

University of Southampton Research Repository ePrints Soton

Copyright © and Moral Rights for this thesis are retained by the author and/or other copyright owners. A copy can be downloaded for personal non-commercial research or study, without prior permission or charge. This thesis cannot be reproduced or quoted extensively from without first obtaining permission in writing from the copyright holder/s. The content must not be changed in any way or sold commercially in any format or medium without the formal permission of the copyright holders.

When referring to this work, full bibliographic details including the author, title, awarding institution and date of the thesis must be given e.g.

AUTHOR (year of submission) "Full thesis title", University of Southampton, name of the University School or Department, PhD Thesis, pagination

UNIVERSITY OF SOUTHAMPTON

FACULTY OF MEDICINE

Human Development and Health

Bone structure and function in adult rat offspring is affected
by maternal protein restriction during pregnancy

by

Stephanie Meakins

Thesis for the degree of Doctor of Philosophy

August 2014

UNIVERSITY OF SOUTHAMPTON

ABSTRACT

FACULTY OF MEDICINE

Human Development and Health

Thesis for the degree of Doctor of Philosophy

BONE STRUCTURE AND FUNCTION IN ADULT RAT OFFSPRING IS AFFECTED BY MATERNAL PROTEIN RESTRICTION DURING PREGNANCY

Stephanie Amanda Meakins

Background Epidemiological studies have shown that poor growth during fetal life, infancy and childhood is associated with an increased risk of fracture and decreased bone mass in adulthood. Previous animal studies have shown that maternal protein restriction (PR) during gestation affects the bone structure and mechanical properties of rat offspring at 75 weeks. However, little is known regarding the effects of maternal PR on subsequent generations and if these effects may be changed with the addition of folic acid (FA) during periods of plasticity such as puberty. **Methods** The gestational PR model was used to evaluate if the effects of gestational PR (F0) are evident in subsequent offspring (F1-F3) and if the effect of PR can be changed by folic acid addition to juvenile rats. Analysis included anthropometric, histological, micro-computed tomography, microindentation, three point bending and qPCR gene expression of femurs and vertebrae in order to assess bone microarchitecture, structure and molecular profiles in offspring. **Results** FA addition to juvenile offspring from PR dams induced site specific negative effects on the neck of femur trabecular bone of male offspring and midshaft femur of female offspring. It also predicted advantageous structural changes to the trabecular and cortical vertebra of the female offspring (increased bone volume and concavity). Differences in bone structure and mechanical properties were observed in the F1-F3 generation female offspring from PR dams. These changes were not transmitted between generations and do not suggest an altered phenotype is visible in bone at 10 weeks of age. F1 PR rats had shorter femurs, F2 PR rats showed a decreased osteocalcin expression and F3 PR rats had heads of femur more resistant and necks of femur less resistant to fracture than the control rat offspring. **Conclusions** This thesis demonstrates that maternal PR induces minor structural changes in 10 week old offspring for three subsequent generations, and this phenotype is altered but not reversed by FA addition to juvenile offspring.

Contents

Abstract	i
Contents	iii
List of tables.....	ix
List of figures	xvii
Declaration of authorship.....	xxv
Acknowledgements	xxvii
Abbreviations.....	1
1. Introduction.....	5
1.1 Bone structure and functions	5
1.1.1 Anatomical features	5
1.1.2 Bone cells	7
1.1.3 Micro and macroscopic structure of bone.....	9
1.1.4 Osteoblast markers	13
1.2 Osteoporosis	15
1.2.1 Overview	15
1.2.2 Bone health	17
1.2.3 Diagnosis	18
1.2.4 Sex and ethnic differences in bone mineral density (BMD)	20
1.2.5 Osteoporosis treatment	23
1.2.6 Genetic influences	28
1.2.7 Environmental influences.....	28
1.2.8 Dietary effects	28
1.3 Developmental origins of health and disease (DOHaD).....	30
1.3.1 DOHaD theory	30
1.3.2 Epidemiological evidence	32
1.3.3 Developmental plasticity.....	32
1.3.4 Window of opportunity	36
1.4 Development and remodelling of bone	37
1.4.1 Processes of bone formation.....	37
1.4.2 Bone remodelling	39
1.4.3 Human skeletal development	40
1.5 Perinatal growth and nutrition	42

1.5.1	Effect of nutrition on embryonic and fetal growth	42
1.5.2	Nutritional influences during pregnancy on fetal bone.....	43
1.6	Epigenetics and cellular programming.....	44
1.6.1	Epigenetics	44
1.6.2	Skeletal programming	46
1.7	Intrauterine environment and osteoporosis.....	47
1.7.1	Epidemiological evidence	47
1.7.2	Animal studies.....	48
1.8	Intrauterine environment effects on other tissues	51
1.8.1	Maternal protein restriction and other tissues.....	51
1.8.2	Maternal high fat and other tissues.....	52
1.9	Conclusions	53
2.	General methods	55
2.1	Anthropometric analysis.....	55
2.2	Histology	55
2.2.1	Sample fixation and decalcification	55
2.2.2	Processing and embedding	56
2.2.3	Cutting sections	56
2.2.4	Alcian Blue Sirius Red staining	57
2.2.5	Section analysis	57
2.3	Micro computed tomography (μ CT) data	58
2.3.1	SkyScan 1176 scanning and reconstruction.....	58
2.3.2	X-Tek HMX scanning and reconstruction.....	58
2.3.3	X-Tek HMX scans: trabecular bone analysis	59
2.3.4	X-Tek HMX scans: cortical bone analysis.....	60
2.3.5	SkyScan 1176 scans: trabecular bone analysis	60
2.3.6	SkyScan 1176 scans: cortical bone analysis.....	61
2.3.8	Parameters investigated	62
2.4	Bone mineral density analysis	65
2.4.1	Hounsfield unit analysis of scans from the HMX	65
2.4.2	Bone mineral density (BMD) analysis of scans from the SkyScan 1176.....	66
2.5	Three point bend testing.....	67
2.5.1	Method 1 conducted for data in Chapter 3	67
2.5.2	Improved method 2 conducted for data in Chapter 4	68

2.6	Micro indentation	68
2.7	Molecular analysis	68
2.7.1	RNA/DNA extraction from bone tissue	71
2.7.2	cDNA production	71
2.7.3	qPCR	71
2.8	Statistical analysis	73
3.	The effect of folic acid dietary addition to offspring from protein restricted mothers on bone structure and quality.....	75
3.1	Introduction	75
3.2	Methods	76
3.2.1	Animal experimentation	76
3.2.2	Histology	79
3.2.3	Micro computed tomography data	79
3.2.4	Bone mineral density	79
3.2.5	Three point bend testing	80
3.2.6	Statistical analysis	80
3.3	Results	81
3.3.1	Anthropometric analysis of femurs	81
3.3.2	Histological analysis of distal femurs from 12 week female rats ..	82
3.3.3	Micro computed tomography analysis of bone structure	86
3.3.4	Three point bend testing	102
3.3.5	Body weight of animals	104
3.3.6	Result summary	106
3.4	Discussion	108
4.	Multigenerational study into the effect of protein restriction during pregnancy (F0) on the bone structure, mechanical properties, and gene expression of offspring up to F3 generation.....	115
4.1	Introduction	115
4.2	Methods	117
4.2.1	Animal experimentation	117
4.2.2	Anthropometric analysis of femurs	120

4.2.3	Micro computed tomography	120
4.2.4	Bone Mineral density.....	120
4.2.5	Three point bend testing.....	120
4.2.6	Microindentation testing	120
4.2.7	Molecular analysis.....	120
4.2.8	Statistical analysis.....	120
4.3	Results	121
4.3.1	Anthropometric analysis.....	121
4.3.2	Micro computed tomography analysis of bone structure	121
4.3.3	Bone mineral density	132
4.3.4	Three point bend testing.....	133
4.3.5	Microindentation analysis.....	134
4.3.6	Quantitative PCR analysis	136
4.3.7	Results summary.....	138
4.4	Discussion	139
5.	General discussion.....	143
6.	References.....	155
7.	Appendices.....	169

List of tables

Table 1-1 Remaining lifetime percentage probability of common osteoporotic fractures in Swedish men and women aged 50 years. Taken from Kanis et al. (2008)	22
Table 3-1 Diet fed during pregnancy, lactation and after weaning	77
Table 3-2 Sample information and codes for offspring	79
Table 3-3 Anthropometric measurements of 12 week young adult rat femurs. Values are mean \pm SD with P-values. Diet groups- C/CFA (control/control folic acid) n=6, C/HFA (C/High folic acid) n=4 , PR/CFA (protein restricted/CFA) n=5 , PR/HFA n= 4 and the diet comparisons were juvenile pubertal diet (JP) and maternal diet (M). - indicates no significance.....	81
Table 3-4 Vertebral body trabecular bone data for 12 week young adult offspring from control/ protein restricted dams, with control/ high folic acid during the juvenile period. Data displayed as mean \pm SD with associated P-values. Diet groups- C/CFA (control/control folic acid) n=6, C/HFA (C/High folic acid) n=4 , PR/CFA (protein restricted/CFA) n=5 , PR/HFA n=4 and the diet comparisons were JP (juvenile pubertal diet) and M (maternal diet). - indicates no significance.....	87
Table 3-5 Vertebral body cortical bone data for 12 week young adult offspring from control/ protein restricted dams, with control/ high folic acid during the juvenile period. Data displayed as mean \pm SD with associated P-values. Diet groups- C/CFA (control/control folic acid) n=6, C/HFA (C/High folic acid) n=4 , PR/CFA (protein restricted/CFA) n=5 , PR/HFA n=4 and the diet comparisons were JP (juvenile pubertal diet) and M (maternal diet). - indicates no significance.....	88
Table 3-6 Vertebral body bone mineral density (BMD) data for 12 week young adult offspring from control/ protein restricted dams, with control/ high folic acid during the juvenile period. Data displayed as mean \pm SD with associated P-values. Diet groups- C/CFA (control/control folic acid) n=6, C/HFA (C/High folic acid) n=4 , PR/CFA (protein restricted/CFA) n=5 , PR/HFA n=4 and the diet comparisons were JP (juvenile pubertal diet) and M (maternal diet). - indicates no significance.....	89

Table 3-7 Femoral head trabecular bone data for 12 week young adult offspring from control/ protein restricted dams, with control/ high folic acid during the juvenile period. Data displayed as mean \pm SD with associated P-values. Diet groups- C/CFA(control/control folic acid) n=6, C/HFA (C/High folic acid) n=4 , PR/CFA (protein restricted/CFA) n=5 , PR/HFA n=4 and the diet comparisons were JP (juvenile pubertal diet) and M (maternal diet). - indicates no significance.....93

Table 3-8 Femoral neck trabecular bone data for 12 week young adult offspring from control/ protein restricted dams, with control/ high folic acid during the juvenile period. Data displayed as mean \pm SD with associated P-values. Diet groups- C/CFA (control/control folic acid) n=6, C/HFA (C/High folic acid) n=4 , PR/CFA (protein restricted/CFA) n=5 , PR/HFA n=4 and the diet comparisons were JP (juvenile pubertal diet) and M (maternal diet). - indicates no significance.....94

Table 3-9 Distal femur trabecular bone data for 12 week young adult offspring from control/ protein restricted dams, with control/ high folic acid during the juvenile period. Data displayed as mean \pm SD with associated P-values. Diet groups- C/CFA (control/control folic acid) n=6, C/HFA (C/High folic acid) n=4 , PR/CFA (protein restricted/CFA) n=5 , PR/HFA n=4 and the diet comparisons were JP (juvenile pubertal diet) and M (maternal diet).97

Table 3-10 Midshaft cortical femur μ CT data for 12 week young adult offspring from control/ protein restricted dams, with control/ high folic acid during the juvenile period. Data displayed as mean \pm SD with associated P-values. Diet groups- C/CFA (control/control folic acid) n=6, C/HFA (C/High folic acid) n=4 , PR/CFA (protein restricted/CFA) n=5 , PR/HFA n=4 and the diet comparisons were JP (juvenile pubertal diet) and M (maternal diet). - indicates no significance..... 99

Table 3-11 Midshaft femur three point bend testing data for 12 week young adult offspring from control/ protein restricted dams, with control/ high folic acid during the juvenile period. Data displayed as mean \pm SD with associated P-values. Diet groups- C/CFA (control/control folic acid) n=6, C/HFA (C/High folic acid) n=4 , PR/CFA (protein restricted/CFA) n=5 , PR/HFA n=4 and the diet comparisons were JP (juvenile pubertal diet) and M (maternal diet). - indicates no significance.....103

Table 4-1 Diet compositions. PR-protein restriction.....	118
Table 7-1 Housekeeping gene CT data used to determine stability.....	171
Table 7-14 Primer sequences for qPCR	172
Table 7-2 Mean values for the microindentation data for the midshaft femur 2 cortical bone of female F1 offspring (n=5) from protein restricted mothers (F0) compared to controls (n=5). P-values are derived from the One-Way ANOVA analysis.....	174
Table 7-3 Mean values for the microindentation data for the midshaft femur 3 cortical bone of female F1 offspring (n=5) from protein restricted mothers (F0) compared to controls (n=5). P-values are derived from the One-Way ANOVA analysis.....	174
Table 7-4 Mean values for the microindentation data for the midshaft femur 4 cortical bone of female F1 offspring (n=5) from protein restricted mothers (F0) compared to controls (n=5). P-values are derived from the One-Way ANOVA analysis.....	175
Table 7-5 Mean values for the microindentation data midshaft femur 2 cortical bone of female F2 offspring (n=5) from protein restricted mothers (F0) compared to controls (n=5). P-values are derived from the One-Way ANOVA analysis.....	175
Table 7-6 Mean values for the microindentation data midshaft femur 3 cortical bone of female F2 offspring (n=5) from protein restricted mothers (F0) compared to controls (n=5). P-values are derived from the One-Way ANOVA analysis.....	176
Table 7-7 Mean values for the microindentation data midshaft femur 4 cortical bone of female F2 offspring (n=5) from protein restricted mothers (F0) compared to controls (n=5). P-values are derived from the One-Way ANOVA analysis.....	176
Table 7-8 Mean values for the microindentation data for the midshaft femur 2 cortical bone of female F3 offspring (n=5) from protein restricted mothers (F0) compared to controls (n=4). P-values are derived from the One-Way ANOVA analysis.....	177

Table 7-9 Mean values for the microindentation data for the midshaft femur 3 cortical bone of female F3 offspring (n=5) from protein restricted mothers (F0) compared to controls (n=4). P-values are derived from the One-Way ANOVA analysis.....	177
Table 7-10 Mean values for the microindentation data for the midshaft femur 4 cortical bone of female F3 offspring (n=5) from protein restricted mothers (F0) compared to controls (n=4). P-values are derived from the One-Way ANOVA analysis.....	178
Table 7-11 Mean values for the microindentation data for the epicondyle cortical bone of female F1 offspring (n=5) from protein restricted mothers (F0) compared to controls (n=4). P-values are derived from the One-Way ANOVA analysis.....	178
Table 7-12 Mean values for the microindentation data for the epicondyle cortical bone of female F2 offspring (n=5) from protein restricted mothers (F0) compared to controls (n=4). P-values are derived from the One-Way ANOVA analysis.....	179
Table 7-13 Mean values for the microindentation data for the epicondyle cortical bone of female F3 offspring (n=5) from protein restricted mothers (F0) compared to controls (n=4). P-values are derived from the One-Way ANOVA analysis.....	179
Table 7-15 Bone sialoprotein gene expression $\Delta\Delta\text{CT}$ (ddCT) for F1 Control and protein restricted samples	180
Table 7-16 Bone sialoprotein gene expression $\Delta\Delta\text{CT}$ (ddCT) for F2 Control and protein restricted samples	180
Table 7-17 Bone sialoprotein gene expression $\Delta\Delta\text{CT}$ (ddCT) for F2 Control and protein restricted samples	181
Table 7-18 Collagen 1 gene expression $\Delta\Delta\text{CT}$ (ddCT) for F1 Control and protein restricted samples	181
Table 7-19 Collagen 1 gene expression $\Delta\Delta\text{CT}$ (ddCT) for F2 Control and protein restricted samples	182
Table 7-20 Collagen 1 gene expression $\Delta\Delta\text{CT}$ (ddCT) for F3 Control and protein restricted samples	182

Table 7-21 IGF II gene expression $\Delta\Delta\text{CT}$ (ddCT) for F1 Control and protein restricted samples	183
Table 7-22 IGF II gene expression $\Delta\Delta\text{CT}$ (ddCT) for F2 Control and protein restricted samples	183
Table 7-23 IGF II gene expression $\Delta\Delta\text{CT}$ (ddCT) for F3 Control and protein restricted samples	184
Table 7-24 IGF I gene expression $\Delta\Delta\text{CT}$ (ddCT) for F1 Control and protein restricted samples	184
Table 7-25 IGF I gene expression $\Delta\Delta\text{CT}$ (ddCT) for F2 Control and protein restricted samples	185
Table 7-26 IGF I gene expression $\Delta\Delta\text{CT}$ (ddCT) for F3 Control and protein restricted samples	185
Table 7-27 Osteocalcin gene expression $\Delta\Delta\text{CT}$ (ddCT) for F1 Control and protein restricted samples	186
Table 7-28 Osteocalcin gene expression $\Delta\Delta\text{CT}$ (ddCT) for F2 Control and protein restricted samples	186
Table 7-29 Osteocalcin gene expression $\Delta\Delta\text{CT}$ (ddCT) for F3 Control and protein restricted samples	187
Table 7-30 Osteonectin gene expression $\Delta\Delta\text{CT}$ (ddCT) for F1 Control and protein restricted samples	187
Table 7-31 Osteonectin gene expression $\Delta\Delta\text{CT}$ (ddCT) for F2 Control and protein restricted samples	188
Table 7-32 Osteonectin gene expression $\Delta\Delta\text{CT}$ (ddCT) for F3 Control and protein restricted samples	188
Table 7-33 Osteopontin gene expression $\Delta\Delta\text{CT}$ (ddCT) for F1 Control and protein restricted samples	189
Table 7-34 Osteopontin gene expression $\Delta\Delta\text{CT}$ (ddCT) for F2 Control and protein restricted samples	189
Table 7-35 Osteopontin gene expression $\Delta\Delta\text{CT}$ (ddCT) for F3 Control and protein restricted samples	190

Table 7-36 Runx-2 gene expression $\Delta\Delta\text{CT}$ (ddCT) for F1 Control and protein restricted samples	190
Table 7-37 Runx-2 gene expression $\Delta\Delta\text{CT}$ (ddCT) for F2 Control and protein restricted samples	191
Table 7-38 Runx-2 gene expression $\Delta\Delta\text{CT}$ (ddCT) for F3 Control and protein restricted samples	191
Table 7-39 Results of the Mann-Whitney U test for F1 C vs F1 PR samples. ..	192
Table 7-40 Results of the Mann-Whitney U test for F2 C vs F1 PR samples. ..	193
Table 7-41 Results of the Mann-Whitney U test for F3 C vs F3 PR samples. ..	194

List of figures

Figure 1-1 Anatomy of a long bone. Diagram adapted from Blaus (2013)	6
Figure 1-2 Osteoblast, osteocyte (A) and osteoclast (B) differentiation. Preosteoblasts start to differentiate slowly from mesenchymal stem cells in the bone marrow until they have the location and phenotype of osteoblasts. As the osteoid becomes mineralized by osteoblasts, these cells become enclosed in lacuna as osteocytes. Osteoclasts are giant multinucleate cells that differentiate from hematopoietic cells of the monocytes/macrophage lineage in the bone marrow (Marquis et al. 2009).....	7
Figure 1-3 Osteoclast. Breakfast, lunch and dinner for an osteoclast! Boyde (2010). An electron microscope image of an osteoclast and the crater in the bone surface it produced by bone resorption.	8
Figure 1-4 Structure of cortical bone and its components (SEER 2014).....	11
Figure 1-5 Finite element analysis model of a proximal femur for (a) healthy and (b) osteoporotic femurs during the stance-phase of walking. Yellow-to-red represent increasing compressing strains (squashing); blue-green increasing tensile strength (stretching). Taken from Van Rietbergen et al. (2003).	12
Figure 1-6 Normal trabecular bone (left), osteoporotic trabecular bone (right) Images from Bone and Joint Research Group.	13
Figure 1-7 Healthy proximal femur (Normal hip bone) and low bone mass proximal femur (Osteoporotic hip bone). Taken from http://www.hughston.com/hha/a.osteo.htm	15
Figure 1-8 Typical sites of osteoporotic fracture; wrist (left), spine (centre) and hip (right) (Kanis 2010).	16
Figure 1-9 A. Bone mass increases during childhood and adolescence to reach a peak by the age of about 20; bone mass remains stable thereafter in both genders until the age of about 50 when age-related bone loss starts to commence; women experience an accelerated phase of bone loss after the menopause (blue box); B. Increasing incidence of hip, spine and wrist fractures with age in women (Ralston 2012).	17
Figure 1-10 Graph showing the bone and muscle strength increasing up to peak bone mass and decreasing in later life. Also shows how differences in	

peak bone mass affect the range of bone mass and strength in later life. (created by S Meakins).....18

Figure 1-11 T-score cut-offs for the diagnosis of osteoporosis, osteopenia and normal BMD; the solid line indicates the average change in BMD with age in Caucasian women; about 50 per cent of women age 80 have osteoporosis as defined by DEXA (Ralston 2012).....19

Figure 1-12 Percentage of initial BMD vs. age for women (left) and men (right) from age 50 onwards. Both trabecular (broken line) and cortical bone (solid line) are shown. Note that women have two phases of bone loss, the first phase is fast, and the second phase is slow, with only the fast phase having disproportionate loss of trabecular bone. Men have one continuous phase that is generally proportionate. Taken from Riggs et al. (1998).....21

Figure 1-13 Ethnic variation in osteoporotic fracture risk and diagnosis of osteoporosis (T-score, -2.5 or lower). Ratios were adjusted for multiple covariates, and White women were the reference group. Data are from the National Osteoporosis Risk Assessment (NORA) Cohort. Taken from Leslie (2012).....23

Figure 1-14 Osteoclast inhibition with denosumab vs bisphosphonates (BPs). OPG (osteoprotegerin). RANK (receptor activator of nuclear factor kappa-B). RANKL (receptor activator of nuclear factor kappa-B ligand) Baron et al. (2011)27

Figure 1-15 The fetal origins of adult disease hypothesis. Taken from Langley-Evans and McMullen (2010).31

Figure 1-16 Pre-adult periods of adaptive plasticity (Hochberg et al. 2011). IC (infant to childhood transition).....33

Figure 1-17 A diagrammatical representation of the different factors affecting phenotypic programming (created by S Meakins).....34

Figure 1-18 Predictive adaptive response (PAR)- red lines represent the potential nutritional environment that an organism could be exposed to. The grey area represents the zone of PARs that reduces disease risk. The risk of disease due to excessive nutrition increases if the level of developmental nutrition was low. Individual 'A' was exposed to a richer intrauterine environment than 'B' and so would cope better in an excessive nutritional

environment than 'B', who is more likely to be at risk of disease. Adapted from Gluckman and Hanson (2004)..... 35

Figure 1-19 Schematic diagram of endochondral ossification. (A, B) Mesenchymal cells condense and differentiate into chondrocytes to form the cartilaginous model of the bone. (C) Chondrocytes in the centre of the shaft undergo hypertrophy and apoptosis while they change and mineralize their extracellular matrix. Their death allows blood vessels to enter. (D, E) Blood vessels bring in osteoblasts, which bind to the degenerating cartilaginous matrix and deposit bone matrix. (F-H) Bone formation and growth consist of ordered arrays of proliferating, hypertrophic, and mineralizing chondrocytes. Secondary ossification centres also form as blood vessels enter near the tips of the bone Gilbert (2000). 38

Figure 1-20 Schematic diagram of intramembranous ossification Gilbert (2000). 39

Figure 1-21 Bone remodelling (Coxon et al. 2004) 40

Figure 1-22 Epigenetics- Two primary processes in epigenetic modification: DNA methylation and histone modification 44

Figure 1-23 Adapted from Gluckman (2008) detailing gene expression regulation through epigenetic processes.....45

Figure 2-1 X-ray images of the same femur and tibia at different stages of demineralisation. Fully mineralised on the left through to demineralised on the right..... 56

Figure 2-2 Illustration of a more concave cortical bone..... 62

Figure 2-3 Fern leaf image to demonstrate fractal dimension as taken from Structural parameters measured by the Skyscan™ CT-analyser software..... 64

Figure 3-4 Schematic of a load displacement graph for a rat femur to demonstrate parameter origins 67

Figure 2-5 Illustration showing the microindentation sites investigated..... 70

Figure 2-6 Microindentation probe- the microindentation probe consists of a reference probe and a test probe. Figure adapted from Diez-Perez et al. (2010). 71

Figure 2-7 An illustration of a typical Indentation curve for one cycle-force versus distance indentation curve with load, hold and unload regions. Courtesy of Tom Jenkins, Bioengineering Research Group, University of Southampton..71

Figure 2-8 Microindentation cycles-for each microindentation cycle, the reference probe is loaded on the bone surface and the testing probe is used to indent the bone. The indentation distance (in relation to the reference probe) is recorded. Figure adapted from Diez-Perez et al. (2010).72

Figure 2-9 Example of 96 plate lay out and colour guide for the two qPCR required to compare 40 samples.....74

Figure 3-1 Diagram displaying the timeline and dietary conditions of the offspring. Both males and female offspring were studied from each diet group78

Figure 3-2 Organisation of the distal femur including cortical bone, trabecular bone and growth plate. Sections labelled and provided as a template guide ...82

Figure 3-3 Female femur histology samples stained with Alcian Blue and Sirius Red. A. C/CFA group (n=3) B. C/HFA group (n=3).83

Figure 3-4 Female femur histology samples stained with Alcian Blue and Sirius Red. A. PR/CFA group (n=3) B. PR/HFA group (n=3).84

Figure 3-5 3D reconstructions of a whole rat vertebra and a segmented vertebral body section. The trabecular and cortical regions of interests (ROI) are shown and labelled on the diagram. The vertebral body trabecular section has been digitally clipped in order to show the interior structure using VG Studio Max.86

Figure 3-6 3D reconstruction of a whole femur (middle), a femoral head (left) and distal femur (right). The femoral head and distal femur have been digitally clipped in order to show the internal trabecular structures using VG Studio Max.....91

Figure 3-7 3D reconstruction of femoral head and neck, digitally clipped to display the trabecular in the inner structure, with cuboids to illustrate sections segmented for trabecular analysis for both the femoral head (blue) and neck (green).92

Figure 3-8 3D reconstruction of distal femur that has been digitally clipped to display the trabecular in the inner structure, with a cuboid to illustrate the section segmented for trabecular analysis for the distal femur (red). 96

Figure 3-9 Whole femur bone mineral density data for male 12 week young adult offspring from C (control)/ PR (protein restricted) dams, with CFA (control folic acid)/ HFA (high folic acid) during the juvenile period. Data displayed as mean \pm SD. 100

Figure 3-10 Whole femur bone mineral density data for female 12 week young adult offspring from C (control)/ PR (protein restricted) dams, with CFA (control folic acid)/ HFA (high folic acid) during the juvenile period. Data displayed as mean \pm SD. 101

Figure 3-11 from (Burdge et al. 2009) Whole body weight gain from weaning (mean \pm 1SD) in (A) male C, (B) male PR, (C) female C and (D) female PR offspring. The periods of feeding diets with different folic acid contents, and the high fat diet are indicated above the x-axis. Comparisons between groups at each time point are indicated by ^aP<0.05, ^bP<0.01, ^cP<0.001 and ^dP<0.0001. Since there were no significant effect of maternal diet, only comparisons between control/control folic acid C/CFA (C/AF) vs. control/ high folic acid C/HFA (C/FS) and protein restricted/ control folic acid PR/CFA (PR/AF) vs. protein restricted/ high folic acid PR/HFA (PR/FS) are shown. 105

Figure 4-1 Taken from Drake and Liu. (2010) Mechanisms for the intergenerational transmission of programming effects. (a) Persistence of an adverse external environment can result in the reproduction of the phenotype in multiple generations. (b) The induction of programmed effects in the F1 offspring following in utero exposure (e.g. programmed changes in maternal physiology or size) results in programmed effects on the developing F2 fetus and so on.....115

Figure 4-2 Simplified schematic of the study design and dietary manipulations 119

Figure 4-3 Anthropometric analysis of 10 week old female femur data for F1-F3 10 week old females from F0 PR (protein restricted) and C (control) dams. N = 5 samples per group, per generation. Data are mean \pm SD and significance is displayed as P \leq 0.05 (*). 121

Figure 4-4 Vertebral body trabecular bone data for F1-F3 10 week old females from F0 PR (protein restricted) and C (control) dams. N = 5 samples per group, per generation. Data are mean \pm SD. 122

Figure 4-5 Vertebral body cortical bone data for F1-F3 10 week old females from F0 PR (protein restricted) and C (control) dams. N = 5 samples per group, per generation. Data are mean \pm SD. 123

Figure 4-6 In order to avoid the growth plate at the proximal femur (red), including the femoral head, an offset was applied before analysis. A. proximal femur, B. Close up of femoral head with the growth plate and trabecular bone exposed..... 124

Figure 4-7 Representations of the cortical and trabecular bone analysed for the head of femur. A. cortical bone and B. trabecular bone..... 125

Figure 4-8 Head of femur trabecular bone data for F1-F3 10 week old females from F0 PR (protein restricted) and C (control) dams. N = 5 samples per group, per generation. Data are mean \pm SD. 126

Figure 4-9 Head of femur cortical bone data for F1-F3 10 week old females from F0 PR (protein restricted) and C (control) dams. N = 5 samples per group, per generation. Data are mean \pm SD. 127

Figure 4-10 In order to avoid the growth plate at the distal femur (red) an offset was applied so that the growth plate was not analysed. A. distal femur, B. segment of the distal femur with the growth plate and trabecular bone exposed..... 128

Figure 4-11 Illustration representing the cortical and trabecular bone analysed for the distal femur. A. distal femur after offset, B. cortical bone and C. trabecular bone. 129

Figure 4-12 Distal femur trabecular bone data for F1-F3 10 week old females from F0 PR (protein restricted) and C (control) dams. N = 5 samples per group, per generation. Data are mean \pm SD. 130

Figure 4-13 Distal femur cortical bone data for F1-F3 10 week old females from F0 PR (protein restricted) and C (control) dams. N = 5 samples per group, per generation. Data are mean \pm SD..... 131

Figure 4-14 Bone mineral density data for F1-F3 10 week old females from F0 PR (protein restricted) and C (control) dams. N = 5 samples per group, per generation. Data are mean \pm SD. 132

Figure 4-15 Three point bend testing data for F1-F3 10 week old females from F0 PR (protein restricted) and C (control) dams. N = 5 samples per group, per generation. Data are mean \pm SD. 133

Figure 4-16 Microindentation data for the head and neck of femur and midshaft femur 1 for F1-F3 10 week old females from F0 PR (protein restricted) and C (control) dams. N = 5 samples per group, per generation. Data are mean \pm SD and $P \leq 0.05$ significances are $P < 0.05$ (*) and $P < 0.01$ (**). 135

Figure 4-17 Relative gene expression data for F1-F3 10 week old females from F0 PR (protein restricted) and C (control) dams. N = 5 samples per group, per generation. Data are mean \pm SD and $P \leq 0.05$ significances is displayed as (*). 137

DECLARATION OF AUTHORSHIP

I, Stephanie Meakins

declare that the thesis entitled

Bone structure and function in adult rat offspring is affected by maternal protein restriction during pregnancy

and the work presented in the thesis are both my own, and have been generated by me as the result of my own original research. I confirm that:

- this work was done wholly or mainly while in candidature for a research degree at this University;
- where any part of this thesis has previously been submitted for a degree or any other qualification at this University or any other institution, this has been clearly stated;
- where I have consulted the published work of others, this is always clearly attributed;
- where I have quoted from the work of others, the source is always given. With the exception of such quotations, this thesis is entirely my own work;
- I have acknowledged all main sources of help;
- where the thesis is based on work done by myself jointly with others, I have made clear exactly what was done by others and what I have contributed myself;
- none of this work has been published before submission, or [delete as appropriate] parts of this work have been published as: [please list references]

Signed:

Date:.....

Acknowledgements

I would like to thank my supervisors, Prof. Richard Oreffo, Dr Stuart Lanham and Prof. Cyrus Cooper for all their help, knowledge and encouragement over the last four years. Prof. Richard Oreffo has provided me with direction, understanding, and motivation for which I am very grateful. Dr. Stuart Lanham provided me with expert guidance, unrivalled problem solving skills and a lot of support, especially with micro CT. Kate White and Tsiloon Li have assisted me with fantastic support and technical skills in molecular experimentation design and execution. Thanks must go to David Gibbs and Stef Inglis who provided assistance with proof reading. Thank you to the Bone and Joint Research Group for welcoming and nurturing me during my time with the group.

I would like to also say a special thanks to my family for the infinite support during this PhD especially my parents and sisters. Finally, I would like to thank my husband Ben for all his love, help, and encouragement. I could not have done this without Ben he has made this all possible.

Abbreviations

μ CT Micro computed tomography

aBMD Areal bone mineral density

ANOVA Analysis of variance

BMC Bone mineral content

BMD Bone mineral density

BP Bisphosphonate

BSP Bone sialoprotein

BV Bone volume

C Control

Ca Calcium

CID Creep indentation distance

Col I Collagen I

Conn.Dn Connectivity density

CRF Clinical risk factor

Cu Copper

μ CT micro-computed tomography

CT cycle threshold

DA Degree of anisotropy

DEXA Dual-energy X-ray absorptiometry

DNA Deoxyribonucleic acid

DOHaD Developmental origins of health and disease

EDTA Ethylenediaminetetraacetic acid

ER Oestrogen receptor

ET Oestrogen therapy

F Fluoride

F0 First generation rats

F1 First generation offspring rats
F2 Second generation offspring rats
F3 Third generation offspring rats
FA Folic acid
FD Fractal dimension
FRAX WHO fracture risk assessment tool
GR Glucocorticoid receptor
HBSS Hanks buffered salt solution
HCl Hydrochloric acid
HF High fat
HRT Hormone replacement therapy
HT Hormone therapy
IDI Indentation distance increase
IGF-I Insulin-like growth factor I
IGF-II Insulin-like growth factor II
L3 Lumbar vertebra 3
L4 Lumbar vertebra 4
LDL Low Density Lipoprotein
Mg Magnesium
NAFLD Non-alcoholic fatty liver disease
NICE National Institute for Clinical Excellence
NORA National osteoporosis risk assessment
NTD Neural tube defects
OCN Osteocalcin
ON Osteonectin
OP Osteopontin
OPG Osteoprotegerin
PAR Predictive adaptive response

PBS Phosphate buffered saline
PCR Polymerase chain reaction
PMMA Poly(methyl methacrylate)
PPAR Peroxisomal proliferator-activated receptor
PR Protein restricted
RANKL Receptor activator of nuclear factor kappa-B ligand
ROI Region of interest
Runx 2 Runt-related transcription factor 2
SD Standard deviation
SERM Selective oestrogen receptor modulators
Si Silicon
SMI Structural model index
Sr2 Strontium
SrR Strontium renelate
Tb.N Trabecular number
Tb.Pf Trabecular pattern factor
Tb.Sp Trabecular separation
Tb.Th Trabecular thickness
TID Total indentation increase
VB Vertebral body
Vit D Vitamin D
VTE Venous thromboembolism
Zn Zinc

1. Introduction

1.1 Bone structure and functions

Bone has a number of functions; it acts as a mineral store, supports the musculoskeletal system, provides a site for muscle binding to allow locomotion, protects the internal organs and other tissues, and produces blood and stem cells within the bone marrow (Knight 2003).

1.1.1 Anatomical features

1.1.1.1 Types of bone

There are five types of bone in the human body: I) short, II) sesamoid, III) flat, IV) long, and V) irregular bones.

- I) Short bones are usually cubic and contain mainly trabecular bone, for example the carpal bones in the wrist.
- II) Sesamoid bones are a sub-set of short bones that develop within a tendon, for example the patella.
- III) Flat bones consist of two layers of cortical bone with a layer of trabecular bone in between. As the name suggests they are shorter in one direction than the other two and so are flat and thin, for example the sternum.
- IV) Long bones consist of a long hollow shaft attached to rounded ends. They are longer in length than in width, for example the femur, tibia and humerus are all long bones.
- V) Irregular bones are bones that do not fit into the previous four categories, for example, the pelvis and vertebra.

1.1.1.2 Features of a long bone

The epiphyses are the rounded ends of long bones, at their joint to adjacent bones. Long bones are composed of mainly trabecular bone covered in a thin layer of cortical bone (Marieb 2006). The trabecular bone adds strength along lines of stress. The diaphysis is the shaft that connects the epiphysis of a long

bone, and is made of a dense tube of cortical bone that surrounds the medullary canal. The diaphysis contains yellow bone marrow in adults and red bone marrow in infants (Waugh et al. 2001; Marieb 2006). The wider section of a long bone between the diaphysis and epiphysis is called the metaphysis (Figure 1-1).

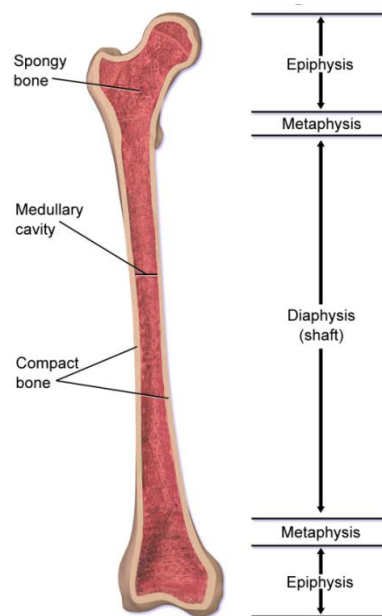


Figure 1-1 Anatomy of a long bone. Diagram adapted from Blaus (2013)

The plate of cartilage (hyaline) found in the metaphysis at the end of long bones is referred to as the epiphyseal plate. This growth plate ossifies when growth is complete in humans (Waugh et al. 2001). The periosteum is a tough membrane encapsulating all bones, except the ends of long bones involved in joints. It is attached to the bone by hundreds of perforating fibres (Marieb 2006). During growth, new bone is laid down under this membrane (Waugh et al. 2001). Similarly, the membrane that surrounds the inside of the medullary canal and separates it from the bone marrow is called the endosteum.

1.1.2 Bone cells

There are four types of bone cells: osteoblasts, osteoclasts, osteocytes and bone lining cells. Osteoblasts are cells responsible for the formation of bone through secretion of osteoid-containing collagen. They are derived from mesenchymal stem cells (Figure 1-2) and either mature into osteocytes or

continue until apoptosis (Aubin 2001). Osteoblasts are located in immature bone ossification centres, in the periosteum during new bone formation, in fracture sites, and on the diaphysis sides of the growth plate of long bones. Osteoblasts are specialised fibroblasts.

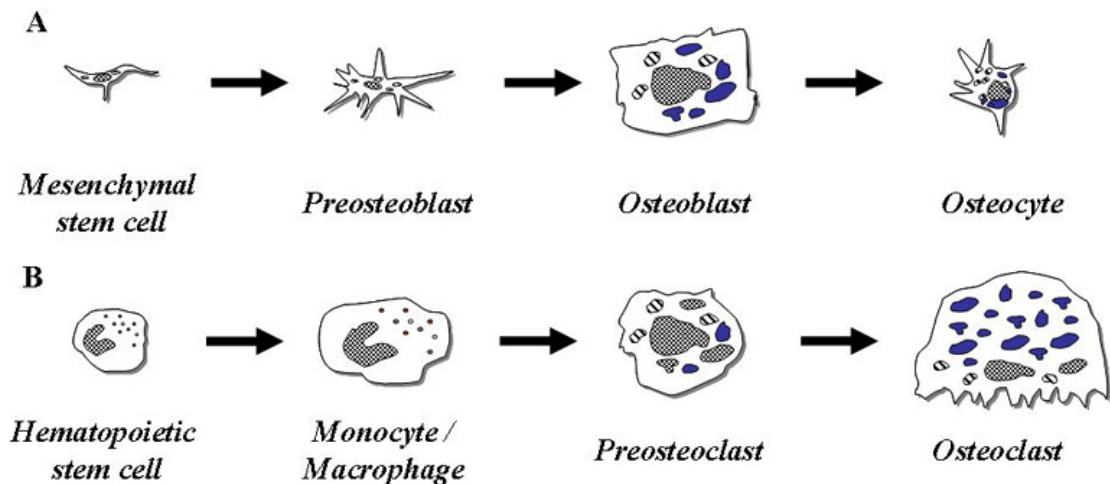


Figure 1-2 Osteoblast, osteocyte (A) and osteoclast (B) differentiation. Preosteoblasts start to differentiate slowly from mesenchymal stem cells in the bone marrow until they have the location and phenotype of osteoblasts. As the osteoid becomes mineralized by osteoblasts, these cells become enclosed in lacuna as osteocytes. Osteoclasts are giant multinucleate cells that differentiate from hematopoietic cells of the monocytes/macrophage lineage in the bone marrow (Marquis et al. 2009).

Osteocytes progress from osteoblast cells that become trapped in the lamella. Osteocytes do form new osteoid but at a much slower rate than osteoblasts (Knight 2003). Osteocytes are connected by the canaliculi and fed by the tissue fluid. It is thought that osteocytes are involved in the movement of minerals such as calcium (Ca) between bone and blood (Vaugh et al. 2001). Osteocytes may also have other roles, for example in sensing mechanical strain and transmitting biochemical signals relating to resorption and formation of bone tissue according to the strength and location of the signals (Bonewald 2007).

Osteoclasts are large multinuclear cells that resorb bone matrix in order to remodel and maintain the matrix. They are derived from haematopoietic stem cells (Figure 1-2). Bone is remodelled around the walls of the medullary canal

and under the periosteum during growth and healing. Osteoclasts leave a trough behind them as they resorb the bone matrix (Figure 1-3).

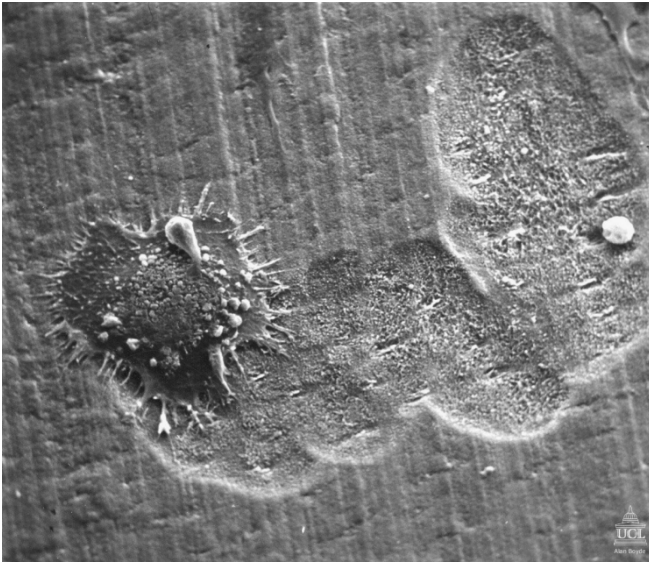


Figure 1-3 Osteoclast. Breakfast, lunch and dinner for an osteoclast! (Boyde 2010). An electron microscope image of an osteoclast and the crater in the bone surface it produced by bone resorption.

Bone lining cells are derived from osteoblasts and cover the bone surface of adult bones. They are important in cellular signalling and are thought to have a role in bone remodelling.

1.1.3 Micro and macroscopic structure of bone

1.1.3.1 Molecular structure

On a molecular level, bone can be divided into matrix and minerals.

Organic bone matrix is a 3D structure composed of mainly type I collagen (Col I) and water, but may also contain silicon (Si) or copper (Cu) within its structure (Rey et al. 2009). Collagen is mainly responsible for the tensile strength of bone. Other less abundant noncollagenous proteins, for example osteonectin, osteopontin and osteocalcin (Aubin 2001), are also within the organic matrix; these proteins control the cell mediated deposition of osteoid and its remodelling (Boskey 2006). Osteonectin (ON) is a bone specific protein that links type I collagen and inorganic bone mineral (hydroxyapatite) (Jundt et al. 1987). Osteopontin (OP) is expressed by osteoblasts and osteoclasts in bone, but is also expressed by other cells such as smooth muscle and endothelial cells. Although not bone specific, OP plays an important role in bone resorption during remodelling (Mazzali et al. 2002). Osteocalcin (OCN) is a protein found in bone and dentin (Hauschka et al. 1983) and is one of the most abundant non-collagenous proteins found in bone. OCN is expressed by mature osteoblasts (Hopyan et al. 1999).

Inorganic bone mineral is composed mainly of a calcium phosphate structure referred to as hydroxyapatite, which is responsible for the compressive strength of bone. The precise atomic arrangement of the hydroxyapatite depends on the amount of Ca present. As bone is used to store Ca, the relative amount of these ions varies at times. Other ions such as fluoride (F⁻), Strontium (Sr²⁺) are present and zinc (Zn) is also present in the solid phase (Rey et al. 2009). These ions can be substituted for Ca in the hydroxyapatite structure. Mineralisation of the collagen matrix gives the bone strength while the collagen fibres provide additional elasticity (Marieb 2006).

1.1.3.2 Collagen structural arrangements

Depending on the method of formation there are a number of possible collagen fibre arrangements.

- Immature or woven bone consists of irregular coarse collagen fibres with a low mineral content. Immature bone initially develops in the embryo and is also formed during fracture repair.
- Mature or lamella bone consists of ordered collagen fibres and has a systematic structure consisting of concentric circles, which makes lamella bone much stronger than immature bone (Marieb 2006)

1.1.3.3 Cortical and trabecular bone

Cortical or compact bone is made up of osteons that consist of a Haversian canal at the centre, encapsulating nerves, lymph and blood vessels, surrounded by concentric layers of lamella bone (Figure 1-4). These are separated by spaces containing osteocytes and tissue fluid called lacuna (Waugh et al. 2001). The lacuna are connected by tunnels called canaliculi, that allow the osteoclasts to extract nutrients from the tissue fluid and dispose of their waste (Marieb 2006). The collagen fibres are aligned parallel to one another providing dense, strong bone that makes up the cortex of most bones. The cortical bone is affected later in life by decreasing bone density although it is thought the effect is less dramatic than that of trabecular bone due to its lower metabolic activity in comparison to trabecular bone (Meunier 1998).

Compact Bone & Spongy (Cancellous Bone)

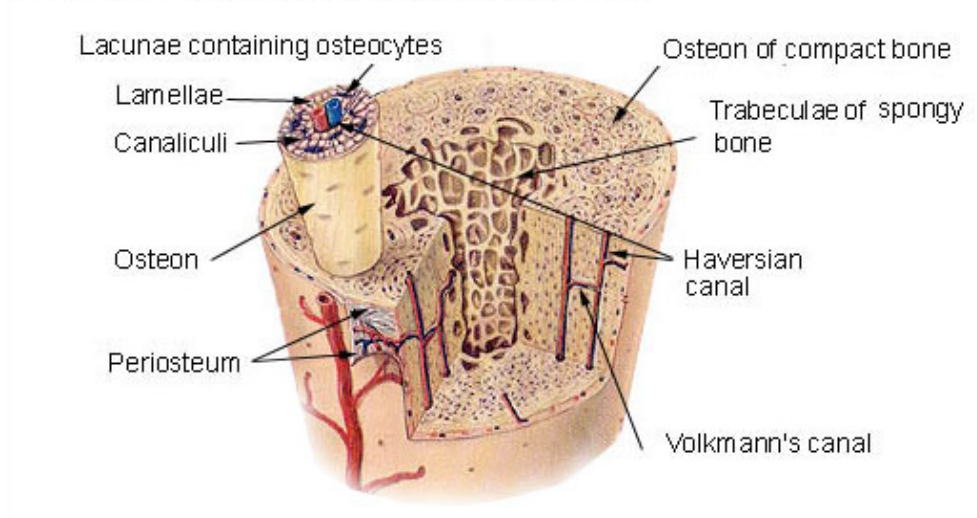


Figure 1-4 Structure of cortical bone and its components (SEER 2014).

Trabecular or spongy bone comprises a fine network of tissue that is less dense and more porous than cortical bone and which occupies the interior of the bones. At the centre of the epiphysis of long bones a vast network of trabecular bone is found. The structure consists of small amounts of lamella with osteocytes interspersed throughout (Waugh et al. 2001). Although the network spans the entire space, the trabeculae are also aligned along stress lines to provide additional strength as shown in Figure 1-5. The healthy femur has greater numbers of trabeculae specifically in the areas that are under strain when in the stance for walking.

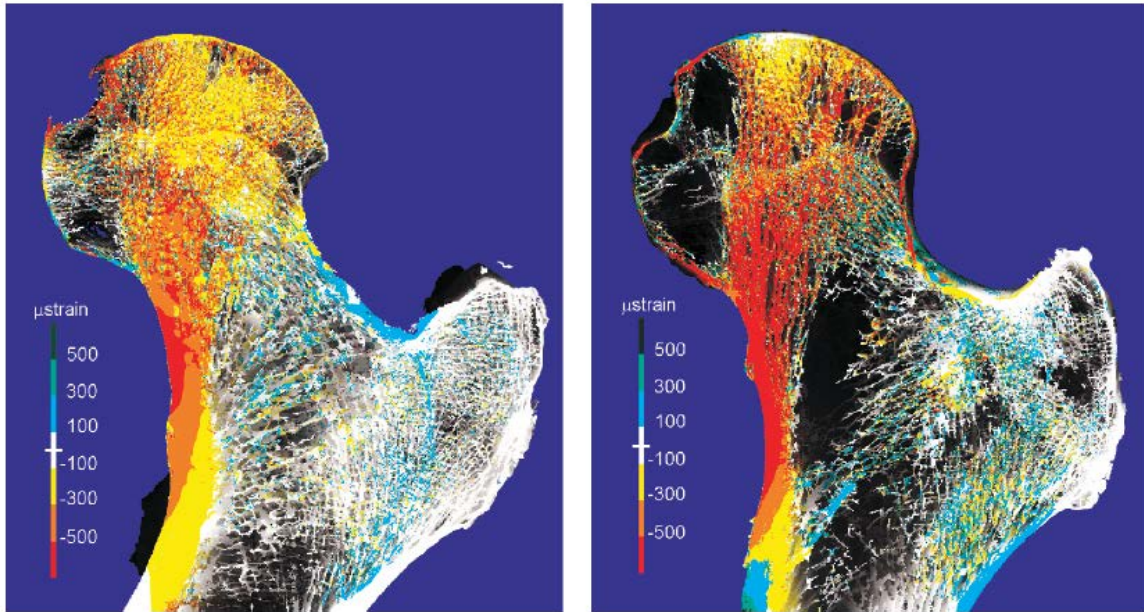


Figure 1-5 Finite element analysis model of a proximal femur for (a) healthy and (b) osteoporotic femurs during the stance-phase of walking. Yellow-to-red represent increasing compressing strains (squashing); blue-green increasing tensile strength (stretching). Taken from Van Rietbergen et al. (2003).

The areas that are most affected by age related fracture have a higher proportion of trabecular bone than cortical bone, for example the neck of femur and lumbar spine (Meunier 1998). Trabecular bone is thought to have a higher metabolic activity in comparison to cortical bone. As bone density decreases in later life, it is the trabecular bone that subsequently becomes thinner due to resorption or a decrease in trabecular number. Although cortical bone is known to decrease in thickness, the effect is less drastic as it is denser to begin with. During age related bone loss, areas with substantial trabecular bone are therefore susceptible to fracture in osteoporotic individuals (Knight 2003). The abundance and connectivity of trabecular bone can influence the appearance of the structure i.e. bone with better connected trabeculae can be described as plate like, bone with less well connected trabeculae can be described as rod like. This is because the connections in dense trabecular bone are thicker and appear wider than the trabeculae in thinner less dense bone. Figure 1-6 illustrates an example of plate like normal bone trabecular bone, and rod like osteoporotic trabecular bone.

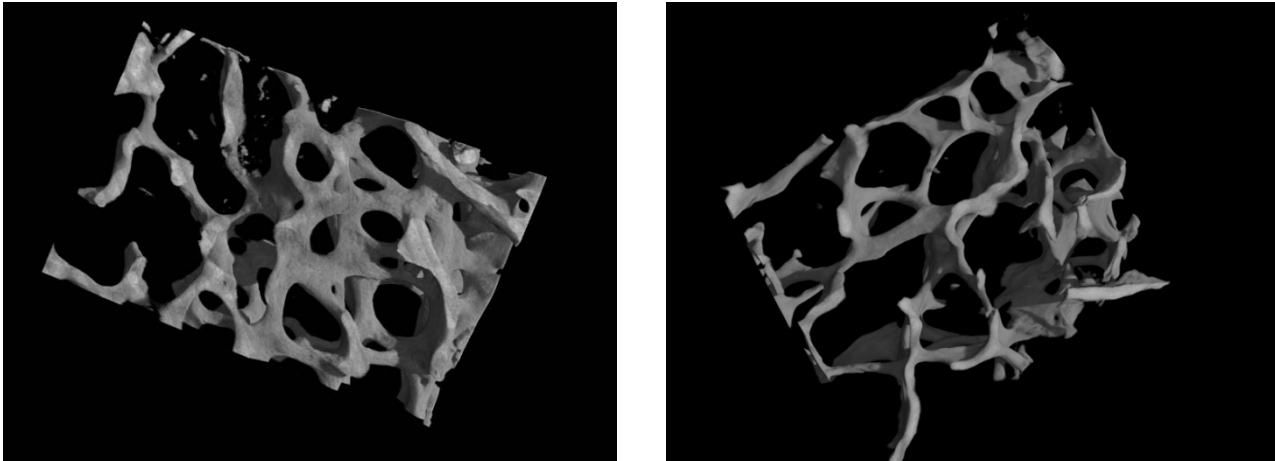


Figure 1-6 Normal trabecular bone (left), osteoporotic trabecular bone (right) Images from Bone and Joint Research Group.

1.1.4 Osteoblast markers

Bone sialoprotein (BSP) is an early osteogenic marker believed to be able to nucleate hydroxyapatite crystals that is involved in the early mineralisation of osteoblasts. BSP has been shown to mediate fibroblast attachment on tissue culture dishes and to participate in collagen binding and cell signalling (Ganss et al. 1999).

Runt-related transcription factor 2 (Runx 2) is essential for bone formation due to its role in osteoblast differentiation from mesenchymal precursors. Runx 2 expression regulates expression of other osteogenic genes such as osteocalcin (Kirkham et al. 2007).

(see section 1.1.3 for other proteins expressed by osteoblasts commonly used as osteoblast markers such as **osteocalcin**, **osteopontin** and **osteonectin**).

1.1.4.1 Insulin-like growth factors I and II

Insulin-like growth factors (IGF-I and IGF-II) are some of the most abundant growth factors expressed by osteoblasts. IGF-I plays a complex role in bone, with involvement in linear bone growth and skeletal acquisition. Zhang et al. showed that IGF-I is essential for coupling matrix biosynthesis to sustained mineralization- which is thought to be of great importance during the pubertal growth spurt when rapid bone formation and consolidation are required (Zhang et al. 2002). IGF-II stimulates bone formation by increasing replication of cells belonging to the osteoblastic lineage. Bone is one of the few adult tissues that expresses IGF-II, along with heart. IGF-II levels decline in extracts of cortical human bone with ageing, suggesting a possible role of IGF-II in the pathogenesis of osteoporosis conservation of bone mass Dequeker and Johnell (1993).

1.2 Osteoporosis

1.2.1 Overview

In 1994 the World Health Organisation defined osteoporosis as “a progressive systemic skeletal disease characterised by low bone mass and micro-architectural deterioration of bone tissue, with a consequent increase in bone fragility and susceptibility to fracture” (Kanis and Kanis 1994).

Figure 1-7 is an illustration representing healthy bone (left) and osteoporotic bone (right). Comparatively, osteoporotic bone has both fewer and thinner trabeculae and thinner cortical bone than healthy bone, which has the effect of decreasing bone strength. Bone with reduced mechanical strength is more likely to fracture when subjected to trauma (Cooper and Aihie 1995). As osteoporotic bone is more fragile than healthy bone, a relatively minor trauma can still lead to a fracture. This is particularly true in the elderly where proximal femoral fractures are typically sustained following a fall from standing height.

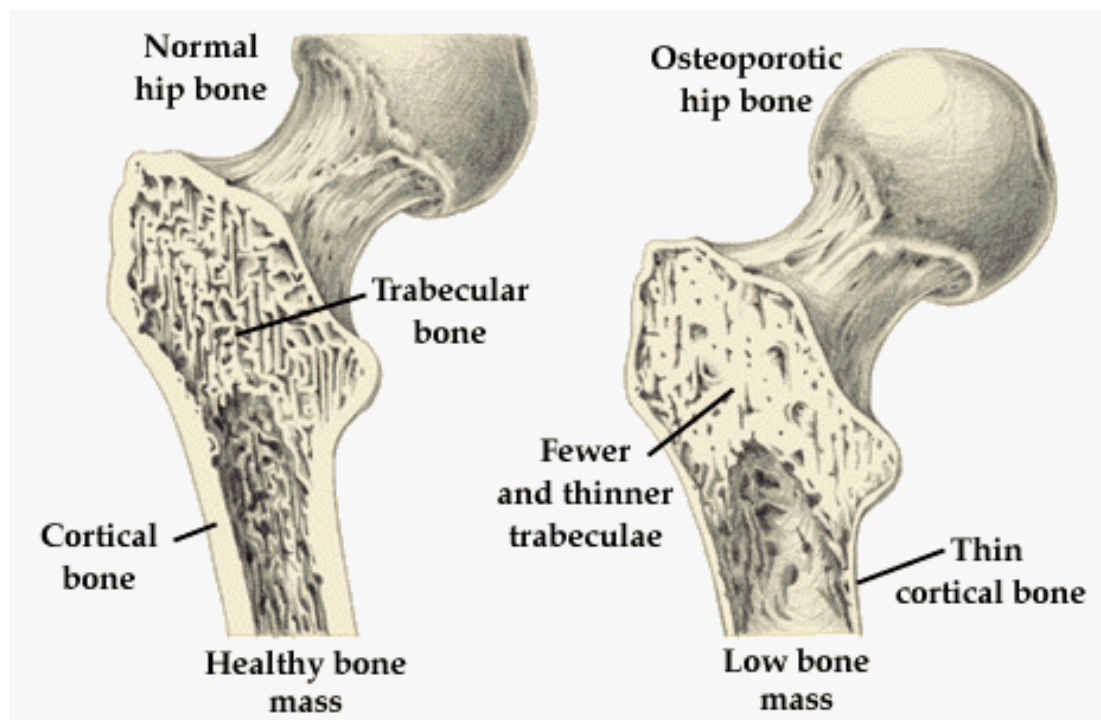


Figure 1-7 Healthy proximal femur (Normal hip bone) and low bone mass proximal femur (Osteoporotic hip bone). Taken from <http://www.hughston.com/hha/a.osteo.htm>

There are both environmental and genetic influences that affect a bone's strength and susceptibility to fracture throughout its life. Within the population it is expected that bone mass will decrease after the age of 50 in both sexes, with this process being even more rapid in females. With an increasingly ageing demographic due to longer life expectancies, there are a greater number of people with low bone mass and thus a rise in diagnosis of osteoporosis within the population. As the 1 year mortality rate of patients who have sustained a proximal femoral fracture is over 20% (Chia et al. 2013), this rise in osteoporotic patients and an associated increase in fracture occurrence has serious consequences for osteoporotic patients. Furthermore those that survive have a reduced quality of life after a fracture and the medical costs associated with rehabilitation are high. As the disease progresses there is an increase in morbidity and mortality after the fracture and this has economic implications for the health care services (Cooper 2010).

Figure 1-8 shows three X-ray images of fractures at the three most common sites of osteoporotic fracture: hip, spine and wrist, with the fractures highlighted in green. When bone is osteoporotic other areas are increasingly likely to fracture, including ribs, humeri and pelvis (Royal college of Physicians. 1999).



Figure 1-8 Typical sites of osteoporotic fracture (encircled in green) wrist (left), spine (centre) and hip (right) (Kanis 2010).

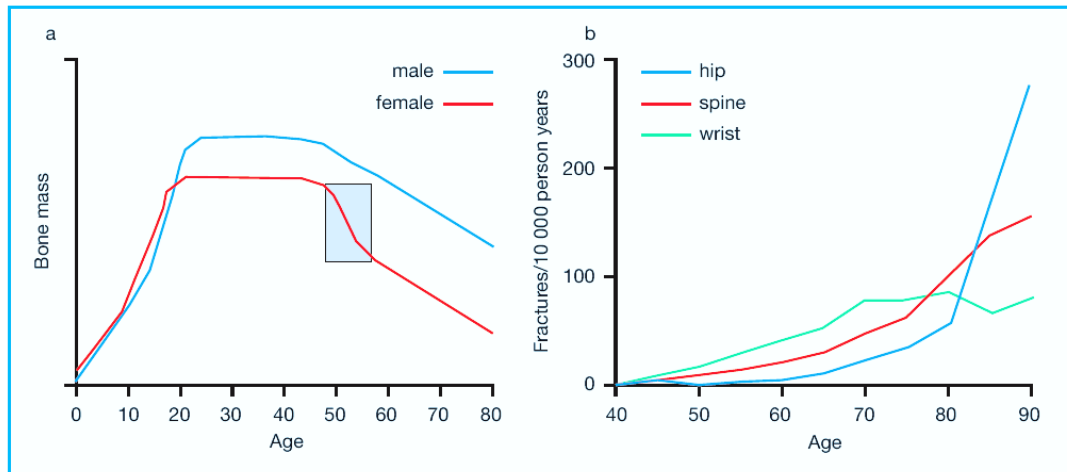


Figure 1-9 A. Bone mass increases during childhood and adolescence to reach a peak by the age of about 20; bone mass remains stable thereafter in both genders until the age of about 50 when age-related bone loss starts to commence; women experience an accelerated phase of bone loss after the menopause (blue box); B. Increasing incidence of hip, spine and wrist fractures with age in women (Ralston 2012).

Figure 1-9 A shows the decrease in bone density with old age for both males and females. The blue box represents menopause for women and the associated increased rate of bone loss. Figure 1-9 B shows the increase in the number of incidences of fracture for hip, spine, and wrist with increasing age.

Over 200,000 fractures occur in the UK each year, causing severe pain and disability to individual sufferers and costing the National Health Service over £1.73 billion per year. In addition, only approximately half of patients are able to live independently after a hip fracture and 20% will die within one year (Kanis 2010). Thus there is a great need to understand the disease progression of osteoporosis and improve strategies for intervention. The role of the intrauterine environment on later bone structure and mechanical strength is one area for investigation.

1.2.2 Bone health

Bone mass status throughout the life course can be divided into three stages (Figure 1-10): 1. **Growth**- bone mass is accrued during skeletal growth, until peak bone mass at approximately age 30, 2. **Remodelling**- where total bone mass is stable and there is no net gain or loss. Bone is constantly being

remodelled, with old bone being reabsorbed and new bone being formed, 3. Loss- bone mass decreases after age 50 in all individuals (Royal College of Physicians 1999). Individuals diagnosed with osteoporosis are said to have a higher than usual rate of bone loss, compared to their rate of bone formation. This imbalance in bone turnover leads to thinning of bone tissue and consequent increased risk of fracture (Cooper et al. 1995). Once bone growth has stopped during the bone remodelling stage, bone mass accumulation thereafter is limited. However, the rate of bone loss can be slowed with treatment and fracture risk can be reduced (Kanis et al. 2008).

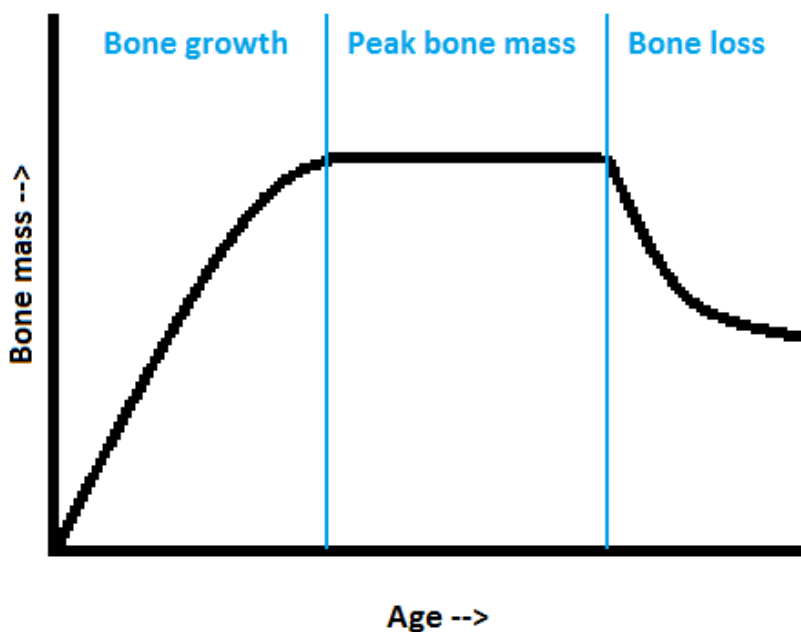


Figure 1-10 Graph showing the bone and muscle strength increasing up to peak bone mass and decreasing in later life. Also shows how differences in peak bone mass affect the range of bone mass and strength in later life (created by S Meakins).

1.2.3 Diagnosis

Osteoporosis is a disease that becomes more prominent with age. The three types of osteoporosis can be defined as postmenopausal (primary type 1), age related (primary type 2) and secondary. Secondary osteoporosis is induced as a side effect from other conditions or their treatments e.g. heparin or as a result of another disease e.g. rheumatoid arthritis or type 1 diabetes (Kanis 2010).

A dual energy X-ray absorptiometry (DEXA) scan at the femoral neck is required to confirm a diagnosis of osteoporosis. However the NICE guidelines suggest that the diagnosis can be assumed if the patient is over 75 years old and has previously suffered a fragility fracture. If an individual has a bone mineral density (BMD) score of 2.5 standard deviations below the population average in healthy adults they are diagnosed as osteoporotic (Figure 1-11). This is referred to as a T-score of -2.5. A T-score of between -1 and -2.5 would result in a diagnosis of osteopenia, meaning that the individual is at risk of developing osteoporosis (Earl et al. 2010; World Health Organisation 1994). A T-score of less than -2.5 does not however guarantee that the individual will have a fracture. Nevertheless, the lower the BMD the more likely a fracture is to occur.

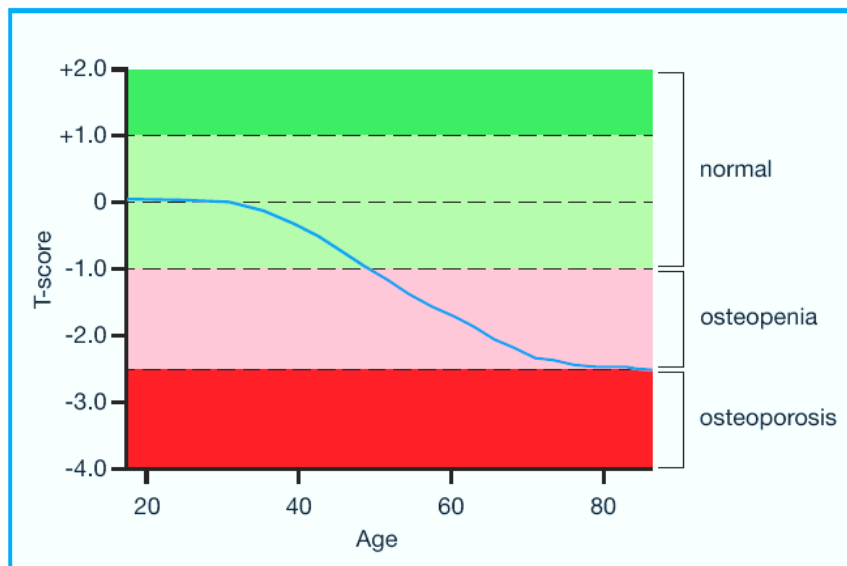


Figure 1-11 T-score cut-offs for the diagnosis of osteoporosis, osteopenia and normal BMD; the solid line indicates the average change in BMD with age in Caucasian women; about 50 per cent of women age 80 have osteoporosis as defined by DEXA (Ralston 2012).

A diagnosis of osteoporosis is not given solely on a T-Score as this only takes into account the overall BMD and not the structural arrangement of the bone, which provides a significant contribution to an individual's risk of fracture. It is difficult however to assess which structural arrangements are more likely to result in bone fracture or indeed to classify variation in bone architecture. For

this reason, an individual may only be diagnosed with severe osteoporosis following a fragility fracture (Kanis 2002).

Alternative methods of predicting fracture risk have recently been developed with multiple risk factors considered within the algorithm. FRAX[®] was developed by the World Health Organisation to assess a patient's 10-year probability of fracture based on clinical risk factors (CRF) with or without BMD. CRF include age, sex, secondary causes of osteoporosis (i.e. rheumatoid arthritis) and smoking. FRAX[®] also gives a suggested care pathway from the National Osteoporosis Guidelines Group (Kanis 2010).

1.2.4 Sex and ethnic differences in bone mineral density (BMD)

Women of postmenopausal age have an increased rate of bone loss compared to men of the same age (Figure 1-12). Although overall, in both men and women as individual age increases, their corresponding BMD decreases together with a drop in T-scores, increasing the risk of fracture. Postmenopausal women have two phases of bone loss, the first of which is faster and disproportionate with respect to the amount of trabecular bone lost compared to cortical bone. The second phase is a slower, more continuous phase. The rate of bone loss in the first phase is due to the alterations in biochemistry associated with the menopause. The second phase is similar in appearance to the slow and continuous phase that men experience, with trabecular and cortical bone loss in equal proportions. As women experience a higher net bone loss, fracture risk is higher for women compared to men of the same age.

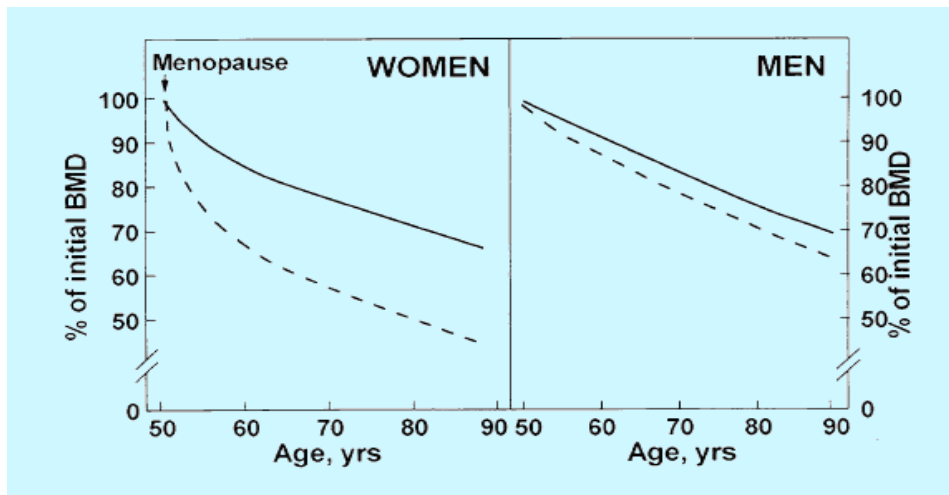


Figure 1-12 Percentage of initial BMD vs. age for women (left) and men (right) from age 50 onwards. Both trabecular (broken line) and cortical bone (solid line) are shown. Note that women have two phases of bone loss, the first phase is fast, and the second phase is slow, with only the fast phase having disproportionate loss of trabecular bone. Men have one continuous phase that is generally proportionate. Taken from Riggs et al. (1998).

The increase in bone loss during the menopause is a consequence of the loss of the protective effect of oestrogen. Oestrogen acts on the oestrogen receptors (ERs) present on osteoblasts and osteoclasts to regulate bone turnover (Riggs et al. 1998). As oestrogen levels fall during the menopause this effect is lost, and the process of bone remodelling becomes unbalanced with rate of bone loss increased with respect to bone formation, resulting in a decrease in bone mass (Cooper 1996; Kanis et al. 2008).

Table 1-1 Remaining lifetime percentage probability of common osteoporotic fractures in Swedish men and women aged 50 years. Taken from Kanis et al (2008).

Site of fracture	Women aged 50 years	Men aged 50 years
Hip	22.9	10.7
Distal forearm	20.8	4.6
Spine (clinical)	15.1	8.3
Proximal humerus	12.9	4.9
Any of the above	46.4	22.4

The probability of fracture in women is significantly higher than in men from the age of 50 onwards at all of the sites detailed above as shown in Table 1-1 in a Swedish population. The remaining lifetime percentage probability at the hip refers to the likelihood of an individual of sustaining a hip fracture during the remainder of their life. Given the similarities within ethnic groups, this trend can be generalised across other Caucasian populations around the world. It is important to note that for other ethnic groups BMD and fracture probability vary from that of Caucasians (Figure 1-13). While osteoporosis and associated fractures affect all ethnic groups, the effect varies due to the multifactorial nature of the disease. Genetics, lifestyle and body size are all known to influence an individual's chance of developing osteoporosis (Ralston et al. 2010).

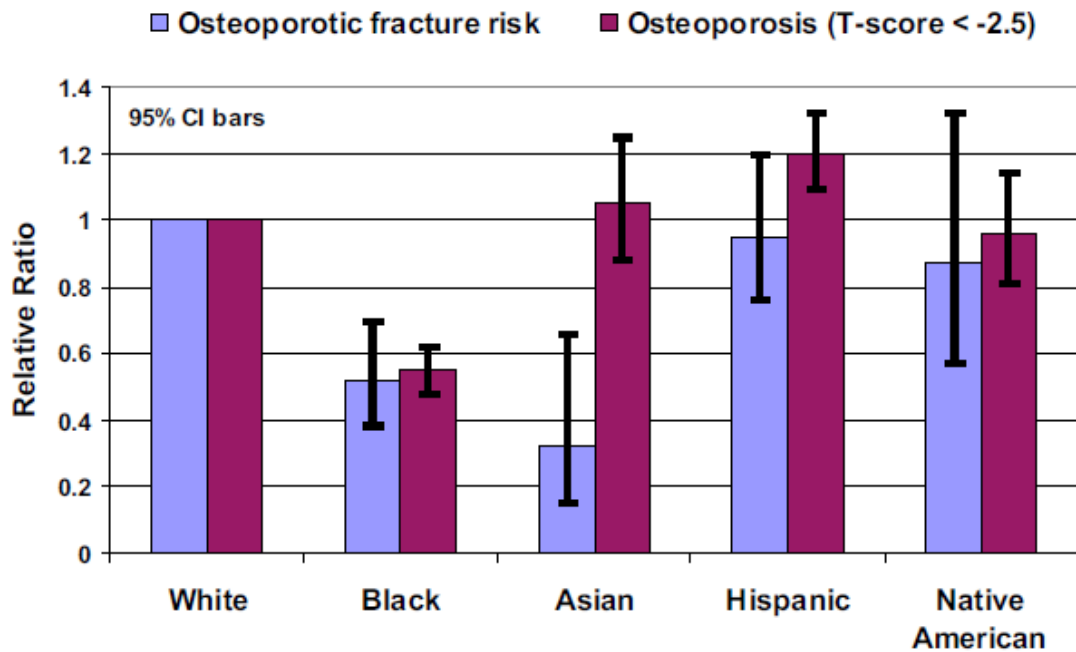


Figure 1-13 Ethnic variation in osteoporotic fracture risk and diagnosis of osteoporosis (T-score, -2.5 or lower). Ratios were adjusted for multiple covariates, and White women were the reference group. Data are from the National Osteoporosis Risk Assessment (NORA) Cohort. Taken from Leslie (2012).

1.2.5 Osteoporosis treatment

Treatments for osteoporosis may be classified as I) agents that reduce the rate of bone loss or II) agents that encourage new bone formation. As osteoporosis is asymptomatic, patient compliance to treatment, particularly those with undesirable side effects, is low. For example, recommendations state that patients should remain upright for 30 minutes after taking alendronate, which can make compliance challenging or even impossible in this demographic. Administration techniques are being developed to increase compliance and overcome some of the common side effects of treatment.

According to the National Institute for Health and Clinical Excellence (NICE) guidelines for the secondary prevention of osteoporotic fragility fractures (after at least one fracture) in postmenopausal women, treatments should be prescribed in the following order in conjunction with Vitamin D (Vit D) and Ca

supplementation if necessary. Initially alendronate is prescribed for women with a T-score of -2.5 SD or below. If alendronate is unsuitable because of intolerance or contraindication to alendronate or inability to comply with administration instructions then other bisphosphonates like risedronate or etidronate are prescribed. If these too are unsuitable then strontium ranelate and raloxifen are recommended, followed finally by teriparatide (National Institute for Health and Clinical Excellence 2008). For primary osteoporosis without a fragility fracture, raloxifen is not prescribed (National Institute for Health and Clinical Excellence 2008). These recommendations are made according to cost benefit analysis. Other treatments not in the NICE guidelines are also listed below.

Bisphosphonates

In 2007, bisphosphonates were the most common osteoporosis treatment regime advocated in the USA (Cramer et al. 2007). Examples of common bisphosphonates prescribed for postmenopausal osteoporosis (primary and secondary) are alendronate, etidronate and risedronate. Bisphosphonates are commonly administered as an oral tablet, taken daily or weekly. However, special dosing requirements are required to take bisphosphonates, for example alendronate requires fasting overnight, 10mg of alendronate is then consumed with 250ml of water with no other food or drink and sitting upright for at least 30 minutes after dosing. Alendronate can also be taken once a week in a 70mg dose under the same dosing conditions. Etidronate is to be taken in 90 day cycles with 400mg/day Etidronate taken for the first 14 days (as with alendronate) followed by calcium carbonate 1.25mg/day for the remaining 767 days (National Institute for Health and Clinical Excellence 2008). Alendronate is approved for treatment of osteoporosis in postmenopausal women and men. Risedronate and Etidronate are approved for prevention and treatment of glucocorticoid-induced osteoporosis in postmenopausal women (Kanis 2010). Side effects include gastric ulcers, difficulty in swallowing and inflammation of the oesophagus (National Osteoporosis Society 2010). As with all osteoporosis treatments, patients' compliance is an issue to be addressed (McHorney et al. 2007). Oral bisphosphonates have a very low bioavailability typically of only a few percent (Major et al. 2000). New treatments are emerging using different administration techniques for bisphosphonates, for example, intravenous

infusion, either every 3 months (pamidronate) (Thiebaud et al. 1997) or once-yearly (Zoledronic Acid) (Black et al. 2007). Further information on bisphosphonate mode of action can be found in Figure 1-14.

Strontium renalate (SrR)

Strontium renalate is thought to decouple the process of bone remodelling, which reduces bone resorption and increases bone formation (Recker et al 2009). During a study conducted by Recker et al (2009) a small statistical significance was found with regard to bone formation. The mechanism by which SrR acts remains under investigation. It is postulated that it may replace Ca bone deposits (National Osteoporosis Society 2010). SrR is administered orally once daily in a 2 g/day sachet dissolved in water (Recker et al 2009). The absorption of SrR is significantly reduced by dairy products and other foods and is therefore recommended to be taken before bed at least 2 hours after eating (National Institute for Health and Clinical Excellence 2008).

Parathyroid hormone (PTH) and Teriparatide

Prior to the development of teriparatide [human recombinant PTH: PTH(1-34)], with the possible exception of SrR, osteoporosis treatment consisted of the aforementioned medications whose mode of action consists of reducing bone turnover by decreasing bone resorption. Teriparatide is a recombinant fragment of the parathyroid hormone which has been shown in both animal and human trials to act as an anabolic agent, increasing bone formation (Recker et al 2009) and reducing risk of fracture. Teriparatide is administered once daily by subcutaneous injection (Recker et al 2009). As many patients are unable to self inject the availability of the therapy only as a subcutaneous injection represents a huge limitation in the use of teriparatide. The treatment lasts for two years and is then usually followed by bisphosphonates or another antiresorptive agent, to reduce bone loss (National Osteoporosis Society 2010).

Oestrogen therapy (ET)/ Hormone Therapy (HT)

As detailed in section 1.2.4, oestrogen is an agonist with strong bone protection properties and hence reduces the rate of bone loss. Oestrogen also acts on receptors in both breast and uterine tissue, and is known to increase

the risk of breast and uterine carcinomas. Oestrogen also reduces LDL (low density lipoprotein) cholesterol levels which decreases the risk of coronary artery disease (Wood et al. 2003). While ET/HT remains an option for osteoporosis treatment, due to the risks associated with use it is not recommended as a primary therapy (Kanis et al. 1997). Other potential side effects include deep vein thrombosis. Common oestrogen agents used include Oestriol, oestradiol, ethinyl oestradiol and oestropipate. These are usually given either orally or trans-dermally via a patch. If the patient has not had a hysterectomy the oestrogen is given in combination with progesterone, although this does increase the risk of bleeding (Kloosterboer and Ederveen 2002).

Selective oestrogen receptor modulators (SERMs)

SERMs are molecules that can interact with the oestrogen receptors in different tissues, as either an oestrogen agonist or antagonist depending on the tissue type. In contrast to oestrogen, SERMs are not steroid based (Wood et al. 2003) and function via a different mode of action. The aim of SERMs is to reduce the negative effects on endometrium and breast tissues while increasing the positive effects on bone. Tamoxifen is a SERM used to treat breast cancer that works as an antagonist in breast tissue and has been observed to display partial agonist properties in bone tissue. Thus, tamoxifen administration as a treatment for breast cancer can also lead to a reduced rate of bone loss. Raloxifen is a SERM that has a similar mode of action to that of Tamoxifen, is licenced for the treatment of postmenopausal osteoporosis and has a recommended dosage of 60mg/day. Raloxifen has similar side effects to hormone replacement therapy (HRT) and is contraindicated for people with venous thromboembolism (VTE) and other conditions (National Institute for Health and Clinical Excellence 2008).

Antibody inhibitor

Denosumab is a human monoclonal antibody inhibitor of RANKL, a vital mediator in survival, function and differentiation of osteoclasts (Brown et al. 2009). Administration is typically via subcutaneous injection at 6 monthly intervals. Denosumab operates via a different mode of action to bisphosphonates (Figure 1-14). Bisphosphonates bind to the mineral content of

the bone and inhibit resorption by osteoclasts, Denosumab blocks RANKL resulting in a reduction of osteoclasts at the bone surface (Baron et al. 2011). Brown et al compared the effectiveness of weekly oral Alendronate and 6 monthly subcutaneous injections of Denosumab. They found Denosumab resulted in significantly higher increases in BMD and larger decreases in bone turnover than Alendronate (Brown et al. 2009; Kloosterboer and Ederveen 2002). Denosumab is only licenced for treatment of primary and secondary osteoporosis in postmenopausal women who are unable to tolerate other therapies due to the higher cost associated with use (National Institute for Health and Clinical Excellence 2010).

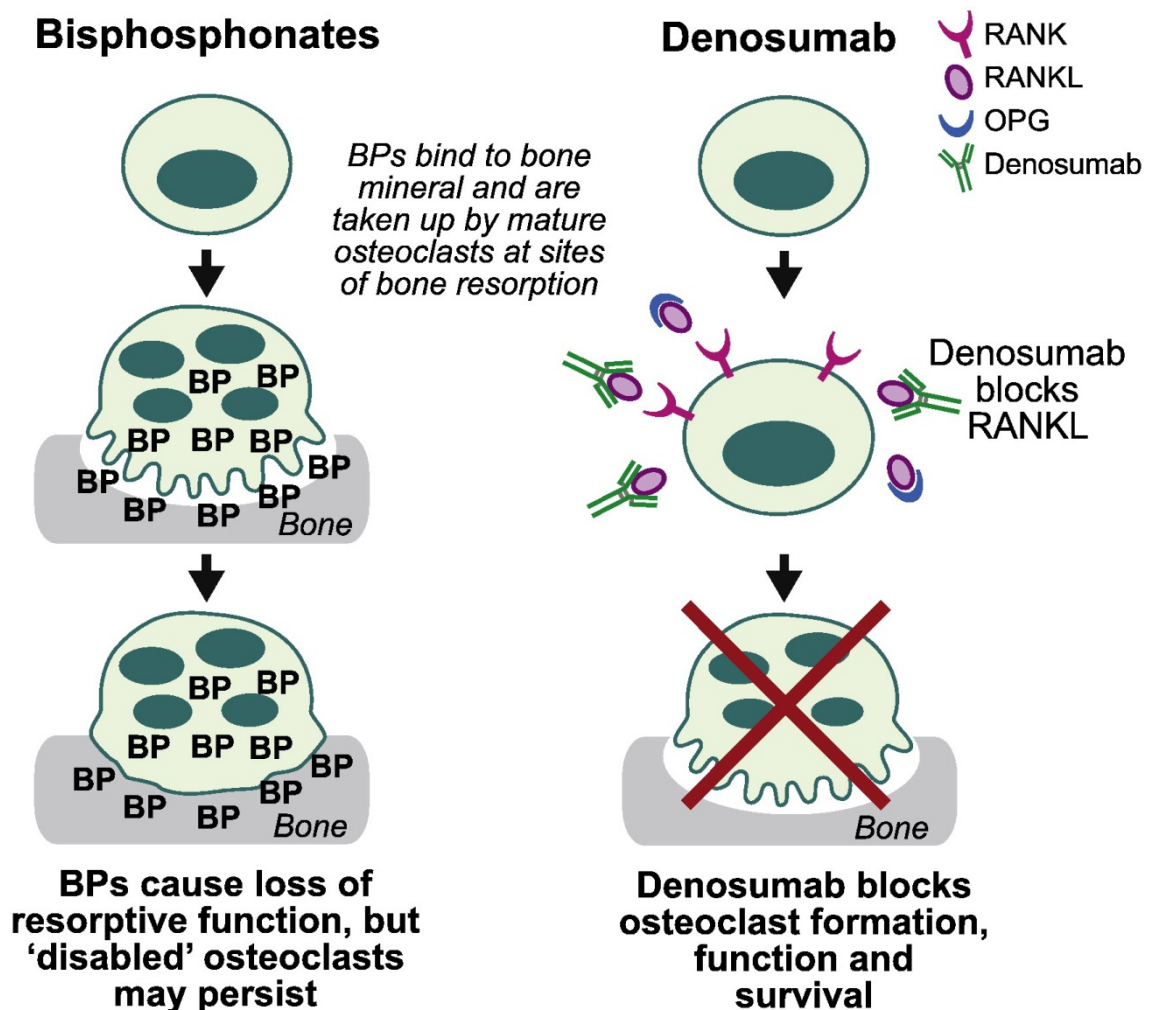


Figure 1-14 Osteoclast inhibition with denosumab vs bisphosphonates (BPs). OPG (osteoprotegerin). RANK (receptor activator of nuclear factor kappa-B). RANKL (receptor activator of nuclear factor kappa-B ligand) Baron et al. (2011).

1.2.6 Genetic influences

Many factors influence bone health and osteoporosis disease progression including diet, the presence of other diseases and lifestyle factors. Twin studies have shown that between 50 and 85% of variation in BMD can be attributed to hereditary influences (Ralston et al. 2010). The estimates of genetic determination of BMD in the hip and spine are higher than in the wrist (Ralston 2002). The influence of the genetic contribution to osteoporotic fractures decreases with age, as factors such as the likelihood of falling increase fracture risk (Ralston and Uitterlinden 2010). There are a large number of candidate genes that have an influence on the genetic component of osteoporosis making this a very complex problem.

1.2.7 Environmental influences

The interactions between genetic and environmental influences on bone are well documented. Cigarette smoking, alcohol consumption, poor nutrition, low body mass and an inactive lifestyle are all associated with low bone mass (Ralston et al. 2010). Cigarette smoking during pregnancy for example, has long been known to have detrimental effects on the child, for example an increased perinatal mortality of 28% and a reduced birth weight of 170g (Butler et al. 1972). With regards to BMD, Jones et al. found a significant decrease in BMD at the lumbar spine and femoral neck in eight year old male and female children whose mothers smoked during pregnancy compared to children whose mothers did not smoke during pregnancy (Jones et al. 1999). Harvey et al. also found that maternal smoking during pregnancy was independently associated with lower neonatal bone mass at birth (Harvey et al. 2010).

1.2.8 Dietary effects

There are many beneficial inorganic minerals, vitamins, and macronutrients that are essential for bone health at all stages of life. In particular, sufficient Ca intake, and Vit D intake or ultra-violet light exposure, are essential for bone (Office of the Surgeon General 2004). Adequate calcium intake in early life is essential for attainment of peak bone mass. A reduced intake of either Ca or Vit D reduces circulating ionised calcium (Ca^{2+}) and increases parathyroid hormone leading to secondary hyperparathyroidism which alters the

remodelling process of bone, leading to an increased risk of fracture due to a decrease in bone mass (Earl et al. 2010). In later life, Ca and Vit D intake decreases due to lack of appetite and reduced time spent outdoors (Earl et al. 2010) which impacts hugely on bone mass and risk of fracture. The recommended Ca and Vit D levels for patients at risk of fracture are 1000mg/day of calcium and 20µg of Vit D (Kanis 2010). Another important period for nutrition and bone health is in early development, from conception into childhood. Due to the rapid speed of growth during this time, inadequate maternal and offspring nutrition can lead to a reduced bone mass in children (Earl et al. 2010).

Protein makes up 50% of the bone volume and 33% of bone mass of bone and therefore adequate protein intake throughout life and especially during old age is very important. Due to the constant remodelling of bone, adequate protein intake on a daily basis is required for bone mass preservation (Earl et al. 2010). The recommended protein intake is 1g/kg of body weight (Kanis 2010). Using an ovariectomized rat model to mimic the effects of oestrogen loss during menopause, Ammann et al showed that a protein restricted diet lead to decreased BMD at the vertebra, femur and tibia (Ammann et al. 2002). However, addition of essential amino acids to the diet improved bone strength at the vertebra, femur and tibia.

The effect of the intrauterine environment, including maternal diet, in the development of osteoporosis in the offspring has been explored in both epidemiological and animal studies and shall be discussed later (Cooper et al. 2000, 2002; Hales et al. 2001; Lanham et al. 2008a, 2008b) see sections 1.7 and 1.8.

1.3 Developmental origins of health and disease (DOHaD)

1.3.1 DOHaD theory

The concept that the perinatal environment can influence disease susceptibility in later life is now referred to as the developmental origins of health and disease (DOHaD) theory. Small changes in an organism's environment during pregnancy and early life can have serious consequences on their susceptibility to chronic diseases, like coronary heart disease (Barker 1995), in later life.

The DOHaD concept evolved from an earlier concept, the fetal origins of adult disease (FOAD) proposed by Barker (Barker 1990). Following increasing evidence that it was not only the fetal stage where later disease susceptibility could be influenced, but from conception through to early childhood, the term 'development' was deemed more accurate. One of the first observations in the field was that individuals with low birth weight and poor growth in infancy were at increased risk of coronary heart disease and type 2 diabetes (Gluckman et al. 2006). This association between low birth weight and later disease risk has been studied and discussed frequently. One explanation of this observation is the 'thrifty phenotype' hypothesis which states that a fetus in a poor nutritional environment will make adaptations that aid its short term survival at the cost of its long term health (Hales et al. 1992). For example, somatic growth may be compromised in order for the fetus to survive, which could result in a phenotype that would be more prone to disease in later life (Hanson and Gluckman 2008). More recently, it has been postulated that the phenotype induced as a response to poor nutritional conditions might not always include a low birth weight. Less extreme nutritional challenges may produce an asymptomatic phenotype that still has structural differences from the norm. Birth weight is however a useful indicator and a viable variable to measure.

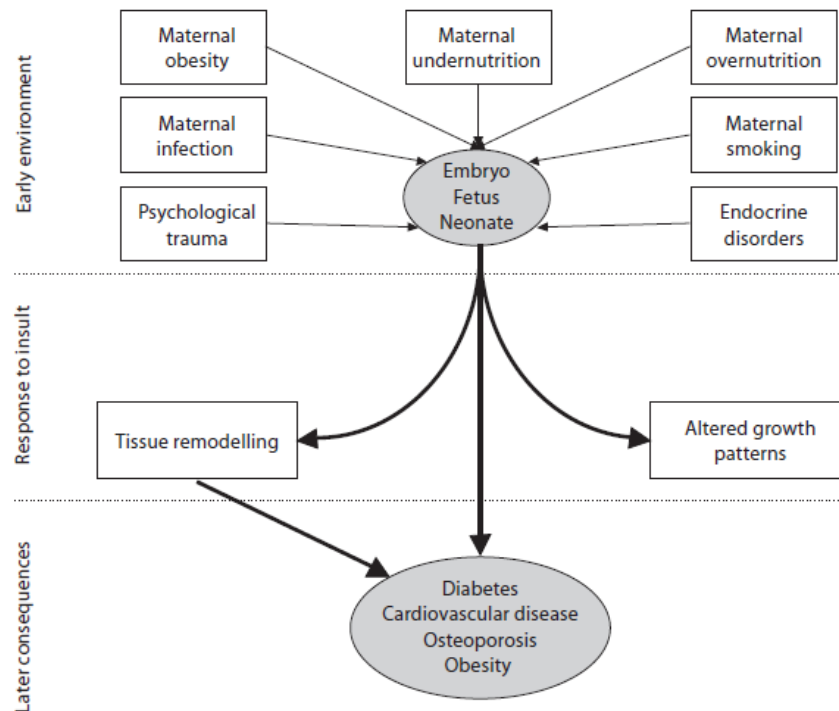


Figure 1-15 The fetal origins of adult disease hypothesis. Taken from Langley-Evans and McMullen (2010).

The DOHaD theory can be summarised by Figure 1-15 which shows some of the influences of the early life environment on the fetus, the responses to these and later life consequences (Langley-Evans and McMullen 2010). Signals from the mother about the adverse environment are passed to the fetus. If the conditions are severe this may lead to loss of the fetus. However, if the conditions permit the fetus may adopt adaptive responses to ensure survival. One potential response would be a decrease in growth that will consequently result in a lower birth weight. The predictive adaptive response may be tissue specific, or may involve other tissues or organs which will modify physiology and metabolism of the tissues or organs. The compromise for overcoming the adverse environment in fetal life could be increased risk of chronic disease in later life.

1.3.2 Epidemiological evidence

Epidemiological data have shown that early life events can influence the susceptibility in later life to chronic diseases, such as metabolic disease, cardiovascular disease, diabetes and osteoporosis (Gluckman et al. 2008; Barker 1995; McCance et al. 1994; Cooper et al. 2002). Barker et al. provided the early epidemiological evidence that supports this theory in connection to cardiovascular disease (Barker 1990). Infant mortality rates from 70 years previously were compared to death rates from myocardial infarctions in different geographical areas. Neonatal deaths were associated with areas that had high maternal death rates during childhood and low birth weights (Hales and Barker 2001). Also, 449 men and women over 50 in Preston had their blood pressure risk of hypertension compared to their birth weight and placental weight. Blood pressure and risk of hypertension taken together give a good estimate of the risk of developing cardiovascular disease (Barker and Osmond 1990). High blood pressure (hypertension) was associated with lower than expected birth weight, as predicted by placental weight. This indicates poor fetal growth as a possible consequence of insufficient maternal nutrition. The association between a low ponderal index (birth weight/length) and metabolic syndrome and type II diabetes in adulthood has been shown reproducibly in numerous different populations (Hales and Barker 2001). Assessing whether a newborn child has had restricted growth in utero is a very complicated process as there are many confounding variables. Birth weight and ponderal index are therefore used as a marker of restricted growth.

1.3.3 Developmental plasticity

The term developmental plasticity describes the ability of one genotype to produce multiple different phenotypes. Hence, allowing the organism to best prepare future generations for current environment conditions. The embryo, fetus, or child takes cues from its environment as to the predicted environment it will face in later life in order to have the highest chance of survival. Periods of transition from one life stage to another are highly plastic (Figure 1-16).

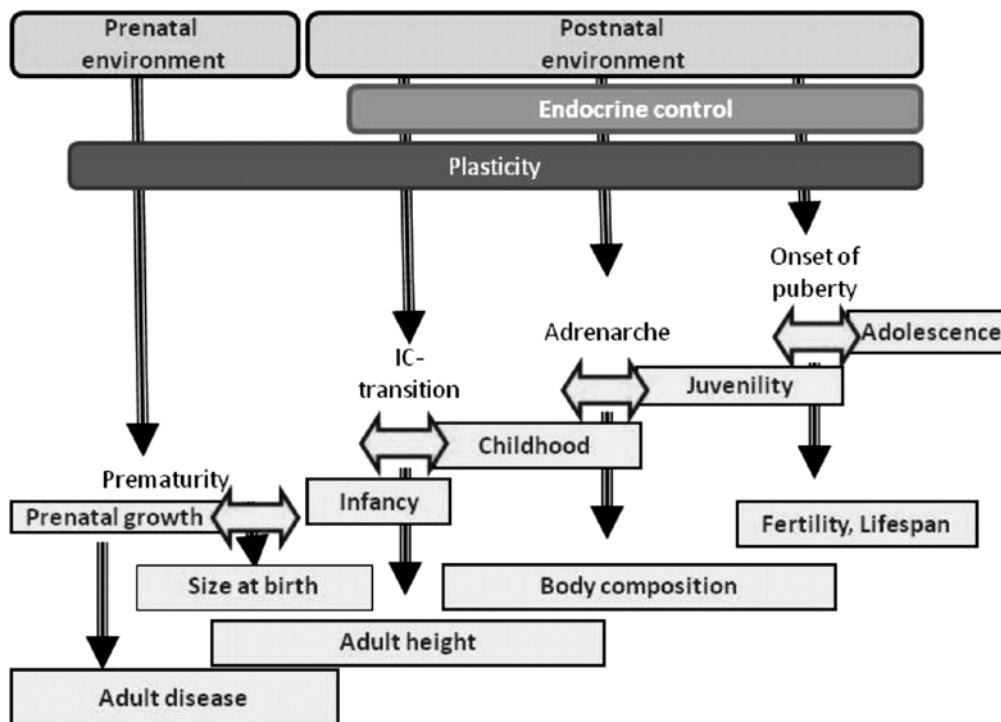


Figure 1-16 Pre-adult periods of adaptive plasticity (Hochberg et al. 2011). IC (infant to childhood transition).

Hochberg et al. describe how using the life-history evolutionary theory can be helpful in understanding growth and development in childhood (Hochberg et al. 2011). This is a very simplified diagram as the systems mentioned here are complex, but it can be used as a guide to intense periods of change. That is not to say that the outcomes of adult disease state, adult height etc. cannot be influenced during other time points merely that these time points are important. The transition from infancy to childhood (IC) determines a period of plasticity where adult height is particularly susceptible to change. Adult height is determined by a combination of bone growth velocity during multiple developmental stages and genetic factors. Similarly, the transition between childhood and the juvenile period confers an adaptive response that helps determine adult body composition and metabolic processes. Finally, the transition from the juvenile period to adolescence governs longevity and the age of reproduction and fertility. Environmental, endocrine and genetic variances during this plastic period all interact to predict the best possible phenotype for long term survival.

The method by which changes during periods of plasticity are enforced is via programming. Programming is defined as 'persisting changes in structure and

function caused by adverse environmental influences at a critical stage of early development' (Barker 1990).



Figure 1-17 A diagrammatical representation of the different factors affecting phenotypic programming (created by S Meakins).

More specifically, these periods of plasticity during perinatal life are influenced by environmental factors which induce epigenetic changes in the DNA through processes such as DNA methylation (see section 1.7). These changes are required to prepare for the expected environment throughout life (Lucas 1991). There is evidence that suggests once set, these epigenetic changes cannot easily be altered, and if mismatched to the environment encountered, can result in a less well adapted offspring and increased disease susceptibility in later life. The resultant phenotype is influenced by environmental factors, including epigenetic variance and environmental factors, as shown in Figure 1-17.

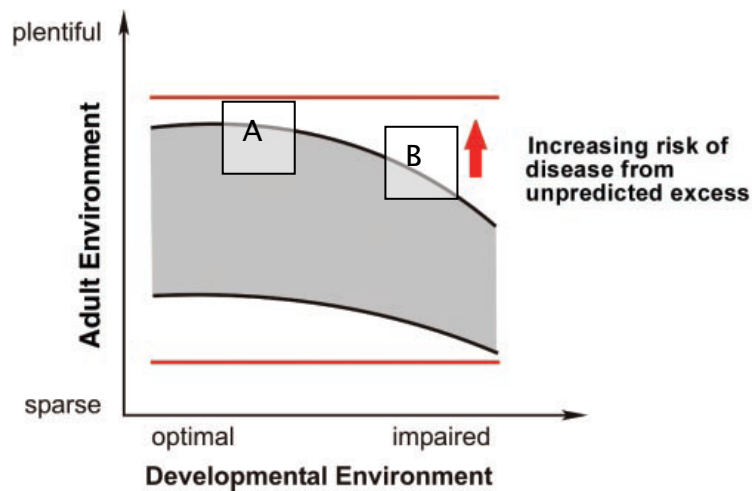


Figure 1-18 Predictive adaptive response (PAR)- red lines represent the potential nutritional environment that an organism could be exposed to. The grey area represents the zone of PARs that reduces disease risk. The risk of disease due to excessive nutrition increases if the level of developmental nutrition was low. Individual 'A' was exposed to a richer intrauterine environment than 'B' and so would cope better in an excessive nutritional environment than 'B', who is more likely to be at risk of disease. Adapted from Gluckman and Hanson (2004).

These differences in phenotype are called predictive adaptive responses (PARs). PARs are a response to the environment and are intended to help aid the survival of the offspring. They can be induced prenatally and in early life at critical periods of plasticity (Cooper et al. 2000; Lucas 1991). Figure 1-18 gives a diagrammatic representation of this theory showing two individuals, A and B and their predicted risk of disease. During intrauterine life, the signals received induce a developmental trajectory that cannot be altered and that holds influence from then onwards. If this trajectory is correct then the organism will have an increased chance of survival and the PARs are said to be appropriate. However, if there is a mismatch between the environment and PARs the organism's chances of survival are reduced (Figure 1-18). This holds for overnutrition as well as undernutrition if the PARs and encountered environment are different (see high fat diet discussion in sections 1.7.3.3 and 1.8.2).

In humans, epidemiological evidence suggests that apart from the effect of the maternal diet on the offspring, other factors can also have an effect on the intrauterine growth of the offspring and its birth weight and size, for example maternal fat stores, maternal smoking and season of birth (Cooper et al. 2002; Doblhammer and Vaupel 2001; Godfrey et al. 2001). Maternal smoking during pregnancy reduced birth weight by on average 170g (Barker 1990; Butler et al. 1972).

1.3.4 Window of opportunity

Different tissues and organs have different periods of plasticity in which they develop during fetal life. These periods of plasticity are called windows of opportunity. According to Barker these windows are different depending on the tissue (Barker 2007). This window of opportunity is the critical development period for the tissue concerned. Compromised development could lead to persistent impairment. Nutritional challenge during a critical period of developmental plasticity causes reduced potential total growth as a whole, and to a greater extent to those tissues whose critical developmental period is at the time of the nutritional challenge. If inadequate nutrition is given during a critical development period for a tissue or organ, this limits the potential growth of the tissue or organ. The potential growth then cannot be exceeded by catch up growth after the critical period for that tissue or organ has passed (Widdowson and McCance 1963). This means that the consequence of incorrect nutrition, even if only for a short time, can have profound effects in the long term.

1.4 Development and remodelling of bone

1.4.1 Processes of bone formation

Bone can be formed by one of two processes: endochondral ossification and intramembranous ossification. Bone produced from either type of ossification displays an indistinguishable structure after formation.

1.4.1.1 Endochondral ossification

Bone formation in long bones is mainly accounted for by endochondral ossification (Figure 1-19). Mesenchymal condensation results in cells that produce and maintain cartilage cells (chondrocytes). During primary ossification the chondrocytes at the centre of the new diaphysis enlarge and begin to produce alkaline phosphatase, an enzyme which is essential for bone mineralisation. As mineralisation occurs producing a bone collar, the chondrocytes undergo apoptosis, leaving a void in the centre of the shaft (Martini 2007). Blood vessels then surround the diaphysis and the outer layer is converted into a primitive form of bone. The perichondrium then progresses to form osteoblasts. Eventually vascularisation occurs and bone formation spreads towards the epiphysis. Growth then continues forming the medullary canal and growth plate. Secondary ossification produces bone within the epiphysis (Martini 2007).

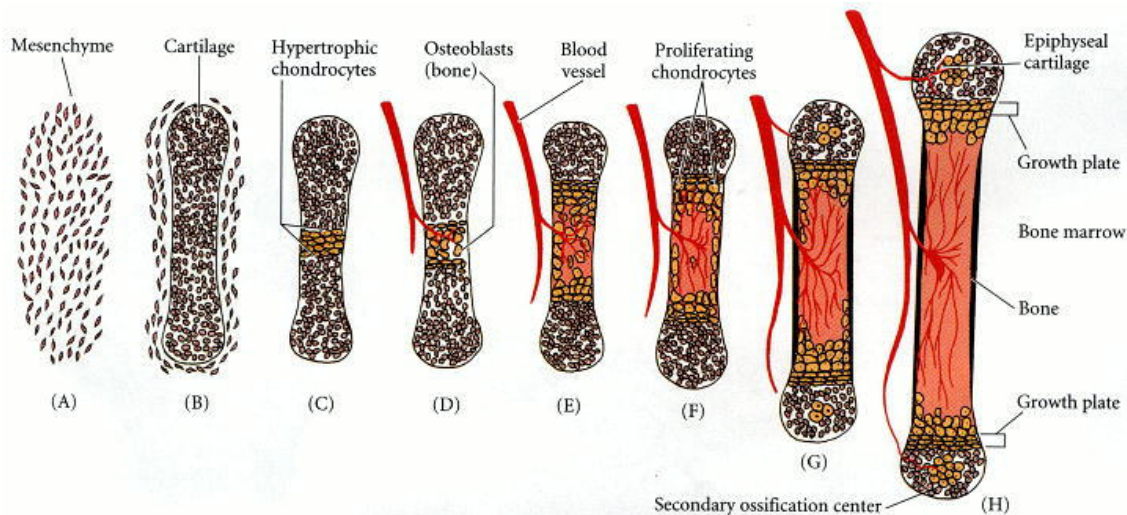


Figure 1-19 Schematic diagram of endochondral ossification. (A, B) Mesenchymal cells condense and differentiate into chondrocytes to form the cartilaginous model of the bone. (C) Chondrocytes in the centre of the shaft undergo hypertrophy and apoptosis while they change and mineralize their extracellular matrix. Their death allows blood vessels to enter. (D, E) Blood vessels bring in osteoblasts, which bind to the degenerating cartilaginous matrix and deposit bone matrix. (F-H) Bone formation and growth consist of ordered arrays of proliferating, hypertrophic, and mineralizing chondrocytes. Secondary ossification centres also form as blood vessels enter near the tips of the bone Gilbert (2000).

1.4.1.2 Intramembranous ossification

Intramembranous ossification occurs without the presence of cartilage. In intramembranous ossification bone develops straight from primitive mesenchyme tissue. Osteoblasts are produced from mesenchymal cells and produce osteoid matrix. In the calcified region, osteoblasts become trapped within the bone and become osteocytes (Figure 1-20) (Gilbert 2000). For example, fetal development of the clavicle and some flat bones in the skull are formed by intramembranous ossification. Fracture repair also progresses through this mechanism.

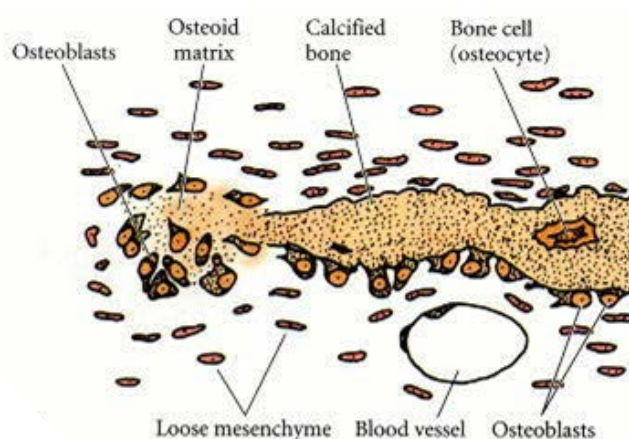


Figure 1-20 Schematic diagram of intramembranous ossification (Gilbert 2000).

1.4.2 Bone remodelling

Remodelling is a process whereby old bone is constantly being resorbed and new bone laid in its place, with approximately 10% of the skeleton being remodelled each year (Kanis 2010). There are four stages involved: resorption, reversal, formation and resting. The bone surface is lined with bone lining cells (Figure 1-20). When the preosteoclasts have been activated they differentiate into osteoclasts and the resorption stage occurs. As shown in Figure 1-21, the osteoclast moves over the bone creating an erosion cavity as it resorbs the matrix and mineral of the bone. In the reversal phase macrophages occupy the erosion cavity preparing it for osteoblasts to lay down new bone matrix. The signals that are transmitted by the osteoclasts regarding mechanical strain, are detected by the osteoblasts which migrate to the site of remodelling and in waves lay down new osteoid. This is mineralised to form new bone, and osteoblasts either become incorporated into the bone and differentiate into osteocytes or remain on the surface and become flattened bone lining cells, which remain on the surface of bone that is not being remodelled and may have a role to play in mechano-sensing in cortical bone (Mullender and Huiskies 1997).

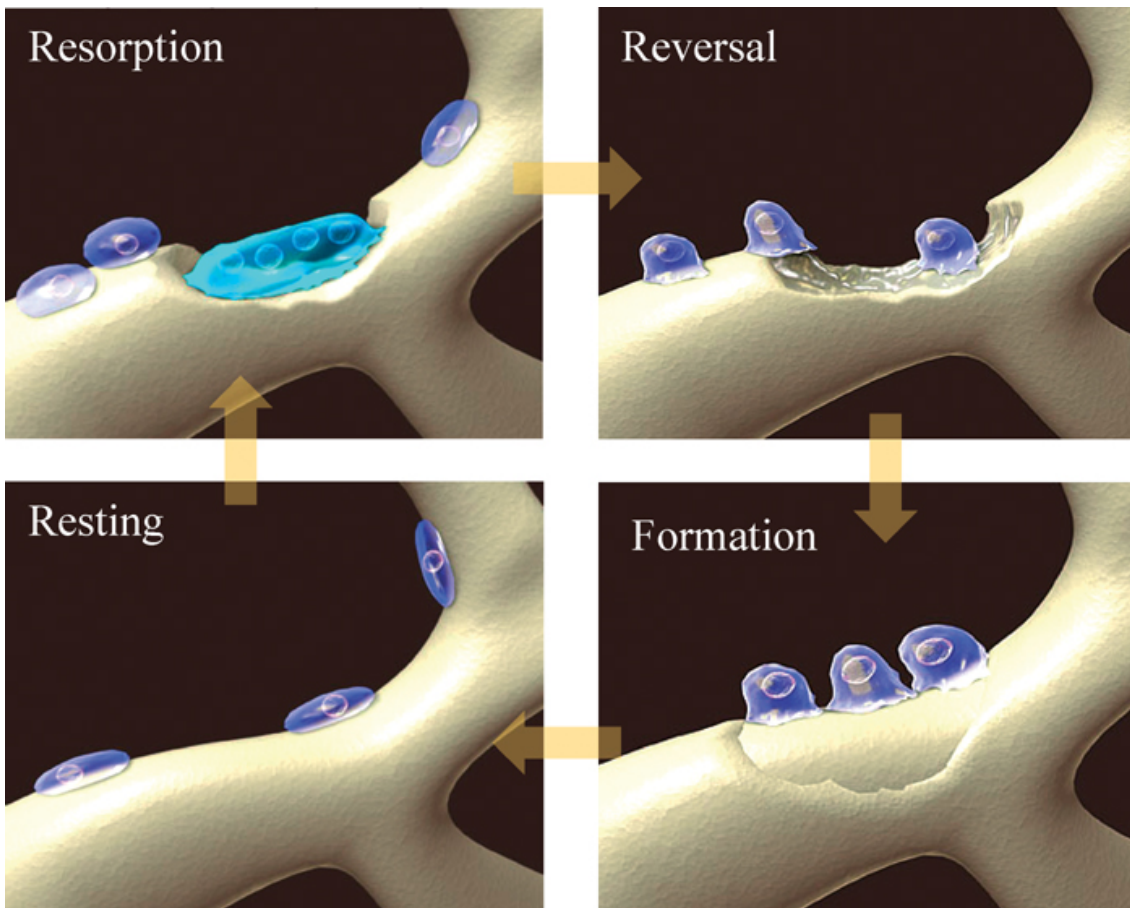


Figure 1-21 Bone remodelling (Coxon et al. 2004)

Mechanical stress influences the architecture of the bone indicating that bone remodelling is controlled locally with a process of cellular events (Hill 1998). If bone osteoclast and osteoblast activity are equal, net bone density stays constant.

1.4.3 Human skeletal development

As discussed in section 1.2.2 Bone health, the development and maturation of the skeleton after birth in humans can be divided into three periods: initially the growth period which lasts for the first 30 years after birth, when bone formation is more active than bone resorption. In this phase osteoblast activity dominates and new bone is laid down, leading to growth of the long bones from the growth plates, and hence more bone is formed than lost. Next, between the ages of approximately 30 and 50 years remodelling of the bone predominates. This is the desired state for adult bone. Finally, after about 50 years this modelling process begins to fail and more bone is removed than is

replaced (osteoblast activity is lower than osteoclast activity). As previously stated, total bone mass in postmenopausal women predominately the trabecular bone mass, decreases year after year (Bilezikian et al. 2009). Decreasing bone mass with age is a normal process; however environmental factors and genetic factors can influence the rate of bone loss, both in adulthood and in early life.

Epiphyseal plate fusion in humans is complete in most long bones by the age of 20 (Ralston 2012). Peak bone mass is reached by the age of approximately 30 in humans (Heaney et al. 2000).

1.5 Perinatal growth and nutrition

1.5.1 Effect of nutrition on embryonic and fetal growth

Growth in utero is rapid and specific in both humans and animals. The embryonic period in humans is from conception to pre natal week eight. During this time the initial architecture of the body is laid down. The organs and tissues are defined from week nine and grow rapidly onwards during the fetal stage in humans. This time is particularly important in terms of nutrition. With such intense growth, inadequate nutrition can lead to retarded growth and small size at birth. However, this is not the only consequence. Sacrifices for short term survival over long term health can be made, leaving chronic disease more likely in later life (Gluckman et al. 2008). Due to the difficulties in comparing one woman's nutritional intake with another, most of the data on the effects of maternal nutrition have been conducted using animal models.

Supplements are recommended in order to ensure adequate nutrition during pregnancy. Folic acid supplementation during pregnancy reduces neural tube defects (NTDs). NTDs are formed when the neural tube does not close properly during embryogenesis, leaving nerve and brain tissue exposed. The rate of NTD occurrence varies with geographic location. Ireland and Scotland have the highest rates of NTD in the Western world with a frequency of approximately 10 per 1000 births (Pitkin 2007). The recommended levels for folic acid supplementation are 0.4mg for all women who could potentially bear children and 4mg for women who have previously have a NTD pregnancy (Wald 1991). Other studies suggest a supplementation of 5mg for all women could reduce NTD by an extra 50%, compared to a 0.4mg supplementation (Wald et al. 2001). Folic acid is now fortified into cereals, bread and other grain products in the UK because of its importance as a methyl donor during pregnancy.

It has been shown that nutrition can affect bone development and subsequent bone health (Ammann et al. 2002; Tobias et al. 2005). There are critical periods in development where boundaries of maximum potential growth are set and this also applies to bone. During the fetal period rapid cell division occurs in tissues and growth can be stunted by undernutrition at this time (Gluckman et al. 2008). There are substantial amounts of epidemiological evidence linking gestational and postnatal undernutrition with increased

chronic disease in later life. An epidemiological example would be the study of the Dutch hunger winter which showed that people who are exposed to famine during their late gestation are born small, remain small and have lower obesity rates than people born after the famine (Schulz 2010). Those exposed during early pregnancy experienced high rates of obesity and cardiovascular disease in later life. Furthermore, the Dutch hunger winter highlighted the importance of gestational nutritional restriction timing on disease outcomes in later life.

1.5.2 Nutritional influences during pregnancy on fetal bone

Due to the rate and intensity of growth during gestation, maternal dietary content is very important. The dietary factors likely to influence fetal bone development include Ca and Vit D and protein nutrition. More evidence is needed to verify this association in humans. Low maternal Ca intake during pregnancy may influence fetal bone development. The human fetus requires 30g of Ca during gestation; most of this is acquired in the last trimester by active transport across the placenta. The concentration of Ca content in the fetus is higher than in the mother leading to a concentration gradient. An insufficient amount of Ca in the maternal diet may result in low Ca available to the fetus. A study involving healthy mothers supplemented with at least 2g per day of Ca during the last two trimesters showed an association with increased fetal bone mineralization, for women whose dietary intake of Ca was low. Giving supplementation to women who have an adequate dietary calcium intake would be of little benefit to the total fetal bone mineralization (Koo et al. 1999). This does however show that during the third trimester nutrition is important in fetal bone development. Maternal diet during pregnancy and bone mass of the offspring aged 9, was assessed by the Avon Longitudinal Study of Parents and Children (Tobias et al. 2005). Tobias et al. found an association between the magnesium (Mg) intake in the maternal diet and the total body BMC (bone mineral content) and BMD of the children. It is unclear how maternal Mg intake affects bone development: but it maybe that the Mg and Ca compete for Ca receptor binding, leading to lower parathyroid hormone secretion (Tobias et al. 2004; Tobias et al. 2005).

1.6 Epigenetics and cellular programming

1.6.1 Epigenetics

Epigenetics is described as ‘molecular mechanisms that establish and maintain mitotically stable patterns of gene expression, but that do not alter the genomic DNA sequence’ (Gluckman et al. 2009). Modification of the genome in this way allows an organism to produce different phenotypes from the same genotype. Among other things, it is the means by which developmental plasticity is progressed. The trajectory established in intrauterine life is marked out using epigenetics. Two of the main mechanisms that epigenetic changes are induced by are histone modifications and DNA methylation (Figure 1-22).

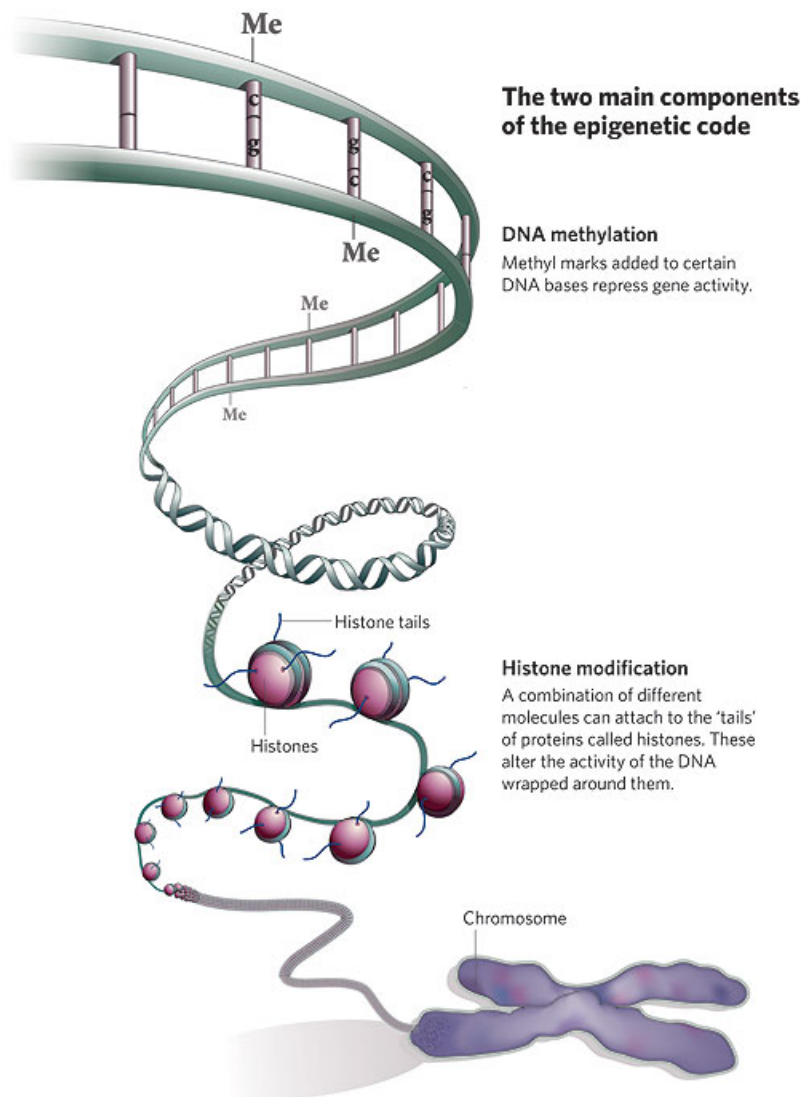


Figure 1-22 Epigenetics- Two primary processes in epigenetic modification: DNA methylation and histone modification

<http://neuroanthropology.files.wordpress.com/2008/07/epigenetics.jpg>

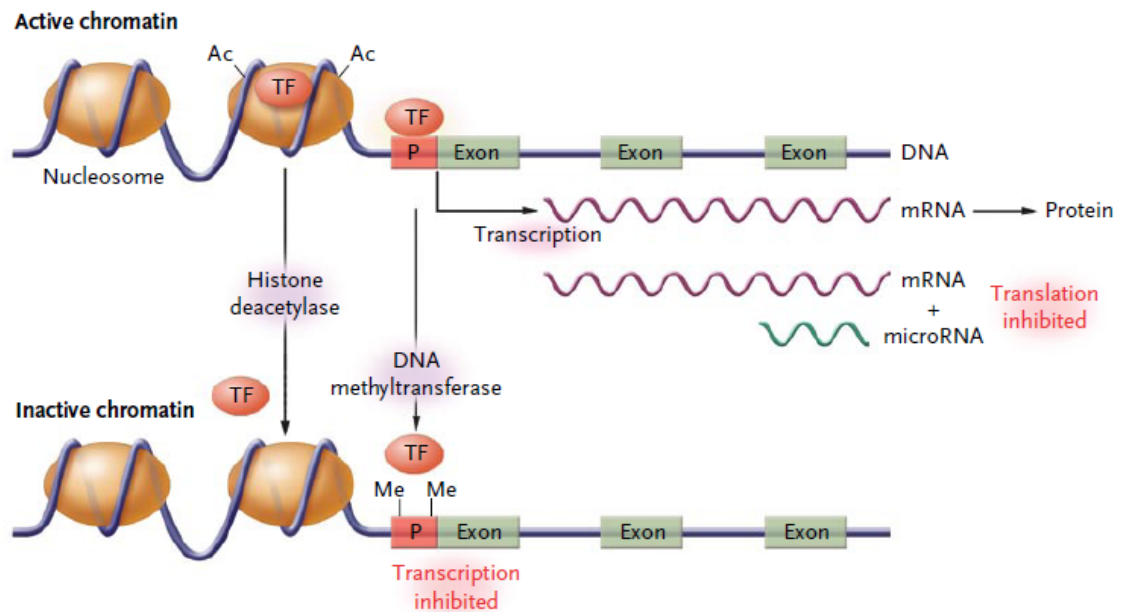


Figure 1-23 Adapted from Gluckman (2008) detailing gene expression regulation through epigenetic processes.

Figure 1-23 describes how the epigenetic modification of the DNA, either through histone modification or DNA methylation, influences gene expression by controlling transcription factor (TF) access to the DNA and hence dictating the rate of mRNA transcription. Active chromatin can be determined by the presence of acetyl (Ac) groups on lysine residues on the surface of the histone nucleosome. The presence of the lysine residues reduced the binding affinity of the DNA to the histone and therefore this allows TF access and subsequent translation. Another feature of active chromatin is that CpG sites on the promoter regions are generally unmethylated which allows easy access for TFs. Conversely, inactive chromatin lacks Ac groups, leading to a tightly packed DNA structure which hinders TF access and increased CpG site methylation at the promoter. This obstructs TF binding and translation. Finally a third method of epigenetic control is found at the microRNA level. microRNAs are short RNA sequences that are complementary to the 3' end of mRNA sequences and upon binding reduce the rate of RNA translation, again reducing the level of expression. It is with control of these three mechanisms that epigenetics can regulate protein expression of the genome (Gluckman et al. 2008).

Dietary folic acid is known to act as a methyl donor that is important in many processes including synthesis of DNA, protein synthesis and cell membrane biosynthesis (Giudicelli et al. 2013). Using the one-carbon metabolic pathway,

folic acid provides methyl groups for DNA methylation and therefore is important in epigenetic regulation of gene expression.

1.6.2 Skeletal programming

Cooper et al. investigated skeletal programming and the associated impact on osteoporosis risk in later life (Cooper et al. 2000). Structural differences as a result of programming are present throughout life, however the phenotype will not manifest until later in life in the case here of osteoporosis. Initially during early life, no phenotypic difference will be seen as a result of the different nutritional conditions. If the cellular level or epigenetic status of the bone were examined, then a difference may be detected. If a fetus has encountered a challenging nutritional environment in its intrauterine life, epigenetic differences in its epigenome will have been induced that lead to bone formation progressing to aid its short term survival (due to the limited resources). These differences will only be noticeable when age related bone loss takes hold, and the structurally inferior bones succumb to fracture. Differences have been found in the rates of bone loss, differences in bone mass, different proportions of adipose cells in the bone, decreased cortical bone thickness or connectivity of the microarchitecture of the trabecular bone, induced by intrauterine nutritional challenges compared to controls. This has been shown in both human epidemiological studies and animal studies (Cooper et al. 2000; Lanham et al. 2008a, 2008b; Tobias et al. 2005).

1.7 Intrauterine environment and osteoporosis

It is well established that nutrition impacts on health. The human body requires the right balance of carbohydrates, protein and fats, as well as adequate vitamins and minerals in order to build and maintain healthy organs. The demand for each of these components of diet changes with each stage of life so appropriate diet at each stage is important. Diet is particularly important during early development where nutritional needs due to rapid growth are different to that of an adult. Epidemiological research has shown us that nutrition throughout life impacts on bone health. It is well known that Ca and Vit D are important for bone health and there is now mounting evidence that the protein content of the diet and Vitamin K intake are also important (Ammann et al. 2002; Weber 2001). The significance of Ca intake during childhood is well established but skeletal development starts in utero. Now there is evidence that the maternal diet during pregnancy has an effect on the long-term bone health of the offspring. Animal studies have been used to show that an alteration in just the maternal diet can alter the bone structure of the offspring by changing the subsequent bone microarchitecture (Lanham et al. 2008b; Lanham et al. 2009; Romano et al. 2009).

Changes in microarchitecture induced by maternal nutritional challenge result in a structure similar to osteoporotic bone, which is thought to predispose the bone to fracture in later life.

1.7.1 Epidemiological evidence

There are epidemiological studies linking birth weight or childhood growth to bone mass, and thus fracture risk, in later in life. Cohorts in Bath and Hertfordshire have shown that weight at one year is associated with BMC in later life (Cooper et al. 1997). Cooper et al. conducted DEXA scans, serum osteocalcin and urinary type 1 collagen cross linked N-telopeptide measurements on 224 women and 189 men aged 63-73 years. There was found to be a statically significant relationship between BMC and weight at 1 year at the spine and femoral neck for women and at the spine for men (Cooper et al. 1997). A unique cohort from Helsinki provided an opportunity to look at 112 subjects who had sustained hip fractures and who had accurate birth records and on average 10 measurements of height and weight

throughout childhood. It was determined that the two major factors evident from this study to contribute to fracture risk were tall maternal height and low rate of childhood growth (Cooper et al. 2001).

Factors that have been shown to influence neonatal and childhood bone mass in humans include low maternal birth weight, maternal smoking in late pregnancy, low maternal fat stores and last-trimester vigorous exercise. They all predict lower whole-body BMC in the neonate (measured by DEXA after birth) (Barker 1990; Godfrey et al. 2001). Women with lower than normal fat stores during pregnancy have children with lower BMD and BMC compared to women with higher fat stores (Godfrey et al. 2001). Women who smoke have been shown to have children with a lower birth weight and lower BMD and BMC (Bernstein et al. 2000; Godfrey et al. 2001). Other studies using human models to assess the effect of nutrition on bone structure include, for example, Cole et al. who showed that a high prudence diet (containing fruit, vegetable and wholegrain foods and not containing processed foods) during pregnancy increased whole body and lumbar spine BMD and BMC in 9 year old children (Cole et al. 2009). Harvey et al. showed that factors other than maternal nutrition during pregnancy can be used to predict fetal whole body bone area (BA) such as maternal parity, late pregnancy triceps skinfold thickness and late pregnancy walking speed (Harvey et al. 2010). No studies investigating the effects of protein intake during pregnancy on the child's subsequent bone structure are present at this time.

1.7.2 Animal studies

1.7.2.1 Total nutrient restriction

Animal studies have long been used to investigate bone development. A rat model was used by Widdowson et al. to show that under nutrition during weaning had a long term effect on the animal's size (Widdowson and McCance 1963). Romano et al. showed that total nutritional restriction (using a bilateral uterine vessel ligation surgery) during pregnancy in rats resulted in decreased BMC and bone strength in offspring at 6 months of age (Romano et al. 2009).

1.7.2.2 Maternal protein restriction and bone

Small changes in maternal dietary composition during pregnancy have been shown to change the structure and quality of the offspring's bone, via in utero programming. A well known model used in order to investigate a under nutritional environment is maternal protein restriction during pregnancy. Lanham et al. gave a relatively mild isocaloric protein restriction diet (18% control and 9% protein restricted) to Wistar rats during pregnancy (Lanham et al. 2008b). The offspring, all kept on a control diet, were then studied at 4, 8, 12, 16, 20, 47 and 75 weeks of age. It was found that maternal protein restriction did not affect the anthropometric length of the femurs and tibias of the offspring rats. However, it did cause changes in the microarchitecture of the trabeculae: reduced thickness and density of the trabecular bone in the femoral head, closer packed trabeculae in the femoral neck and thicker, denser vertebral trabeculae at 75 weeks. The tibial midshaft cortical bone was also noted to be thicker. Mechanical testing showed that maternal protein restriction increased the structural strength of the femoral neck and vertebra and decreased the structural strength of the femoral heads and tibial midshafts. Overall Lanham et al. concluded that maternal protein restriction lead to site specific differences in bone structure in 75 week female offspring were found with both favourable and undesired structural consequences depending on the site being investigated. These findings support the idea that small alterations in maternal diet composition can change the resulting bone structure and bone density of the offspring and consequently highlights the need to understand the influences that early life factors can have on long term bone health. It shows that even with alterations in protein restriction while maintaining an isocaloric diet, the tissue being examined is structurally and biologically different (Lanham et al. 2008a, 2008b).

1.7.2.3 Maternal high fat and bone

Maternal protein restriction in rodents is used to model undernutrition during pregnancy. Therefore further to this maternal high fat was investigated in order to model an over nutritional environment. This is of particular importance due to the increased rate of obesity in the developed world. Lanham et al. investigated if differences in maternal and offspring dietary fat content were demonstrated to affect the bone structure of the offspring

(Lanham et al. 2009). Mouse dam offspring were fed either lifetime high fat or a standard chow diet. The femurs were removed and the adiposity, strength and bone structure were analysed. There was found to be higher adiposity in the femurs of the offspring from high fat dams and the female offspring from high fat dams had different trabecular structure at the femur.

1.7.2.4 Evaluation of animal models

Animal studies are commonly used to model human disease states in a controlled environment and often for a much shorter time scale than human studies. Using animal models is however not without its limitations, but it is accepted that some parallels can be drawn between animal models and humans. In general the larger the animal, the more similarities can be drawn between the bone structure of the animal and humans. However, quadrupeds will have very different load on their joints than humans; specifically the hip joint is loaded at a significantly different angle. This limits the extent to which the findings of animal studies can be applied to humans, especially when the proximal femur is one area commonly studied in osteoporosis research in humans. Bone growth and development is different between species, and larger animals have bone growth and development processes similar to our own, but it takes longer to acquire the samples and is more costly. As long as these limitations are taken into consideration, animal research does provide a quick and informative method to gather evidence about the long term effects of nutrition on bone structure and quality.

Rat skeletal development has similarities to human skeletal development that make it a useful model for studying osteoporosis. In the rat, long bone growth is similar to humans and progresses through endochondral ossification. However, contrary to human development growth plates do not fuse around peak bone mass at 40 weeks of age in rats (Jee and Yao 2001) and some bone, for instance many of the long bones in male rats continue to grow until 30 months (Lelovas et al. 2008) and the female lumbar vertebrae continue to grow for 21 months.

1.8 Intrauterine environment effects on other tissues

Intrauterine programming has been shown to affect many tissues as discussed in section 1.3.2. Both maternal low protein and maternal high fat studies have been conducted in order to investigate tissues and related diseases such as hypertension, diabetes, and fatty liver disease. These tissues were chosen in order to further investigate the chronic non communicable diseases investigated by epidemiological DOHaD research.

1.8.1 Maternal protein restriction and other tissues

As mentioned in section 1.7.3.2 maternal protein restriction has been used extensively to investigate intrauterine programming of a variety of tissues. Lillycrop et al. showed that folic acid addition reverses the negative effects of protein restriction during pregnancy on hepatic gene expression in the liver, in a Wistar rat model (Lillycrop et al. 2005). More specifically PPAR (peroxisomal proliferator-activated receptor) gene methylation was 20.6% lower and expression 10.5-fold higher in PR offspring compared with control offspring. Glucocorticoid receptor (GR) gene methylation was 22.8% lower and expression 200% higher in PR offspring compared with controls. Maternal protein restriction in rats was found by Woods et al. to impair renal development and to programme adult hypertension in later life (Woods et al. 2001). Fernandez-Twinn et al. showed that protein restriction during gestation resulted in increased insulin resistance and risk of type II diabetes in later life (Fernandez-Twinn et al. 2005). Maternal protein restriction during pregnancy may also affect fetal brain by inducing alterations in maternal liver metabolism, as shown by Torrens et al. (2010). In order to investigate if a smaller window of intervention leads to an adapted phenotype Watkins et al. investigated protein restriction during just the implantation stage. Using a mouse model Watkins gave a maternal low protein diet during the periconception period. This increased the offspring's chances of developing cardiovascular disease and metabolic syndrome at 1 year (Watkins et al. 2011). This further highlights the significant effects of protein restriction on rodent development. Differences in phenotype were observed depending on the time point of the low protein diet. A protein restricted diet was administered either during oocyte maturation (3.5 days before mating), preimplantation (3.5 days after mating) or throughout

gestation. All three offspring groups showed decreased body weight and increased systolic blood pressure relative to controls. In all these studies there is strong evidence that protein restriction during pregnancy has persistent and detrimental effects in rodent models on a variety of tissues.

1.8.2 Maternal high fat and other tissues

As previously mentioned, in order to investigate an overnutritional environment maternal high fat diet studies were conducted. Bruce et al. used a mouse maternal high fat model to investigate non-alcoholic fatty liver disease (NAFLD), metabolic syndrome and obesity (Bruce et al. 2009). From a month before conception until after lactation mothers were fed either a control (C) diet or high fat (HF) diet. Offspring were then assigned to either a C or HF diet, resulting in the following groups C/C, C/HF, HF/C and HF/HF. At 30 weeks the Kleiner scoring and histological analysis concluded that the C/HF and HF/C groups both showed signs of NAFLD and the HF/HF groups showed the most severe signs. Thus, exposure to HF during pregnancy and early life affects a rodent's likelihood of developing NAFLD in later life. Torrens et al. later showed in a mouse model in male offspring that a high fat diet preconception, throughout gestation and lactation leads to increased body weight and systolic blood pressure (Torrens et al. 2012). This disadvantageous phenotype is likely to increase the risk of obesity in later life.

1.9 Conclusions

As osteoporotic fractures increase with age, the ageing demographic in the UK means that research in this area is crucial. There are numerous serious socioeconomic implications of having both an ageing population and a population with increasingly poor diet that is going to require more medical treatment as time progresses. There is considerable evidence to suggest that perinatal nutritional conditions programme skeletal development and structure, and hence influence bone structure and fracture risk in later life. Influencing how the public think of nutrition, especially during pregnancy and early life can have influences on the future rates of osteoporosis and other chronic diseases. Education about appropriate nutrition throughout life is important for chronic disease prevention in later generations. Perinatal nutrition offers the unique opportunity to impact life-long health, influence during this relatively short time can have such a fundamental effect on later life disease states.

If due to poor nutrition in utero there is a mismatch between the PARs and the encountered environment, this can lead to a less well adapted individual that is at greater risk of osteoporosis and fracture in later life. Research into the genetic and epigenetic mechanisms of this are being conducted as a greater understanding of the effects and mechanisms involved in the alteration of the epigenome during perinatal life, under different conditions and its influence on bone development. The findings from these investigations progress our understanding of bone development and its later influence of long term structure.

Aim

The two aims of this study are 1. To investigate the effects of protein restriction during pregnancy on young adult rats and the influence of additional juvenile folic acid, 2. To investigate the effects of maternal protein restriction on subsequent generations of young adult rats up to F3.

Hypothesis

Folic acid addition to juvenile offspring from protein restricted dams improves bone structure and mechanical properties compared to offspring from protein

restricted dams without folic acid addition. Protein restriction during F0 pregnancy reduces bone quality and mechanical properties in F1 and F2, but not F3 offspring

2. General methods

2.1 Anthropometric analysis

2.1.1 Measurements

The longitudinal measurements of the right femur were conducted using digital callipers (Mitutoyo Absolute Digimatic, Mitutoyo (UK) Ltd, Andover, UK).

2.2 Histology

2.2.1 Sample fixation and decalcification

Femurs for histological analysis were fixed after dissection in 4% (w/v) formaldehyde solution. The samples were washed in phosphate buffered saline and put into 5% ethylenediaminetetraacetic acid (EDTA) (w/v) solution with 0.1M Tris base pH 7.3. Samples were then placed on a gyro rocker at 4°C to aid demineralisation. X-ray images were taken on a Faxitron MX20 (Faxitron Bioptics, Tucson, Arizona, USA) over time to follow demineralisation. The EDTA solution was changed twice weekly for between 8 and 10 weeks until demineralisation occurred, evidenced by X-ray image analysis. Images were taken with the voltage 26kV and the exposure time 20 sec. Images were saved as .jpeg files. Representative images are displayed in Figure 2-1.

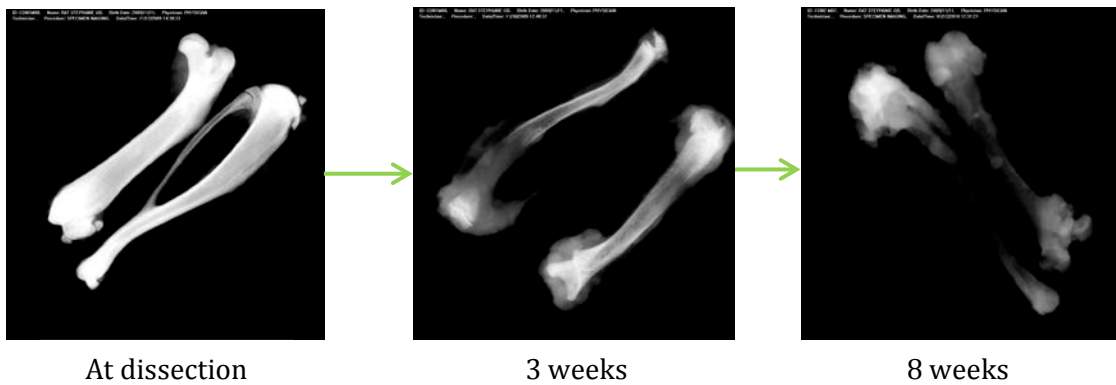


Figure 2-1 X-ray images of the same femur and tibia at different stages of demineralisation. Fully mineralised on the left through to demineralised on the right.

2.2.2 Processing and embedding

Femurs were divided into both transverse and longitudinal portions, and placed into labelled processing cassettes in PBS. The Shanden Citadel 2000 processing machine (Thermo Fisher Scientific, Leicestershire, UK) was used to process all samples. Samples were taken through a series of solutions (PBS 30 minutes, 50% ethanol 2 hours, 90% ethanol 2 hours, 100% ethanol 2 hours, 100% ethanol 2 hours, chloroform 2 hours, Chloroform 2 hours, Paraffin wax 2 hours, Paraffin wax 2 hours) before being embedded in molten paraffin wax using a Raymond A Lamb Blockmaster III embedding machine (Raymond A Lamb, London, UK).

Two distal and two proximal paraffin blocks were obtained from each femur with longitudinal sections of the femur and a transverse section of the diaphysis.

2.2.3 Cutting sections

Blocks were cut into 7 μ m sections on a Microm Heidelberg HM330 microtome (Microm International Gmb, Walldorf, Germany) to procure. Sections were placed onto glass slides and labelled. The slides were dried and stored at -4°C.

2.2.4 Alcian Blue Sirius Red staining

Slides were selected and stained for collagen using Alcian blue and bone using Sirius red. Slides were then de-waxed in histoclear and rehydrated through a series of methanol concentrations from 100%-50%. Weigert's Haematoxylin A and B solutions were then used to stain the cell nuclei. Slides were then rinsed in an acid alcohol solution (1% HCl and 50% methanol), stained with Alcian blue, then molybdophosphoric acid and finally Sirius red. Finally, the slides were dehydrated through graded methanols (50%-100%) and then histoclear. Cover slips were mounted on the slides using DPX mountant.

2.2.5 Section analysis

Three distal femur samples from each female group were sectioned and stained with haematoxylin (to stain cell nuclei), Alcian Blue (to stain for cartilage matrix proteoglycans) and Sirius red (to stain for bone matrix collagen) in order to compare the samples a qualitative analysis of the cortical and trabecular bone and growth plates was performed. As changes have previously been seen primarily in female offspring (Lanham et al. 2008), only female samples were analysed in this study.

2.3 Micro computed tomography (μ CT) data

The two scanners used in the project were designed for different purposes. The SkyScan1176 scanner was designed for scanning a high throughput of small lab animals at fixed resolutions in order to study biological tissues. The X-Tek HMX scanner was originally designed for scanning engineering material samples at high resolution for example in order to detect small fractures in the material of interest. The HMX is very capable of scanning rat bones as described here, however the subsequent analysis of the data is better formatted from the SkyScan machine. For this reason the HMX machine was no longer used in the project once the SkyScan machine was made available.

2.3.1 SkyScan1176 scanning and reconstruction

Samples were scanned using the SkyScan1176 in-vivo μ CT (Brucker-MicroCT, Kontich, Belgium). The resolution of samples was set at 18 μ m, a frame averaging of four was employed together with a filter of 1 mm copper and aluminium (used to set the μ A and kV), a rotation step of 0.4° and a rotation angle of 360° were also selected. Scans were reconstructed with NRecon using a smoothing of 2, automatic misalignment compensation, object larger than field of view, ring artifacts reduction of 5 and 40% beam-hardening correction. The dynamic range was set to 0-0.035 for all scans and exported as a .bmp file 8bit.

2.3.2 X-Tek HMX scanning and reconstruction

Samples were scanned on the X-Tek HMX μ CT (Nikon Metrology UK Ltd, Tring, UK) at 60kV, 120 μ A and 23.7 μ m resolution, using a molybdenum target. Images were taken at 1415ms exposure, 1 frame averaging, 2000 projections (over 360°), 1x binning and 2xdigital gain. The panel used was a Perkin Elmer XRD 1621 AN3 HS detector panel. All scans were reconstructed using CTPro version 2.2 (Nikon Metrology) at 100% quality resulting in 23.7 μ m resolution. A beam hardening 5 was selected using appropriate hydroxyapatite standards. Noise reduction 1 was selected to give the best signal to noise ratio. A water image was entered into CTPro to calibrate all voxels into Hounsfield units.

Reconstructed volume images were opened in VGStudio Max 2.1 software (Volume Graphics GmbH, Heidelberg, Germany). All the voxels that formed the structure were assigned Hounsfield units automatically. Each femur was then exported as a .bmp file stack in the transaxial orientation.

2.3.3 X-Tek HMX scans: trabecular bone analysis

Bruker software including Data Viewer and CTAn, were used to analyse the trabecular cuboids within the femoral head, femoral neck and distal femur. The .bmp stack was loaded into CTAn and the resolution was corrected to 23.7 μm . For sites such as the distal femur the region of interest (ROI) started when the desired trabecular bone was approximately 50% of the total bone on that slice i.e. in the middle of the knee joint. Each of the trabecular cuboids were selected at the same point and had a predefined size as described below. The optimum size for each cuboid was selected to be the largest area of trabecular bone that could be segmented from all samples without any cortical bone present. Illustrations provided in Chapter 3 section 3.2.1.

Sites

- Femoral head 2.3mm x 2.3mm x 20 slices
- Femoral neck 1.2mm x 1.2mm x 10 slices
- Distal femur 3.0mm x 3.0mm x 60 slices

Datasets and ROIs were loaded into Batch Manager (BatMan) in CTAn and a custom processing task list was used for all trabecular bone samples consisting of adaptive thresholding, despeckle, 3D analysis and save bitmaps. A detailed version of the task list used for trabecular bone analysis can be found in Appendix 1. The data for the 3D analysis were exported as a text table for each dataset and a single line .csv file for each site.

Trabecular 3D bone sample analysis produced data for 33 parameters. However, only the nine most physiologically relevant were looked at in detail: bone volume BV (mm^3), trabecular pattern factor $TbPf$ ($1/\text{mm}$), trabecular thickness $Tb.Th$ (mm), trabecular number $Tb.N$ ($1/\text{mm}$), trabecular separation

Tb.Sp (mm), degree of anisotropy *DA*, fractal dimension *FD*, structural model index *SMI* and connectivity density *Conn.Dn* (1/mm³).

2.3.4 X-Tek HMX scans: cortical bone analysis

Using VGStudio Max 2.1 software the cortical midshaft slice midway between the trabecular bone at the proximal and distal ends of the bone was identified. The midshaft area (μm²) and lumen area (μm²) were measured with the segmentation polygon lasso tool. From the midshaft area and the lumen area the cortical area was calculated. The midshaft radius and lumen radius were calculated using the equation below where *A* is area of a circle and *r* is the radius of the circle.

$$r = \sqrt{\frac{A}{\pi}}$$

The mean cortical wall thickness was calculated as shown below.

$$\text{Mean wall thickness } (\mu\text{m}) = \text{midshaft radius } (\mu\text{m}) - \text{lumen radius}(\mu\text{m})$$

The cross sectional moment of inertia (CSMI) was calculated from the midshaft radius and lumen radius based on the standard material properties equation.

$$CSMI = \left(\frac{\pi}{4}\right) (\text{midshaft radius}^4 - \text{lumen radius}^4)$$

2.3.5 SkyScan 1176 scans: trabecular bone analysis

Bruker software including Data Viewer and CTAn, were used to analyse the trabecular areas within the vertebral body, femoral head and distal femur. At each site a trabecular region was separated from the cortical and both were saved for analysis. For the vertebral body (VB), for example, an offset from each of the two growth plates was applied in order to exclude the primary spongiosa from the trabecular analysis, leaving an area of interest in the middle. The trabecular bone was segmented out into one ROI and the cortical

bone into another. These ROIs were then used to analyse both the trabecular and cortical sections of the vertebra body. The femoral head and distal femur trabecular regions ROIs were offset from the growth plate and continued until the end of the trabecular bone.

Datasets and ROIs were loaded into BatMan in CTAn and a trabecular custom processing task list was used for all trabecular bone samples consisting of adaptive thresholding, despeckle, 3D analysis and save bitmaps. A detailed version of the task list used for trabecular bone analysis can be found in Appendix 1. The data for the 3D analysis were exported as a text table for each dataset and a single line .csv file for each site.

The parameters interrogated are as detailed in section 2.3.3.

2.3.6 SkyScan 1176 scans: cortical bone analysis

ROIs obtained during trabecular analysis were inverted so just the cortical area was observed and saved. Datasets and ROIs were loaded into BatMan (Batch Manager) in CTAn and a cortical custom processing task list was used for all trabecular bone samples consisting of global thresholding, bitwise operation, morphological operation, despeckle, 3D analysis, 2D analysis and save bitmaps. A detailed version of the task list used for trabecular bone analysis can be found in Appendix 1. The data for the 3D analysis were exported as a text table for each dataset and a single line .csv file for each site.

Cortical 3D bone sample analysis produced data for 31 parameters, as trabecular separation and number were not calculated. However the seven most physiologically relevant will be looked at in detail-bone volume BV (mm^3), trabecular pattern factor $TbPf$ ($1/\text{mm}$), cortical thickness $Tb.Th$ (mm), degree of anisotropy DA , fractal dimension FD , structural model index SMI and connectivity density $Conn.Dn$ ($1/\text{mm}^3$).

2.3.7 Parameters investigated

Physiologically relevant data often show a pattern within the data, rather than a single significant result. This is key here as with multiple sites analysed, nine parameters studied and four different groups, it is possible to generate false positive results.

Definitions of the parameters analysed follow and are defined according to the structural parameters measured by Bruker™ μ CT-analyzer software (available from the Bruker website: http://www.skyscan.be/next/ctan_ctvol_02.pdf). A brief definition of the relevant parameters can be found below.

The ROI refers to the 3D volume selected for analysis. The ROI is binarised, before the analysis, in a process called thresholding. The volume of interest (VOI) is defined as the total volume of all voxels within the ROI, regardless of binarisation. The VOI is also referred to as the tissue volume (TV).

Bone volume (BV) mm^3 - the total volume of the binarised objects within the VOI. The 3D volume measurement is based on the marching cubes volume model of the binarised objects within the ROI. A higher value indicates a higher bone volume.

Trabecular pattern factor (Tb.Pf) $1/mm$ - this is an inverse index of connectivity, which was developed and defined by Hahn et al. (2007) for application to trabecular bone. It was applied originally to 2D images of trabecular bone, and it calculates an index of relative convexity or concavity of the total bone surface, on the principle that concavity indicates connectivity (and the presence of “nodes”), and convexity indicates isolated disconnected structures (struts). As a result, lower Tb.Pf signifies better connected trabecular lattices while higher Tb.Pf indicates a more disconnected trabecular structure. A prevalence of enclosed cavities and concave surfaces can push Tb.Pf to negative values. When analysing cortical bone a more negative Tb.Pf indicates a more concave

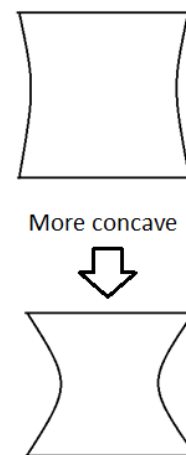


Figure 2-2
Illustration of
a more
concave
cortical bone

structure- that is associated with an increase in strength (Figure 2-2).

Structural model index (SMI) - indicates the relative prevalence of rods and plates in a 3D structure such as trabecular bone. SMI involves a measurement of surface convexity. This parameter is of importance in osteoporotic degradation of trabecular bone which is characterised by a transition from plate-like to rod-like architecture. An ideal plate, cylinder and sphere have SMI values of 0, 3 and 4 respectively. The calculation of SMI is based on dilation of the 3D voxel model, that is, artificially adding one voxel thickness to all binarised object surfaces (Hildebrand et al. 1997).

Trabecular thickness (Tb.Th) *mm* - with 3D image analysis by μ -CT, a true 3D thickness can be measured which is model-independent. Distance transform methods described by Remy et al. (2002) are the basis for the implementation by CT-analyser of local thickness measurement. The method starts with a “skeletonisation” identifying the medial axes of all structures. Then the “sphere-fitting” local thickness measurement is made for all the voxels lying along this axis. All trabecular thicknesses were measured in 3D.

Trabecular number (Tb.N) *1/mm* - trabecular number describes the number of traversals across a trabecular or solid structure made per unit length on a random linear path through the VOI. Again, the complexities of model dependence associated with 2D measurements are eliminated by true 3D calculation of trabecular number from 3D μ CT images. This parameter is measured by application of the equation for the parallel plate model (fractional volume/thickness Equation 3-1), but using a direct 3D measurement of trabecular thickness (Tb.Th).

$$Tb.N = \frac{1}{(Tb.Th + Tb.Sp)}$$

Trabecular separation (Tb.Sp) *mm* - trabecular separation is essentially the size of the spaces between trabeculae. A more accurate definition is thickness of the spaces as defined by binarisation within the VOI in 3D. Bruker analysis software can measure Tb.Sp directly and model-independently in 3D from μ CT images by the same method used to measure trabecular thickness (see above).

Degree of anisotropy (DA) - isotropy is a measure of 3D symmetry or the presence or absence of preferential alignment of structures along a particular directional axis. An object would be isotropic if it was identical in all directions. Directional dependence is therefore referred to as anisotropy. Apart from percent volume, DA and the general stereology parameters of trabecular bone are probably the most important determinants of mechanical strength (Odgaard 1997). Here DA is 0 for total isotropy and a value of less than 0 describes increasing anisotropy.



Figure 2-3 Fern leaf image to demonstrate fractal dimension as taken from Structural parameters measured by the Skyscan™ CT-analyser software.

Fractal dimension (FD) - fractal dimension is an indicator of the surface complexity of an object. FD quantifies how that object's surface fills space. True fractal objects have surface shapes which are repeated over many spatial scales. So the closer you look i.e. the higher the magnification the more self-similar structure will be observed.

A typical example is a fern leaf, as shown in Figure 2-3, in which each side-branch is very similar to the whole fern leaf, and likewise each side-finger of each side branch also looks the same as the whole fern leaf, and so on. A fractal object essentially has fractional, non-integer dimension, i.e. a line "trying" to fill a plane, or a plane trying to fill a 3d space, having dimension somewhere between 2 and 3. Fractal dimension is

calculated using the Kolmogorov or “box counting” method. It is calculated here in 3D in Bruker CTAn. The surface or volume is divided into an array of equal squares or cubes, and the number of squares containing part of the object surface is counted. This is repeated over a range of box sizes of between 3-100 pixels. The number of boxes containing surface is plotted against box length in a log-log plot, and the fractal dimension is obtained from the slope of the log-log regression. Fractal characteristics of trabecular bone, and methods for measurement of fractal dimension, are discussed by Chappard et al. (2001)

Connectivity density (Conn.Dn) $1/mm^3$ – Euler number is used to calculate Conn.Dn. Euler number is an indicator of the connectedness of a 3D structure. This allows one to calculate how many redundant connections are present when the object is multiply connected and how many of these can be severed before the structure falls into two parts. Euler number is then divided by the volume in the VOI to establish ConnDn.

2.4 Bone mineral density analysis

2.4.1 Hounsfield Unit analysis of scans from the HMX

Histograms were saved in Hounsfield units for each bone in VG Studio Max. These were opened in Microsoft Excel and combined into one file. A mean histogram was obtained for each diet group with the standard deviation calculated and plotted at 50 point intervals. Groups to be compared were overlapped with the standard deviation points staggered. If the standard deviation error bars did not overlap, statistical analysis would be conducted for none overlapping points. None overlapping provides a rapid method to determine which points should be examined with a statistical analysis. A range of consecutive points were examined, to determine a larger bone density region which showed differences between the study groups.

2.4.2 Bone mineral density (BMD) analysis of scans from the SkyScan 1176

According to the Bruker protocol the scans for both the femurs and vertebrae were calibrated to two phantoms of 0.25 g/cm^3 and 0.75 g/cm^3 (purchased from Bruker). This allowed histograms calibrated to BMD to be gathered for each sample. In addition to this, the software generates the mean BMD for the cortical bone and mean regional medullary BMD for the trabecular region. The trabecular region calculation is different in order to take into account that the bone marrow is interspersed throughout the trabecular region.

2.5 Three point bend testing

The load displacement graphs obtained from the three point bend testing were used to determine ultimate force, total displacement, work to failure and stiffness as defined below (Figure 3-4). Definitions of the parameters can also be found below.

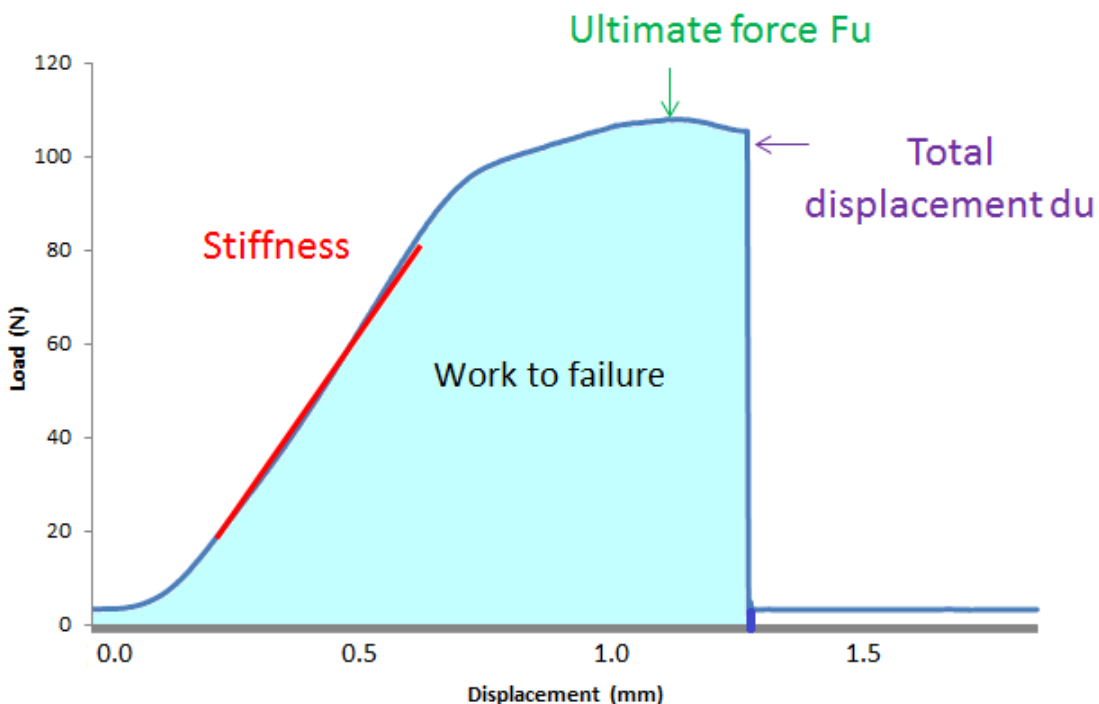


Figure 3-4 Schematic of a load displacement graph for a rat femur to demonstrate parameter origins.

Parameters

Ultimate force (F_u) is the maximum amount of load applied to the femur. At this point both the load in N and displacement in mm were noted and the means for each group determined (see in the graphs below).

Total displacement (d_u) is the maximum displacement of the femur before fracture. At this point both the load in Newtons (N) and displacement in mm were noted and the means for each group determined (see in the graphs below).

Work to failure is the total energy in Joules (J) required to fracture the femur as determined by the area under the curve until failure. The means for each determined (see in the graphs below).

Stiffness in N/mm is slope of the linear region of the force-displacement curve. The means for each group can be seen in the graphs below.

2.5.1 Method 1 conducted for data in Chapter 3

All testing was performed on a Bose Electroforce 3200 electromagnetic test instrument (Bose Corporation, Eden Prairie, Minnesota, USA). The midshaft strength of tibia and femur was tested using a three-point bend test. Samples were placed anterior surface down on two supports equidistant from the ends and 10 mm apart. Samples were centrally loaded at a constant rate (6 mm/min) up to fracture. Load-displacement curves were used to calculate maximum load, maximum deflection, stiffness and work to failure. Stiffness was calculated as the slope of the linear portion of the load-displacement curve. Work to failure was determined as the area under the curve (see Figure 3-10 for illustration).

Data were entered into IBM SPSS 21. All diet groups were assigned a number. The data were then analysed using a One Way ANOVA and Bonferroni post-hoc analysis. The significance level was set as $P \leq 0.05$. The means for each diet group were also calculated using IBM SPSS 21.

2.5.2 Improved method 2 conducted for data in Chapter 4

The testing procedure is as described in method 1 above with the revision that the bone be submersed in HPSS buffer during testing. This is keep the collagen fibres hydrated and provides a better simulation of *in vivo* conditions. The significance of the hydration only came to light after the destruction of the bones in Chapter 3 so this addition is seen in Chapter 4.

2.6 Micro indentation

All investigations were conducted on the BioDent Hfc Reference Point Indenter (Active Life Scientific. Inc, Santa Barbara, CA, USA) with the assistance of Tsiloon Li (Bone and Joint Research Group, University of Southampton) and Tom Jenkins (Bioengineering Research Group, University of Southampton). The probe was validated on poly(methyl methacrylate) (PMMA) plastic with a preload touch down of approximately 150 μm . Femurs were secured with crocodile clips and kept moist with Hank's Balanced Salt Solution (HBSS) when needed. Seven microindentation sites were interrogated as shown in Figure 2-5.

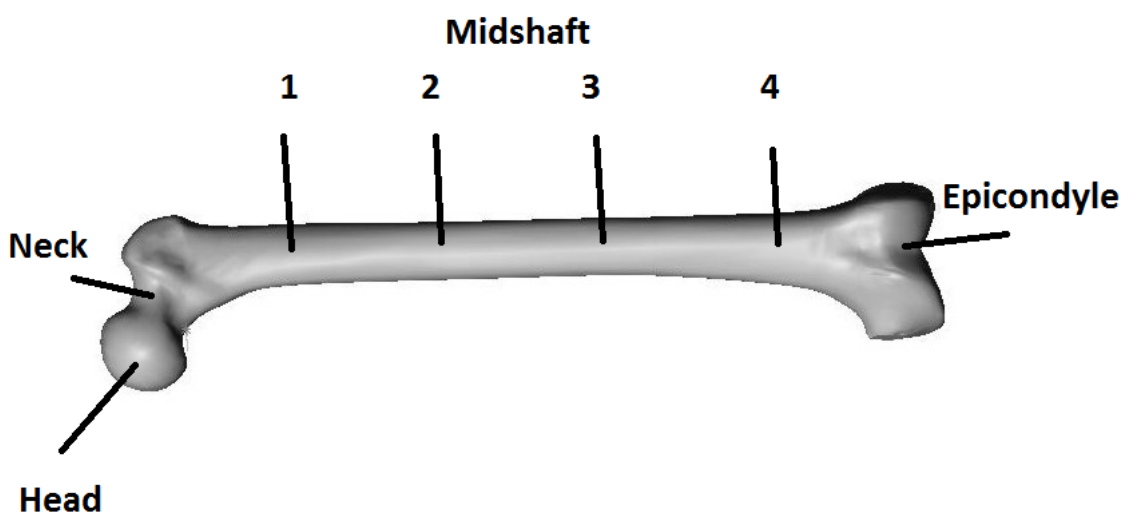


Figure 2-5 Illustration showing the microindentation sites investigated

Reference probe indentation (RPI) involves positioning a probe (Figure 2-6), at a set pre-load, onto the surface of the bone with the reference probe in contact with the bone. The test probe then indents the bone at a predetermined force in cycles consisting of -load, hold and unload, at the same sample site (Figure 2-7). Each indentation distance, relative to the reference probe, is recorded, with a typical test consisting of between 10 and 20 cycles. A constant maximum applied force and frequency is used during each cycle.

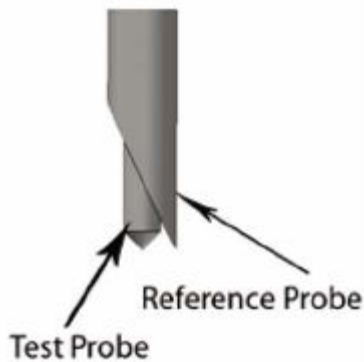


Figure 2-6 Microindentation probe- the microindentation probe consists of a reference probe and a test probe. Figure adapted from Diez-Perez et al. (2010).

A force versus distance curve is produced from the test. Figure 2-7 shows an example indentation curve for one cycle, with the three parts of the cycle labelled-load, hold and unload. The additional cycles would also appear on the graph but are absent in this illustration.

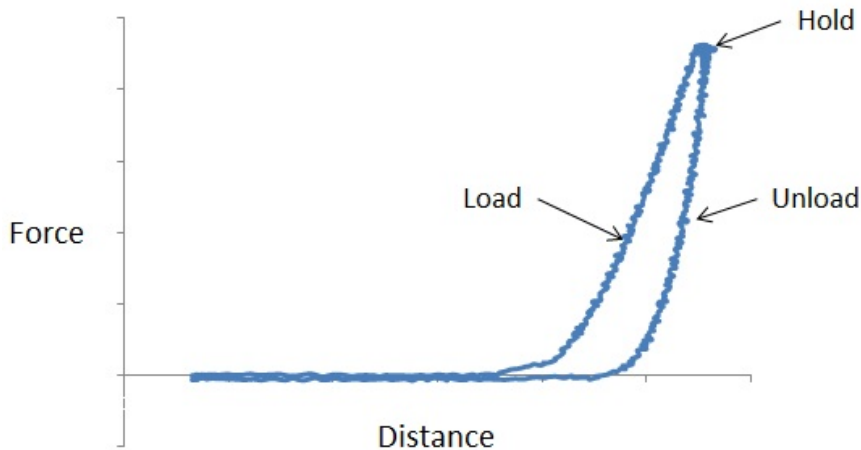


Figure 2-7 An illustration of a typical Indentation curve for one cycle-force versus distance indentation curve with load, hold and unload regions. Courtesy of Tom Jenkins, Bioengineering Research Group, University of Southampton.

The indentation distance increase (IDI) is the distance between the initial indentation of the first cycle and the final indentation distance on the last cycle (Figure 2-8).

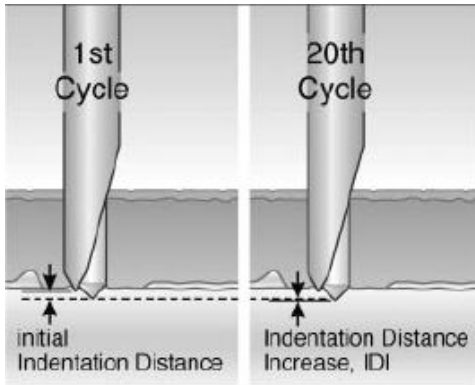


Figure 2-8 Microindentation cycles-for each microindentation cycle, the reference probe is loaded on the bone surface and the testing probe is used to indent the bone. The indentation distance (in relation to the reference probe) is recorded. Figure adapted from (Diez-Perez et al. 2010).

Creep indentation distance (CID) was calculated for the first cycle only in this study. CID is the distance the probe moves during the hold region of the test.

The total indentation distance (TID) is the distance between the initial probe depth for the first cycle and the final probe depth in the final cycle.

Data for IDI, CID and TID were entered into IBM SPSS 21. All diet groups were assigned a number. The data were then analysed using a One Way ANOVA and Bonferroni post-hoc analysis. The significance level was set as $P \leq 0.05$. The means for each diet group were also calculated using IBM SPSS 21.

2.7 Molecular analysis

2.7.1 RNA/DNA extraction from bone tissue

Femurs were dissected and soft tissues removed. The distal femur was removed and crushed using bone cutters. The bone tissue was washed three times in PBS then bone tissue (150mg) was added to 1 ml Trizol (Invitrogen Life Technologies Ltd, Paisley, UK). All samples were then frozen at -80°C until required.

Once defrosted RNA extraction from the trabecular bone was performed in accordance to the Invitrogen Trizol protocol Appendix 2.

The RNA was quantified using a Nanodrop instrument (Thermo Fisher Scientific, Leicestershire, UK). Ultrapure H₂O was added in order to achieve a 100mg concentration of RNA for each sample.

2.7.2 cDNA production

cDNA was synthesised using the SuperScript® VILO™ cDNA Synthesis Kit from Invitrogen according to the manufacturers protocol provided Appendix 2. The 10µl of cDNA was diluted with 40µl ultrapure H₂O to achieve the correct concentration for qPCR.

2.7.3 qPCR

qPCR experiments were carried out using Syber-Green (Invitrogen) according to the manufactures protocol. Three different house keeping genes (R18S, β Actin and GAPDH) were initially investigated in order to establish which produced the most consistent cycle threshold (CT) values across a range of samples. This study involved samples from a large rat population and hence a large genetic diversity, therefor establishing a stable base line is necessary. R18S proved to be the most stable and so was chosen for this study (Appendix 3). Only one house keeping gene was used because with such a large population running two housekeeping genes would have been impractical. Primer sequences for

the genes of interest and the housekeeping gene are shown in Appendix 4. All primers except IGF-I and IGF-II were obtained from Biomers (Biomers.net, Ulm, Germany) and their sequences were taken from reputable journals. Standard curve experiments were carried out for each of the gene of interest primers prior to the study.

The number of genes and volume of samples posed a practical challenge and so each gene of interest and the housekeeping gene were run on a qPCR plate that included each sample in triplicate (Figure 2-9).

Figure 2-9 Example of 96 plate lay out and colour guide for the two qPCR required to compare 40 samples

	1	2	3	4	5	6	7	8	9	10	11	12
A	767	767	767	258	258	258	341	341	341	172	172	172
B	384	384	384	120	120	120	686	686	686	188	188	188
C	1111	1111	1111	768	768	768	730	730	730	370	370	370
D	113	113	113	597	597	597	175	175	175			
E	767	767	767	258	258	258	341	341	341	172	172	172
F	384	384	384	120	120	120	686	686	686	188	188	188
G	1111	1111	1111	768	768	768	730	730	730	370	370	370
H	113	113	113	597	597	597	175	175	175			

	1	2	3	4	5	6	7	8	9	10	11	12
A	707	707	707	1026	1026	1026	1169	1169	1169	149	149	149
B	245	245	245	325	325	325	613	613	613	699	699	699
C	769	769	769	1053	1053	1053	94	94	94	1119	1119	1119
D	474	474	474	903	903	903	731	731	731			
E	707	707	707	1026	1026	1026	1169	1169	1169	149	149	149
F	245	245	245	325	325	325	613	613	613	699	699	699
G	769	769	769	1053	1053	1053	94	94	94	1119	1119	1119
H	474	474	474	903	903	903	731	731	731			

As 30 samples were being analysed for comparison, two 96 well plates were required for each gene. Figure 2-9 above shows the design used to randomise the sample allocation. Samples were run in triplicate and are represented on the figure by their sample number e.g. 767. The housekeeping gene and target gene of interest for each sample were always run on the same plate. The samples were assigned positions so that no samples of the same group were next to each other and an equal number of samples for each group were represented on each plate. The same sample allocation was used for each gene

of interest that was run for practical reasons. CT values for R18S were monitored across all plates to establish consistency in procedure and ensure that the results were comparable across plates.

Large variation was evident in the data due to population variation between rats as expected. All samples were normalised to the highest control sample being analysed using the $\Delta\Delta\text{CT}$ method (Livak et al. 2001).

Data were entered into IBM SPSS 21. Statistical analysis was conducted on the ΔCT level before any transformations were conducted. All diet groups were assigned a number. If two conditions were analysed a Mann-Whitney U test was used, if three conditions were analysed a One Way ANOVA and Bonferroni post-hoc analysis was utilised.

2.8 Statistical analysis

The data for Chapter 3 were analysed with the help of Karen Jameson (statistician at the MRC Lifecourse Epidemiological Unit, Southampton) using a multivariate analysis model in STATA 11 (StataCorp LP, College Station, Texas, USA). As the samples have familial relationships in some cases, this model was designed to compensate for sibling relationships (see Table 3-1 for sibling relationships). This model is similar to a One Way ANOVA but accounts for the sibling relationship within diet groups. The significance level was set as $P \leq 0.05$. As the samples were selected without sibling relationships within groups data for Chapter 4 were analysed in IBM SPSS 21 (IBM UK, Business Analytics - SPSS, Middlesex, UK) using a One Way ANOVA and Bonferroni post-hoc analysis. The significance level was set as $P \leq 0.05$. The means for each diet group were also calculated using IBM SPSS 21.

All data in Chapter 4 were entered into IBM SPSS 21 (IBM UK, Business Analytics - SPSS, Middlesex UK) All diet groups were assigned a number. The data were then analysed using a One Way ANOVA and Bonferroni post-hoc analysis. The significance level was set as $P \leq 0.05$. The means and standard deviation for each diet group were also calculated using IBM SPSS 21.

3. The effect of folic acid dietary addition to offspring from protein restricted mothers on bone structure and quality

3.1 Introduction

As discussed in chapter 1, inadequate nutrition during pregnancy impacts on the risk of chronic diseases in later life such as type II diabetes, coronary heart disease, obesity and osteoporosis. Lanham et al. first showed that protein restriction during pregnancy affects the bone microarchitecture and strength of subsequent rat offspring (Lanham et al. 2008). A negative effect was noted at the trabecular femoral head and trabecular vertebrae and a positive effect was seen at the trabecular femoral necks, in 75 week old female offspring.

Folic acid is a methyl donor that is important in many processes including synthesis of DNA, protein synthesis and cell membrane biosynthesis (Giudicelli et al. 2013). Using the one-carbon metabolic pathway, folic acid provides methyl groups for DNA methylation and therefore is important in epigenetic regulation of gene expression. Lillycrop et al. showed that folic acid addition reverses the negative effects of protein restriction during pregnancy on hepatic gene expression in the liver, in a Wistar rat model (Lillycrop et al. 2005). More specifically peroxisomal proliferator-activated receptor (PPAR) gene methylation was 20.6% lower and expression 10.5-fold higher in PR offspring compared with control offspring. Glucocorticoid receptor (GR) gene methylation was 22.8% lower and expression 200% higher in PR offspring compared with controls. The maternal protein restricted and juvenile high folic acid diet (PR/HFA) prevented these changes. Torres et al. found that folic acid addition during pregnancy restored systolic blood pressure to control levels, which is a reversal of the increased systolic blood pressure induced by maternal protein restriction in Wistar rats (Torrens et al. 2010). Huot et al. investigated the effect of very high folic acid supplementation (20mg/kg) during pregnancy and early life (up to 20 weeks) on bone in female rats (Huot et al. 2013). HFA during pregnancy had a negative effect on the femur morphology, bone mineral content (BMC) and biomechanical strength of 20

week old female rats. HFA after weaning resulted in lower L4 anterior posterior width, BMC and bone mineral density (BMD).

Other periods of rapid growth in juveniles, such as during puberty, may be affected by folic acid addition due to the potential decrease in genome stability at this time (Dolinoy et al. 2007). Due to folic acid fortification in the food chain it is important to study the effects of folic acid on developmental time points. Burdge et al. have previously investigated if folic acid addition to juvenile rat offspring can reverse the effects of maternal protein restriction on hepatic gene expression in the liver (Burdge et al. 2009). The results showed that the effects of maternal protein restriction were not reversed in the hepatic gene expression, as with folic acid supplementation during pregnancy, but the phenotype was altered, showing that puberty is a period of plasticity in the liver. The effect on bone of folic acid addition to juvenile offspring from protein restricted dams has not previously been investigated, particularly at this time point.

Hypothesis- Folic acid addition to juvenile offspring from protein restricted dams improves bone structure and mechanical properties compared to offspring from protein restricted dams without folic acid addition.

3.2 Methods

3.2.1 Animal experimentation

All the animals for this study were taken from a study led by Dr. Graham C. Burdge, (HDH, University of Southampton, UK) investigating the effect of folic acid addition to offspring in the juvenile-pubertal period from mothers fed a protein restricted diet during pregnancy, in order to see if the effects of the protein restriction during pregnancy could be altered (Burdge et al. 2009). The animal experimentation was conducted in accordance with the Home Office

Animals Scientific Procedures Act 1986 and approved by internal ethical review.

The animal work involved virgin female Wistar rats of body weight 200-250g which were mated and kept on control (C) or protein restricted (PR) diets. Feed diets were isocaloric chow (Table 3-1) from the time of conception to delivery at approximately day 21. Within 24 hours of delivery, litters were culled down to eight pups with approximately equal number of males and females maintained where possible. Throughout weaning from postnatal 1-28 days, all the dams were on the same chow diet (Table 3-1).

Table 3-1 Diet fed during pregnancy, lactation and after weaning

	Pregnancy diets		Lactation diet	Juvenile pubertal diets		
	C	PR	AIN-93G	AF	FS	High fat
Casein (g/kg)	170	89	186	170	170	168
Folic acid (mg/kg)	1	1	2	1	5	1
Corn starch (g/kg)	418	478	397	448	448	318
Sucrose (g/kg)	206	236	100	236	236	206
Choline (g/kg)	2	2	1	2	2	2
DL-Methionine (g/kg)	5	5	3	5	5	5
Vitamins ¹ (g/kg)	10	10	10	10	10	10
Minerals ² (g/kg)	35	35	35	35	35	35
Cellulose (g/kg)	43	43	50	43	43	43
Soybean oil (g/kg)	100	100	70	4	4	20
Lard (g/kg)	0	0	0	36	36	180
Total lipid (g/kg)	100	100	70	40	40	200
Total energy (MJ/kg)	17.2	17.3	16.4	15.9	15.9	19.3

Vitamin mix (per kg mix): Retinyl palmitate 13 µg; cholecalciferol 25µg; DL-α-tocopherol acetate 83 mg; menadione 0.3 mg; thiamine hydrochloride 6 mg; riboflavin 6 mg; niacin 30 mg; calcium pantothenic acid 15 mg; pyridoxine hydrochloride 6 mg; biotin 0.2 mg; Cyanocobalamin 25 µg. Mineral mix (per kg mix): Calcium 5 g; available phosphorous 1.4 g; potassium 3.6 g; magnesium 0.5 g; sodium 1 g; chloride 2 g; fluorine 10 mg; iron 350 mg; manganese 110 mg; copper 60 mg; iodine 2 mg; chromium 10 mg; molybdenum 1 mg; selenium 2 mg. All diets were supplied by PMI Nutrition International.

Each animal was randomly assigned to one of two groups at weaning, either normal/control folic acid (CFA) with 1 mg/kg feed folic acid, or high folic acid (HFA) with 5mg/kg feed folic acid. The animals were maintained on these diets for 28 days, until postnatal day 56. Four dietary groups were therefore obtained as a consequence of the maternal diet groupings and subsequent

juvenile-pubertal diet groupings (Figure 3-1). A diet of 5mg of folic acid per kg of feed is a comparable amount to that recommended for women before conception and during early pregnancy in the UK (Wald et al. 2001). All animals were fed a high fat diet from day 56 until harvesting using CO₂ asphyxiation.

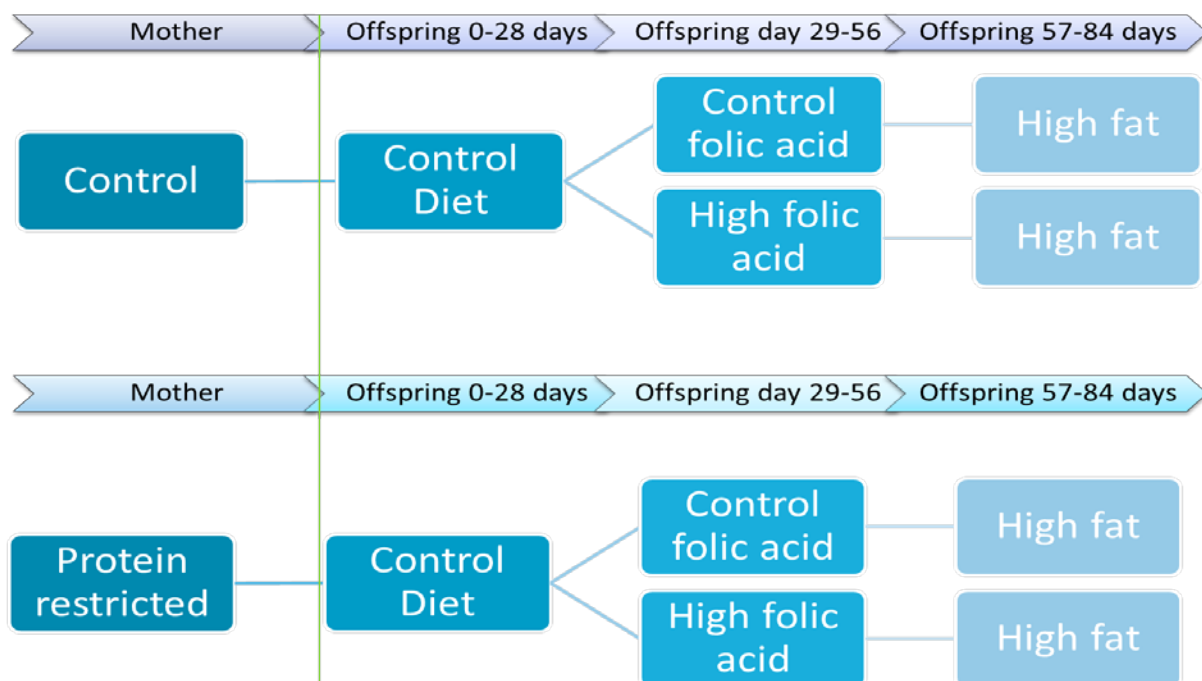


Figure 3-1 Diagram displaying the timeline and dietary conditions of the offspring. Both males and female offspring were studied from each diet group

Between 4 and 6 animals of each sex in each diet group were used in this study. The difference in numbers were due to the samples available at the time of the study. The naming code used consisted of the maternal diet, sample number, sex and year of experiment. The control folic acid experiments were conducted in 2007 and high folic acid experiments in 2008.

Table 3-2 Sample information and codes for offspring

Maternal diet	Juvenile-pubertal diet	Sex of offspring	Number of offspring	Group number	Number of mothers
C	CFA	Male	6	1	3
C	CFA	Female	6	5	2
C	HFA	Male	4	2	2
C	HFA	Female	4	6	2
PR	CFA	Male	5	3	3
PR	CFA	Female	5	7	4
PR	HFA	Male	4	4	2
PR	HFA	Female	4	8	3

3.2.2 Histology

All histological processing and staining was conducted in accordance with the General Methods section 2.2.

3.2.3 Micro Computed Tomography Data

The femur trabecular analysis of the head of femur, neck of femur and distal femur was conducted in accordance with the General Methods sections 2.3.2, 2.3.3 and 2.3.6.

The midshaft cortical femur analysis was conducted in accordance with the General Methods sections 2.3.2, 2.3.4 and 2.3.6.

The vertebral body trabecular analysis was conducted according to General Methods sections 2.3.1, 2.3.5, 2.3.6.

The vertebral body cortical analysis was conducted as detailed in the General Methods sections 2.3.1, 2.3.6, 2.3.6.

3.2.4 Bone mineral density

The whole femur histogram comparisons were conducted according to the General Methods section 2.4.1.

For the vertebral body trabecular and cortical bone, bone mineral density analysis was conducted as detailed in the General Methods sections 2.4.2 and 2.3.6.

3.2.5 Three point bend testing

The three point bend testing and analysis of the midshaft femurs was conducted in accordance with the General Methods section 2.5.1.

3.2.6 Statistical analysis

The statistical analyses were conducted according to General Methods section 2.8.

3.3 Results

3.3.1 Anthropometric analysis of femurs

All femur lengths were measured using digital callipers.

Table 3-3 Anthropometric measurements of 12 week young adult rat femurs. Values are mean \pm SD with P-values. Diet groups- C/CFA(control/control folic acid) n=6, C/HFA (C/High folic acid) n=4 , PR/CFA (protein restricted/CFA) n=5 , PR/HFA n= 4 and the diet comparisons were juvenile pubertal diet (JP) and maternal diet (M). - indicates no significance.

	Dietary groups				P-values		
	C/CFA	C/HFA	PR/CFA	PR/HFA	JP diet	M diet	JP + M diet
Female femur lengths (mm)	30.5 \pm 0.5	29.5 \pm 0.7	30.7 \pm 0.8	31.1 \pm 0.6	-	-	-
Male femur lengths (mm)	34.3 \pm 0.6	33.6 \pm 1.4	33.4 \pm 1.3	33.9 \pm 0.8	-	-	-

No differences were observed between the different diet groups for either male or female offspring (Table 3-3). The male femurs were statistically significantly longer than the female femurs in the C/CFA group ($P < 0.001$), the C/HFA group ($P < 0.001$), the PR/CFA group ($P < 0.001$) and the PR/HFA group ($P < 0.001$). Male femurs would be expected to be longer than females for rats of this age, because of this data from male rats were not compared to those female rats throughout this study.

3.3.2 Histological analysis of distal femurs from 12 week female rats

Figure 3-2 provides a guide to the structural features of the distal femur.

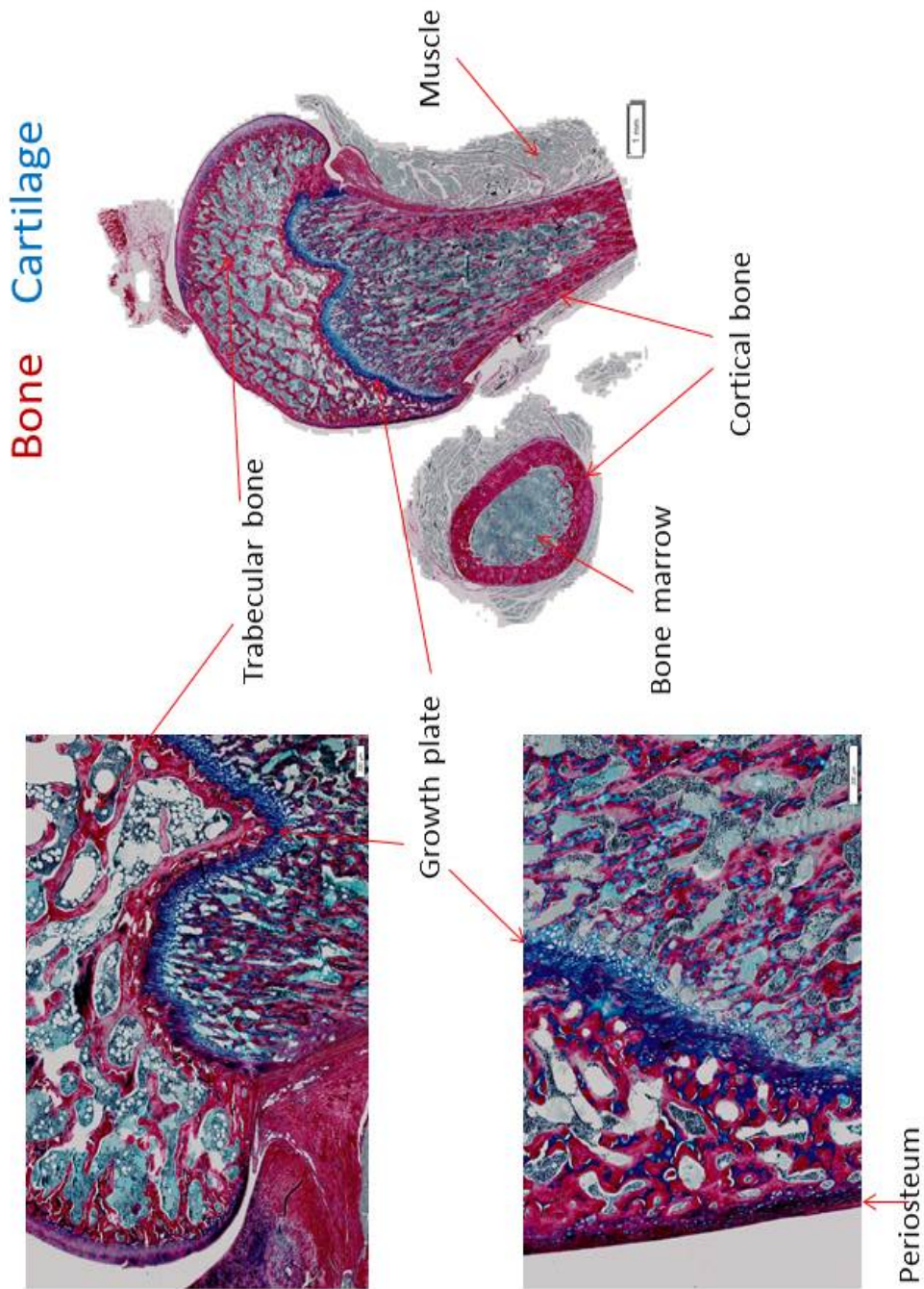
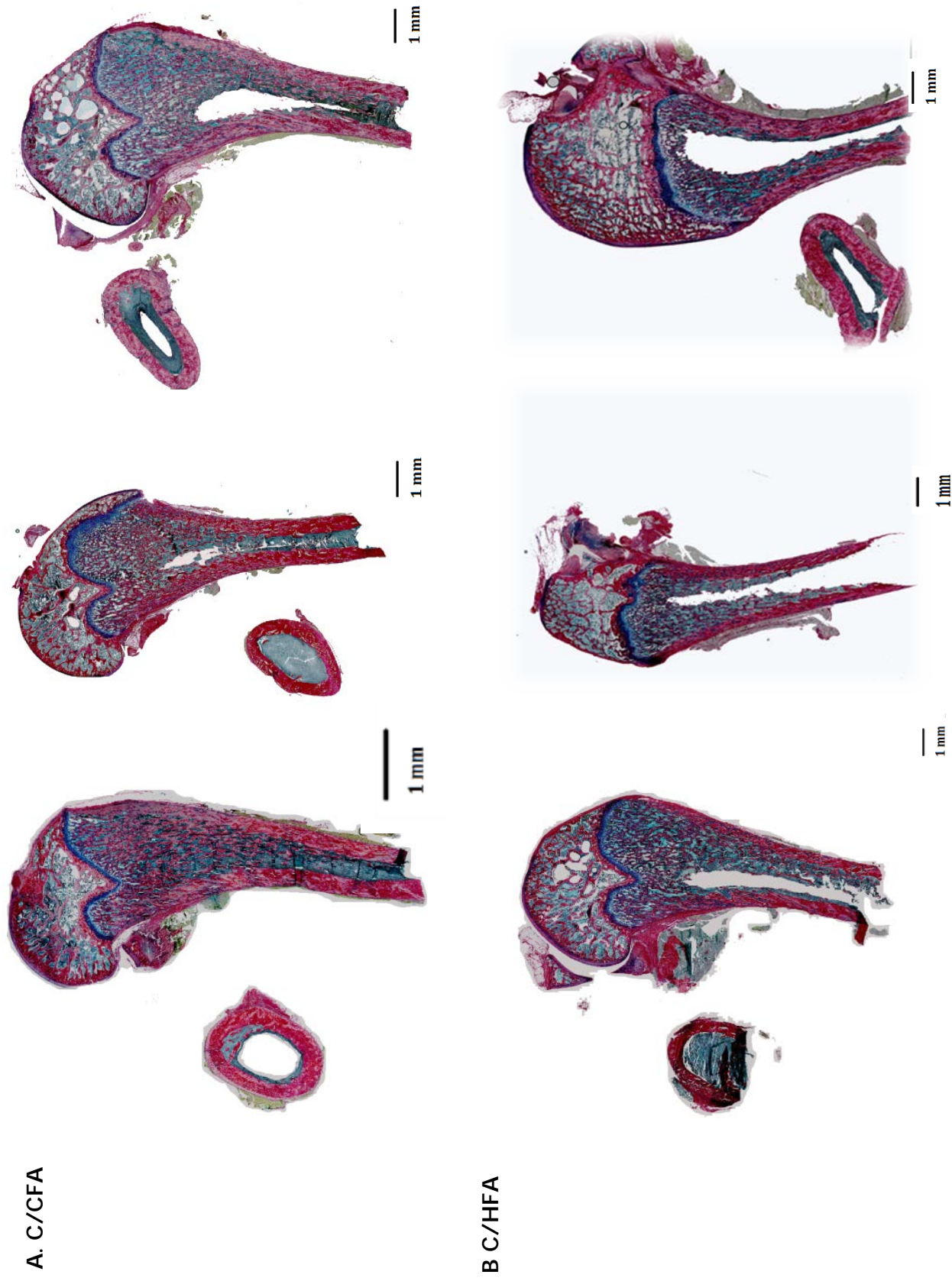
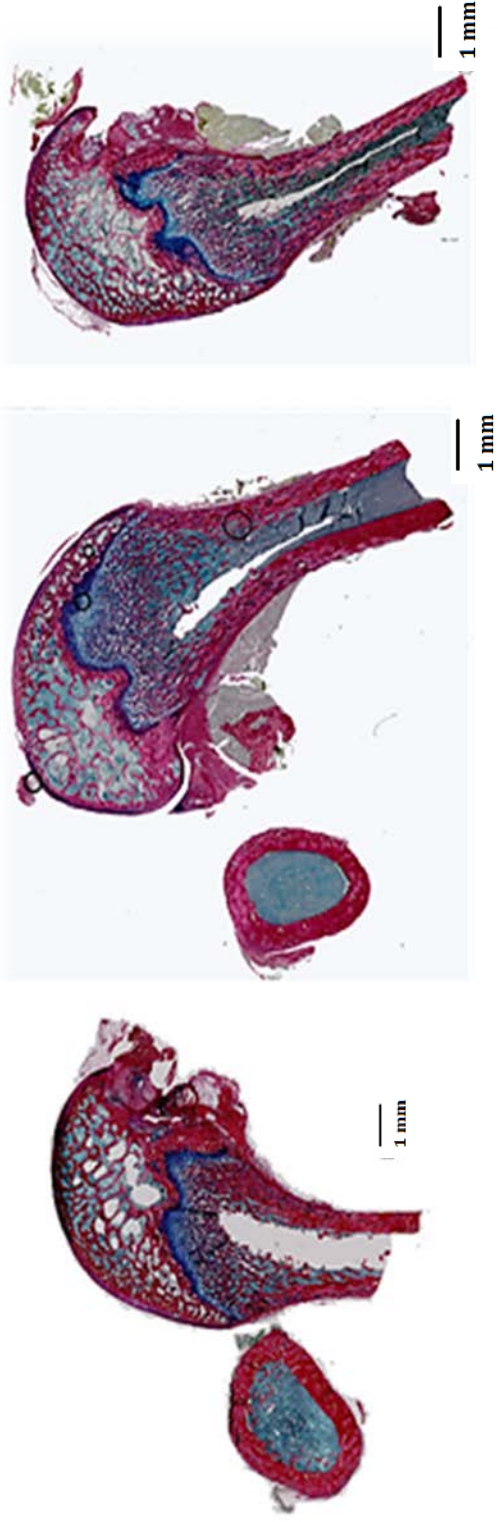


Figure 3-2 Organisation of the distal femur including cortical bone, trabecular bone and growth plate. Sections labelled and provided as a template guide

Figure 3-3 Female femur histology samples stained with Alcian Blue and Sirius Red. A. C/CFA group (n=3) B. C/HFA group (n=3).



A. PR/CFA



B. PR/HFA

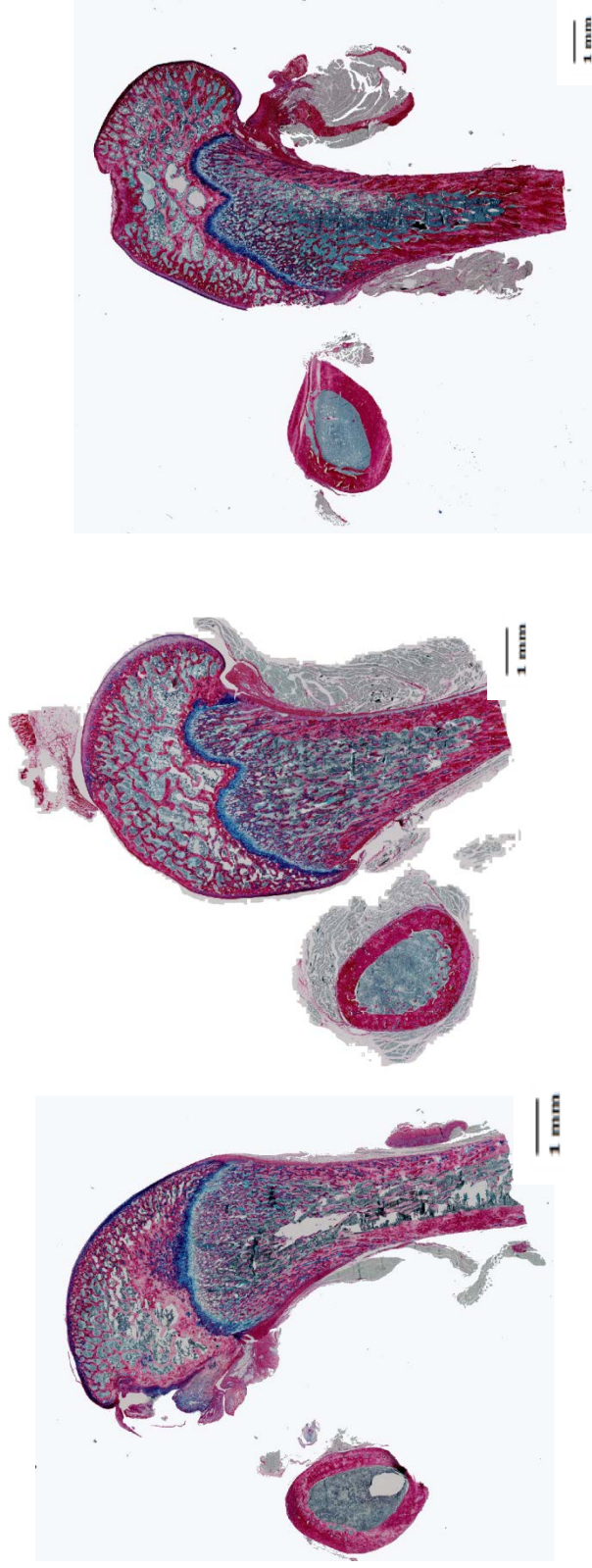


Figure 3-4 Female femur histology samples stained with Alcian Blue and Sirius Red. A. PR/CFA group (n=3) B. PR/HFA group (n=3).

Figure 3-2 is provided as a guide in order to aid interpretation of histological results of this kind, and consists of a longitudinal section from the distal femur and a transverse section from the cortical midshaft. Two high resolution images of the longitudinal section are also provided to further illustrate the features investigated.

Qualitative examination of the growth plate organisation, trabecular and cortical thickness was conducted using Alcian Blue and Sirius Red staining in A- female distal femur C/CFA and B- female distal femur PR/CFA samples (Figure 3-3 and 3-4). No noteworthy differences were observed between samples in either the distal femur longitudinal sections or the transverse cortical midshaft sections.

3.3.3 Micro computed tomography analysis of bone structure

3.3.3.1 Vertebral body micro CT analysis

After the vertebra scans were reconstructed, the L3 vertebra was selected for analysis on all samples. The vertebral body μ CT analysis consisted of segmenting out the vertebral body (VB) and then selecting ROIs of the trabecular and cortical bone in the middle of the VB with an offset from the growth plates at each end of the VB. This is illustrated in Figure 3-5 (ROI shown here for illustrative purposes only).

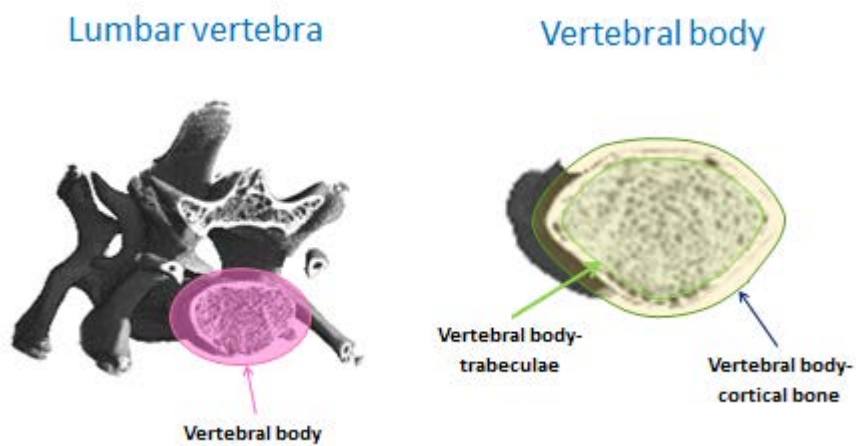


Figure 3-5 3D reconstructions of a whole rat vertebra and a segmented vertebral body section. The trabecular and cortical regions of interests (ROIs) are shown and labelled on the diagram. The vertebral body trabecular section has been digitally clipped in order to show the interior structure using VG Studio Max.

The trabecular and cortical bone analyses were conducted separately as described in the General Methods chapter (sections 2.3.2 and 2.3.3; Figure 3-5). The means and P-values taken from the multi-variance analysis are presented in Tables 3-4 and 3-5. The BMD analyses for the trabecular and cortical vertebral body are displayed in Table 3-5.

Table 3-4 Vertebral body trabecular bone data for 12 week young adult offspring from control/ protein restricted dams, with control/ high folic acid during the juvenile period. Data displayed as mean \pm SD with associated P-values. Diet groups- C/CFA (control/control folic acid) n=6, C/HFA (C/High folic acid) n=4 , PR/CFA (protein restricted/CFA) n=5 , PR/HFA n=4 and the diet comparisons were JP (juvenile pubertal diet) and M (maternal diet). - indicates no significance.

Males	C/CFA	C/HFA	PR/CFA	PR/HFA	P-values		
Vertebra trabecular	Mean	Mean	Mean	Mean	JP diet	M diet	JP x M diet
Bone volume (mm ³)	7.7 \pm 2.3	9.2 \pm 0.9	8.5 \pm 1.3	10.1 \pm 1.4	-	-	0.03
Bone surface density (1/mm)	11.8 \pm 1.0	11.9 \pm 0.6	11.2 \pm 1.0	11 \pm 0.5	-	-	-
Trabecular pattern factor (1/mm)	-1.5 \pm 2.0	-2.5 \pm 1.4	-1.0 \pm 1.6	-2.4 \pm 0.8	-	-	-
Structure model index	0.6 \pm 0.3	0.5 \pm 0.1	0.6 \pm 0.2	0.5 \pm 0.0	-	-	-
Trabecular thickness (mm)	0.1 \pm 0.0	0.1 \pm 0.0	0.1 \pm 0.0	0.1 \pm 0.0	-	-	-
Trabecular number (1/mm)	0.2 \pm 0.0	0.2 \pm 0.0	0.2 \pm 0.0	0.2 \pm 0.0	-	-	-
Trabecular separation (mm)	3.4 \pm 0.3	3.4 \pm 0.2	3.2 \pm 0.3	3.3 \pm 0.1	-	-	-
Degree of anisotropy	1.5 \pm 0.4	1.6 \pm 0.3	1.7 \pm 0.2	1.7 \pm 0.1	-	-	-
Fractal dimension	2.4 \pm 0.0	2.4 \pm 0.0	2.4 \pm 0.0	2.4 \pm 0.0	-	-	-
Connectivity density (1/mm ³)	114 \pm 23	111 \pm 9	98 \pm 15	105 \pm 14	-	-	-
Females							
Bone volume (mm ³)	6.8 \pm 0.9	7.1 \pm 0.9	6.8 \pm 0.6	8.2 \pm 0.6	-	-	0.01
Bone surface density (1/mm)	12.3 \pm 0.8	12.9 \pm 0.8	12.4 \pm 0.7	12.6 \pm 0.8	-	-	-
Trabecular pattern factor (1/mm)	-3.9 \pm 1.4	-3.8 \pm 2.7	-3.7 \pm 1.7	-4.5 \pm 1.0	-	-	-
Structure model index	0.3 \pm 0.3	0.4 \pm 0.5	0.3 \pm 0.2	0.2 \pm 0.3	-	-	-
Trabecular thickness (mm)	0.1 \pm 0.0	0.1 \pm 0.0	0.1 \pm 0.0	0.1 \pm 0.0	-	-	-
Trabecular number (1/mm)	0.2 \pm 0.0	0.2 \pm 0.0	0.2 \pm 0.0	0.2 \pm 0.0	-	-	-
Trabecular separation (mm)	3.6 \pm 0.3	3.7 \pm 0.4	3.6 \pm 0.2	3.7 \pm 0.2	-	-	-
Degree of anisotropy	2.0 \pm 0.3	2.1 \pm 0.4	1.9 \pm 0.4	1.7 \pm 0.2	-	-	-
Fractal dimension	2.5 \pm 0.0	2.5 \pm 0.0	2.4 \pm 0.0	2.5 \pm 0.0	-	-	-
Connectivity density (1/mm ³)	113 \pm 18	133 \pm 16	117 \pm 19	126 \pm 40	-	-	-

Table 3-5 Vertebral body cortical bone data for 12 week young adult offspring from control/ protein restricted dams, with control/ high folic acid during the juvenile period. Data displayed as mean \pm SD with associated P-values. Diet groups- C/CFA(control/control folic acid) n=6, C/HFA (C/High folic acid) n=4 , PR/CFA (protein restricted/CFA) n=5 , PR/HFA n=4 and the diet comparisons were JP (juvenile pubertal diet) and M (maternal diet). - indicates no significance.

Males	C/CFA	C/HFA	PR/CFA	PR/HFA	P-values		
Vertebra cortical	Mean	Mean	Mean	Mean	JP diet	M diet	JP x M diet
Bone volume (mm ³)	13.6 \pm 2.0	13.8 \pm 0.5	13.1 \pm 1.8	12.7 \pm 1.7	-	-	-
Bone surface density (1/mm)	1.0 \pm 0.2	1.0 \pm 0.0	1.2 \pm 0.2	1.1 \pm 0.1	-	-	-
Trabecular pattern factor (1/mm)	-2.9 \pm 1.8	-3.1 \pm 0.7	-2.5 \pm 1.5	-2.2 \pm 0.8	-	-	-
Structure model index	-0.2 \pm 0.5	-0.3 \pm 0.2	0 \pm 0.3	0 \pm 0.2	-	-	-
Cortical thickness (mm)	0.3 \pm 0.0	0.3 \pm 0.0	0.3 \pm 0.0	0.3 \pm 0.0	-	-	-
Cortical separation (mm)	0.3 \pm 0.1	0.3 \pm 0.1	0.4 \pm 0.1	0.4 \pm 0.0	-	-	-
Degree of anisotropy	0.5 \pm 0.4	2.8 \pm 0.2	2.9 \pm 0.2	2.8 \pm 0.1	-	-	-
Fractal dimension	2.2 \pm 0.0	2.2 \pm 0.0	2.2 \pm 0.0	2.2 \pm 0.0	-	-	-
Connectivity density (1/mm ³)	3.6 \pm 1.3	3.7 \pm 1.0	3.8 \pm 1.0	3.4 \pm 0.8	-	-	-
Females							
Bone volume (mm ³)	8.4 \pm 0.8	9.8 \pm 0.5	10.1 \pm 0.9	10.2 \pm 1.2	0.03	<0.01	0.01
Bone surface density (1/mm)	1 \pm 0.2	0.8 \pm 0.5	1.1 \pm 0.3	0.8 \pm 0.2	-	-	-
Trabecular pattern factor (1/mm)	-1.2 \pm 0.9	-2.6 \pm 0.6	-2.4 \pm 1.3	-1.6 \pm 0.8	0.03	0.03	-
Structure model index	0.4 \pm 0.3	-0.1 \pm 0.4	0.1 \pm 0.3	0.3 \pm 0.3	0.02	-	-
Cortical thickness (mm)	0.2 \pm 0.0	0.3 \pm 0.0	0.3 \pm 0.0	0.3 \pm 0.0	<0.01	-	-
Cortical separation (mm)	0.3 \pm 0.1	0.3 \pm 0.2	0.4 \pm 0.1	0.3 \pm 0.1	-	-	-
Degree of anisotropy	3.0 \pm 0.1	2.8 \pm 0.2	2.7 \pm 0.4	2.8 \pm 0.7	-	-	-
Fractal dimension	2.2 \pm 0.0	2.2 \pm 0.0	2.2 \pm 0.10	2.2 \pm 0.0	-	-	-
Connectivity density (1/mm ³)	2.9 \pm 1.4	2.5 \pm 2.2	3.8 \pm 1.5	2.2 \pm 0.6	-	-	-

Table 3-6 Vertebral body bone mineral density (BMD) data for 12 week young adult offspring from control/ protein restricted dams, with control/ high folic acid during the juvenile period. Data displayed as mean \pm SD with associated P-values. Diet groups- C/CFA(control/control folic acid) n=6, C/HFA (C/High folic acid) n=4 , PR/CFA (protein restricted/CFA) n=5 , PR/HFA n=4 and the diet comparisons were JP (juvenile pubertal diet) and M (maternal diet). - indicates no significance.

	C/CFA	C/HFA	PR/CFA	PR/HFA	P-value		
	Mean	Mean	Mean	Mean	JP diet	M diet	JP x M diet
Males							
Vertebral body trabecular bone	0.96 \pm 0.07	0.99 \pm 0.04	0.94 \pm 0.09	0.95 \pm 0.05	-	-	-
Vertebral body cortical bone	1.71 \pm 0.05	1.69 \pm 0.05	1.62 \pm 0.05	1.59 \pm 0.07	-	-	0.03
Females							
Vertebral body trabecular bone	1.01 \pm 0.12	1.00 \pm 0.06	1.01 \pm 0.07	1.04 \pm 0.02	-	-	-
Vertebral body cortical bone	1.69 \pm 0.13	1.62 \pm 0.05	1.66 \pm 0.07	1.66 \pm 0.06	-	-	-

Trabecular vertebral body

In the trabecular vertebral body (Table 3-4), only the combined juvenile and maternal diet produced significant differences compared to controls. The bone volume was significantly higher for both male and female offspring ($P=0.03$ and $P=0.01$ respectively). This combination of maternal low protein and juvenile high folic acid increases bone volume but does not have an effect on the overall trabecular structure at this site.

Cortical vertebral body

However, more significant differences were seen in the cortical vertebral body (Table 3-5) in the female offspring. The largest effects were caused by the juvenile high folic acid diet in females, with increases in bone volume ($P=0.03$) and cortical thickness ($P<0.01$) and decreases in structural model index ($P=0.02$) and trabecular pattern factor ($P=0.03$) compared to controls. These changes indicate a thicker more concave structure, that would result in a stronger cortical vertebra in the C/HFA females.

Effects were also seen in female young adult rats in response to a low protein maternal diet, with an increase in bone volume ($P<0.01$) and decrease in trabecular pattern factor ($P=0.03$) compared to controls. This again would result in a stronger structure.

The combination of maternal low protein and juvenile high folic acid resulted in increased bone volume ($P=0.01$) in young adult females compared to controls. The combination diet PR/HFA reduced the BMD of the cortical vertebral body in male young adult rats ($P=0.03$; Table 3-6).

3.3.3.2 Femur micro CT analysis

The femur μ CT scans were reconstructed into 3D volumes as illustrated in Figure 3-6 and imported into CTAn. Each of the trabecular sample sites were then analysed using the method described in the General Methods (section 2.3.2, 2.3.3. and 2.3.7.1). Three trabecular areas were examined in the femur; the femoral head, femoral neck and distal femur. The cortical bone in the femur was investigated at the cortical midshaft using the .tiff images imported into VGStudioMax.

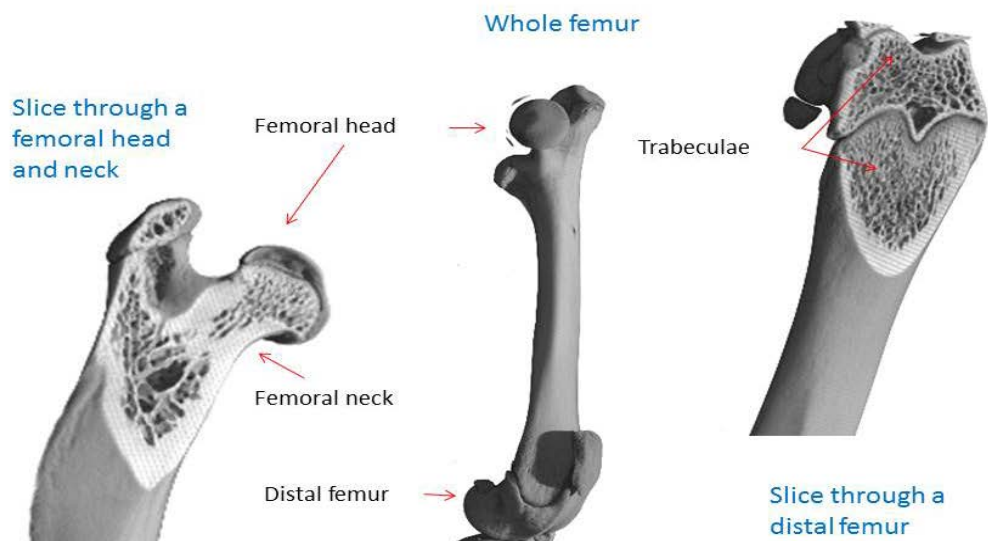


Figure 3-6 3D reconstruction of a whole femur (middle), a femoral head (left) and distal femur (right). The femoral head and distal femur have been digitally clipped in order to show the internal trabecular structures using VG

Figure 3-7 is a digitally clipped slice through the femoral head and neck of a femur and is provided as a guide to where the cuboid sections of trabecular bone from for the femoral head and neck were selected for analysis. The cuboids are not dimensionally accurate (only provided for illustration purposes). For the accurate dimensions and methods followed, see General methods (section 2.3.3.).

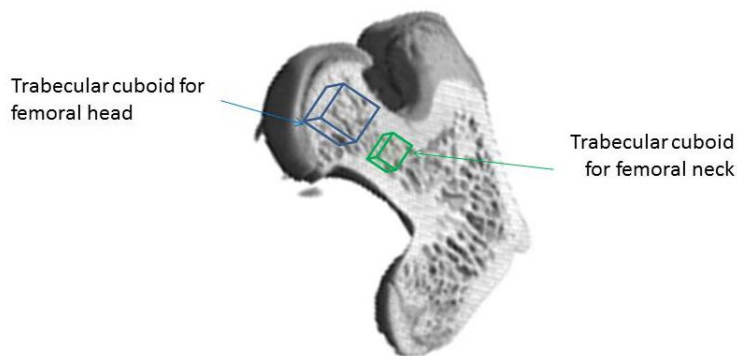


Figure 3-7 3D reconstruction of femoral head and neck, digitally clipped to display the trabecular in the inner structure, with cuboids to illustrate sections segmented for trabecular analysis for both the femoral head (blue) and neck (green).

The means \pm SD and P-values from the multivariate analysis are shown for the head of femur (Table 3-7) and neck of femur (Table 3-8).

Table 3-7 Femoral head trabecular bone data for 12 week young adult offspring from control/ protein restricted dams, with control/ high folic acid during the juvenile period. Data displayed as mean \pm SD with associated P-values. Diet groups- C/CFA(control/control folic acid) n=6, C/HFA (C/High folic acid) n=4 , PR/CFA (protein restricted/CFA) n=5 , PR/HFA n=4 and the diet comparisons were JP (juvenile pubertal diet) and M (maternal diet). - indicates no significance.

Males	C/CFA	C/HFA	PR/CFA	PR/HFA	P-values		
					JP diet	M diet	JP x M diet
Vertebra trabecular	Mean	Mean	Mean	Mean			
Bone volume (mm ³)	1.5 \pm 0.1	1.5 \pm 0.1	1.6 \pm 0.1	1.5 \pm 0.1	-	-	-
Bone surface density (1/mm)	14.3 \pm 0.4	14.8 \pm 1.1	13.8 \pm 0.2	14.5 \pm 0.4	-	-	-
Trabecular pattern factor (1/mm)	-7.7 \pm 2.5	-9.4 \pm 5.0	-7.7 \pm 2.4	-6.0 \pm 1.7	-	-	-
Structure model index	-0.1 \pm 0.4	-0.2 \pm 0.5	-0.2 \pm 0.3	0.1 \pm 0.3	-	-	-
Trabecular thickness (mm)	0.1 \pm 0.0	0.1 \pm 0.0	0.2 \pm 0.0	0.1 \pm 0.0	-	-	-
Trabecular number (1/mm)	4.3 \pm 0.2	4.5 \pm 0.4	4.2 \pm 0.1	4.3 \pm 0.2	-	-	-
Trabecular separation (mm)	0.1 \pm 0.0	0.1 \pm 0.0	0.1 \pm 0.0	0.1 \pm 0.0	-	-	-
Degree of anisotropy	1.8 \pm 0.1	2.0 \pm 0.3	2.0 \pm 0.4	2.2 \pm 0.4	-	-	0.03
Fractal dimension	2.7 \pm 0.0	2.7 \pm 0.1	2.7 \pm 0.0	2.6 \pm 0.0	-	-	-
Connectivity density (1/mm ³)	102 \pm 14	108 \pm 23	84 \pm 9	104 \pm 16	-	-	-
Females							
Bone volume (mm ³)	1.8 \pm 0.2	1.6 \pm 0.2	1.6 \pm 0.2	1.6 \pm 0.4	-	-	-
Bone surface density (1/mm)	13.3 \pm 0.6	15.1 \pm 0.5	14.0 \pm 0.7	14.5 \pm 1.7	-	-	-
Trabecular pattern factor (1/mm)	-12.3 \pm 4.2	-14.9 \pm 1.8	-10.2 \pm 4.4	-10.7 \pm 4.2	-	-	-
Structure model index	-1.1 \pm 0.7	-1.1 \pm 0.3	-0.7 \pm 0.9	-0.6 \pm 1.0	-	-	-
Trabecular thickness (mm)	0.2 \pm 0.0	0.1 \pm 0.0	0.2 \pm 0.0	0.2 \pm 0.0	-	-	-
Trabecular number (1/mm)	4.3 \pm 0.2	4.8 \pm 0.3	4.3 \pm 0.2	4.1 \pm 0.4	-	-	-
Trabecular separation (mm)	0.1 \pm 0.0	0.1 \pm 0.0	0.1 \pm 0.0	0.1 \pm 0.0	-	-	-
Degree of anisotropy	1.9 \pm 0.1	1.9 \pm 0.3	2.1 \pm 0.3	1.9 \pm 0.1	-	-	-
Fractal dimension	2.7 \pm 0.0	2.7 \pm 0.0	2.6 \pm 0.0	2.6 \pm 0.0	-	-	-
Connectivity density (1/mm ³)	62 \pm 7	94 \pm 12	79 \pm 22	121 \pm 84	-	-	-

Table 3-8 Femoral neck trabecular bone data for 12 week young adult offspring from control/ protein restricted dams, with control/ high folic acid during the juvenile period. Data displayed as mean \pm SD with associated P-values. Diet groups- C/CFA(control/control folic acid) n=6, C/HFA (C/High folic acid) n=4 , PR/CFA (protein restricted/CFA) n=5 , PR/HFA n=4 and the diet comparisons were JP (juvenile pubertal diet) and M (maternal diet). - indicates no significance.

<i>Males</i>	C/CFA	C/HFA	PR/CFA	PR/HFA	P-value		
	Mean	Mean	Mean	Mean	JP diet	M diet	JP x M diet
Bone volume (mm ³)	0.22 \pm 0.02	0.20 \pm 0.01	0.21 \pm 0.03	0.17 \pm 0.01	0.05	-	<0.001
Bone surface density (1/mm)	17.0 \pm 0.8	15.8 \pm 0.5	16.4 \pm 0.5	16 \pm 0.6	<0.01	-	0.02
Trabecular pattern factor (1/mm)	-0.5 \pm 1.4	2.4 \pm 0.5	0.9 \pm 3.3	3.9 \pm 1.3	0.03	-	<0.01
Structure model index	1.0 \pm 0.2	1.3 \pm 0.1	1.2 \pm 0.3	1.5 \pm 0.2	0.01	-	<0.001
Trabecular thickness (mm)	0.14 \pm 0.01	0.14 \pm 0.01	0.14 \pm 0.02	0.13 \pm 0.01	-	-	-
Trabecular number (1/mm)	4.5 \pm 0.2	4.1 \pm 0.1	4.2 \pm 0.3	4.0 \pm 0.5	0.03	-	<0.01
Trabecular separation (mm)	0.13 \pm 0.01	0.15 \pm 0.01	0.14 \pm 0.01	0.15 \pm 0.01	0.01	0.01	<0.001
Degree of anisotropy	2.5 \pm 0.4	2.3 \pm 0.4	2.7 \pm 0.3	2.5 \pm 0.2	-	-	-
Fractal dimension	2.5 \pm 0.1	2.5 \pm 0.0	2.5 \pm 0.0	2.5 \pm 0.0	-	-	-
Connectivity density (1/mm ³)	91 \pm 32	77 \pm 14	83 \pm 7	85 \pm 15	-	-	-
<i>Females</i>							
Bone volume (mm ³)	0.23 \pm 0.02	0.23 \pm 0.02	0.23 \pm 0.02	0.20 \pm 0.04	-	-	-
Bone surface density (1/mm)	16.8 \pm 0.5	17.3 \pm 0.8	16.6 \pm 0.4	16.3 \pm 1.0	-	-	-
Trabecular pattern factor (1/mm)	-1.2 \pm 2.6	-2.7 \pm 2.7	-0.8 \pm 2.7	0.8 \pm 4.4	-	-	-
Structure model index	0.9 \pm 0.3	0.9 \pm 0.2	1.0 \pm 0.3	1.2 \pm 0.4	-	-	-
Trabecular thickness (mm)	0.15 \pm 0.01	0.14 \pm 0.02	0.15 \pm 0.01	0.14 \pm 0.02	-	-	-
Trabecular number (1/mm)	0.13 \pm 0.01	0.12 \pm 0.01	0.14 \pm 0.0	0.14 \pm 0.02	-	-	-
Trabecular separation (mm)	4.5 \pm 0.2	4.7 \pm 0.3	4.2 \pm 0.1	4.0 \pm 0.5	-	-	-
Degree of anisotropy	2.7 \pm 0.6	2.5 \pm 0.3	3.1 \pm 0.5	2.4 \pm 0.4	-	-	-
Fractal dimension	2.5 \pm 0.1	2.6 \pm 0.0	2.5 \pm 0.0	2.5 \pm 0.1	-	-	-
Connectivity density (1/mm ³)	75 \pm 9.0	95 \pm 22	84 \pm 12	90 \pm 14	0.03	-	-

Trabecular head of femur

As shown in Table 3-7 both the juvenile and maternal diets had no significant difference on the trabecular head of femur for either male or female young adult rats.

However, the combination of low protein maternal diet and high folic acid juvenile diet in male young adult rats resulted in a significantly higher degree of anisotropy ($P=0.03$) than controls. A more anisotropic trabecular structure would result in an increase in trabecular strength along multiple directional planes- this would therefore lead to a stronger trabecular bone.

Trabecular neck of femur

Significant differences were observed in 84-day young adult male rats with high folic acid during the juvenile period (Table 3-8) compared to controls. C/HFA males showed decreases in bone volume ($P=0.05$), bone surface density ($P<0.01$) and trabecular number ($P=0.03$) and increases in trabecular pattern factor ($P=0.03$), structural model index ($P=0.01$) and trabecular separation ($P=0.01$), therefore resulting in a weaker trabecular structure compared to controls. Female C/HFA young adult rats showed an increase in connectivity density ($P=0.03$) when compared to controls.

Maternal low protein significantly increased trabecular separation ($P=0.01$) in male young adult rats compared to controls- which would result in a weaker trabecular structure.

In young adult male rats, when maternal low protein is combined with the high juvenile folic acid the differences observed for C/HFA are magnified. The PR/HFA males again showed decreases in bone volume ($P<0.001$), bone surface density ($P=0.02$) and trabecular number ($P<0.01$) and increases in trabecular pattern factor ($P<0.01$), structural model index ($P<0.001$) and trabecular separation ($P<0.001$), which results in a weaker trabecular structure compared to controls.

Figure 3-8 shows a 3D μ CT volume that has been digitally clipped to reveal the trabecular structure inside. The cuboids are an example of the trabecular sections that were separated and analysed. For the exact dimensions of the cuboids for the femoral head and neck, see General methods (section 2.5.3).

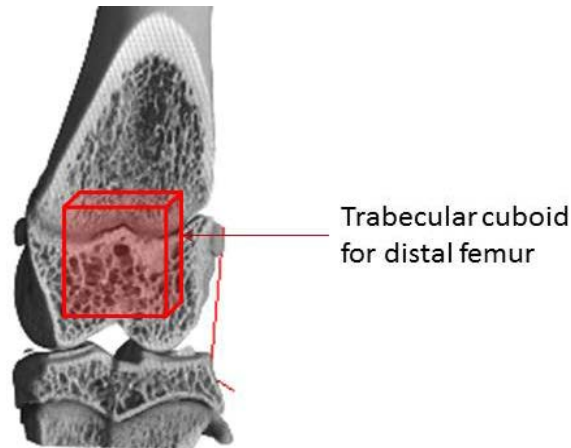


Figure 3-8 3D reconstruction of distal femur that has been digitally clipped to display the trabecular in the inner structure, with a cuboid to illustrate the section segmented for trabecular analysis for the distal femur (red).

The trabecular distal femur means \pm SD and P-values for the multivariate analysis model are shown in Table 3-9.

Table 3-9 Distal femur trabecular bone data for 12 week young adult offspring from control/ protein restricted dams, with control/ high folic acid during the juvenile period. Data displayed as mean \pm SD with associated P-values. Diet groups- C/CFA(control/control folic acid) n=6, C/HFA (C/High folic acid) n=4 , PR/CFA (protein restricted/CFA) n=5 , PR/HFA n=4 and the diet comparisons were JP (juvenile pubertal diet) and M (maternal diet). - indicates no significance.

<i>Males</i>	C/CFA	C/HFA	PR/CFA	PR/HFA	P-value		
	Mean	Mean	Mean	Mean	JP diet	M diet	JP x M diet
Vertebra trabecular							
Bone volume (mm ³)	6.3 \pm 0.6	6.2 \pm 0.7	6 \pm 0.6	6.1 \pm 0.2	-	-	-
Bone surface density (1/mm)	10.7 \pm 0.9	10 \pm 1.0	10.3 \pm 1.0	10.1 \pm 0.5	-	-	-
Trabecular pattern factor (1/mm)	-8.9 \pm 1.9	-8.3 \pm 3.6	-7.1 \pm 2.5	-7.5 \pm 1.4	-	-	-
Structure model index	-0.2 \pm 0.3	-0.3 \pm 0.4	0.1 \pm 0.4	-0.1 \pm 0.1	-	-	-
Trabecular thickness (mm)	0.2 \pm 0.0	0.2 \pm 0.0	0.2 \pm 0.0	0.2 \pm 0.0	-	-	-
Trabecular number (1/mm)	2.8 \pm 0.2	2.8 \pm 0.2	2.7 \pm 0.3	2.7 \pm 0.1	-	-	-
Trabecular separation (mm)	0.2 \pm 0.0	0.3 \pm 0.1	0.3 \pm 0.1	0.2 \pm 0.0	-	-	-
Degree of anisotropy	1.4 \pm 0.1	1.3 \pm 0.1	1.3 \pm 0.1	1.3 \pm 0.1	-	-	-
Fractal dimension	2.5 \pm 0.0	2.5 \pm 0.0	2.5 \pm 0.1	2.5 \pm 0.0	-	-	-
Connectivity density (1/mm ³)	98 \pm 19	85 \pm 25	92 \pm 22	85 \pm 15	-	-	-
<i>Females</i>							
Bone volume (mm ³)	6.2 \pm 0.5	6.4 \pm 0.3	6.6 \pm 0.5	5.9 \pm 0.6	-	-	-
Bone surface density (1/mm)	10.0 \pm 0.7	10.8 \pm 0.1+	11.0 \pm 0.9	9.7 \pm 0.9	-	0.03	-
Trabecular pattern factor (1/mm)	-7.3 \pm 1.6	-9.3 \pm 1.5	-10.3 \pm 4.5	-6.3 \pm 2.5	-	-	-
Structure model index	-0.4 \pm 0.2	-0.5 \pm 0.2	-0.5 \pm 0.4	-0.01 \pm 0.5	-	-	-
Trabecular thickness (mm)	0.2 \pm 0.0	0.2 \pm 0.0	0.2 \pm 0.0	0.2 \pm 0.0	-	-	-
Trabecular number (1/mm)	2.9 \pm 0.2	3.1 \pm 0.1	3.1 \pm 0.3	2.7 \pm 0.3	-	-	-
Trabecular separation (mm)	0.2 \pm 0.0	0.2 \pm 0.0	0.2 \pm 0.0	0.3 \pm 0.1	-	-	-
Degree of anisotropy	1.3 \pm 0.1	1.3 \pm 0.1	1.2 \pm 0.1	1.3 \pm 0.1	-	0.04	-
Fractal dimension	2.5 \pm 0.0	2.5 \pm 0.0	2.6 \pm 0.1	2.5 \pm 0.1	-	-	-
Connectivity density (1/mm ³)	65 \pm 15	83 \pm 10	98 \pm 35	66 \pm 15	-	0.01	-

Trabecular distal femur

A maternal low protein diet give rise to a decrease in bone surface density (P=0.03), degree of anisotropy (P=0.04) and an increase in connectivity density (P=0.01) in young female offspring compared to controls (Table 3-9) - showing a change in trabeculae arrangement with a less dense surface structure with increased connectivity.

The midshaft cortical femur means \pm SD and P-values for the multivariate analysis model for 12 week young adult offspring from either C/PR dams, with either CFA/HFA during the juvenile period are shown in Table 3-10 and the whole femur BMD histograms are shown in Figures 3-9 and 3-10.

Table 3-10 Midshaft cortical femur μ CT data for 12 week young adult offspring from control/ protein restricted dams, with control/ high folic acid during the juvenile period. Data displayed as mean \pm SD with associated P-values. Diet groups- C/CFA(control/control folic acid) n=6, C/HFA (C/High folic acid) n=4 , PR/CFA (protein restricted/CFA) n=5 , PR/HFA n=4 and the diet comparisons were JP (juvenile pubertal diet) and M (maternal diet). - indicates no significance.

Males	C/CFA	C/HFA	PR/CFA	PR/HFA	P-value		
	Mean	Mean	Mean	Mean	JP diet	M diet	JP x M diet
Vertebra trabecular							
Cortical area (mm ²)	6897 \pm 686	5935 \pm 952	6760 \pm 527	6751 \pm 112	-	-	-
Lumen area (mm ²)	1444 \pm 241	1599 \pm 405	1698 \pm 285	1835 \pm 223	-	-	-
Wall mean thickness (mm)	0.71 \pm 0.05	0.60 \pm 0.06	0.66 \pm 0.04	0.64 \pm 0.03	<0.001	-	0.02
Cross sectional moment of inertia (CSMI) x 10 ⁹	8.8 \pm 1.8	7.7 \pm 2.7	9.43 \pm 1.7	9.83 \pm 8.9	-	-	-
Females							
Cortical area (mm ²)	5566 \pm 103	5057 \pm 245	5496 \pm 261	5810 \pm 524	-	-	-
Lumen area (mm ²)	1145 \pm 35	1389 \pm 132	1295 \pm 200	10.39 \pm 235	-	-	-
Wall mean thickness (mm)	0.64 \pm 0.01	0.55 \pm 0.02	0.61 \pm 0.04	0.70 \pm 0.08	-	-	-
Cross sectional moment of inertia (CSMI) x 10 ⁹	5.65 \pm 2.0	5.56 \pm 6.0	5.97 \pm 6.32	5.71 \pm 8.34	-	-	-

Figure 3-9 Whole femur bone mineral density data for male 12 week young adult offspring from C (control)/ PR (protein restricted) dams, with CFA (control folic acid)/ HFA (high folic acid) during the juvenile period. Data displayed as mean \pm SD.

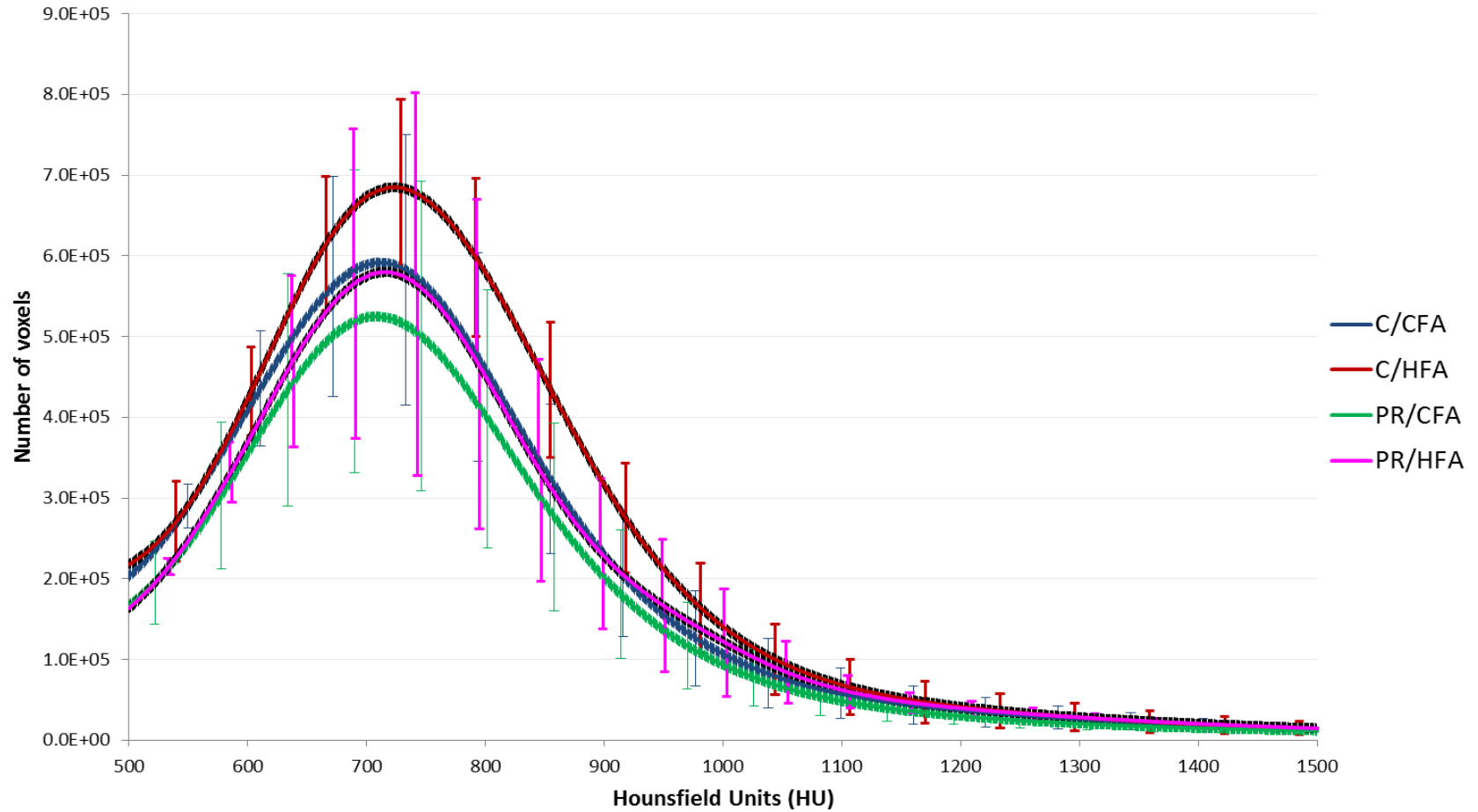
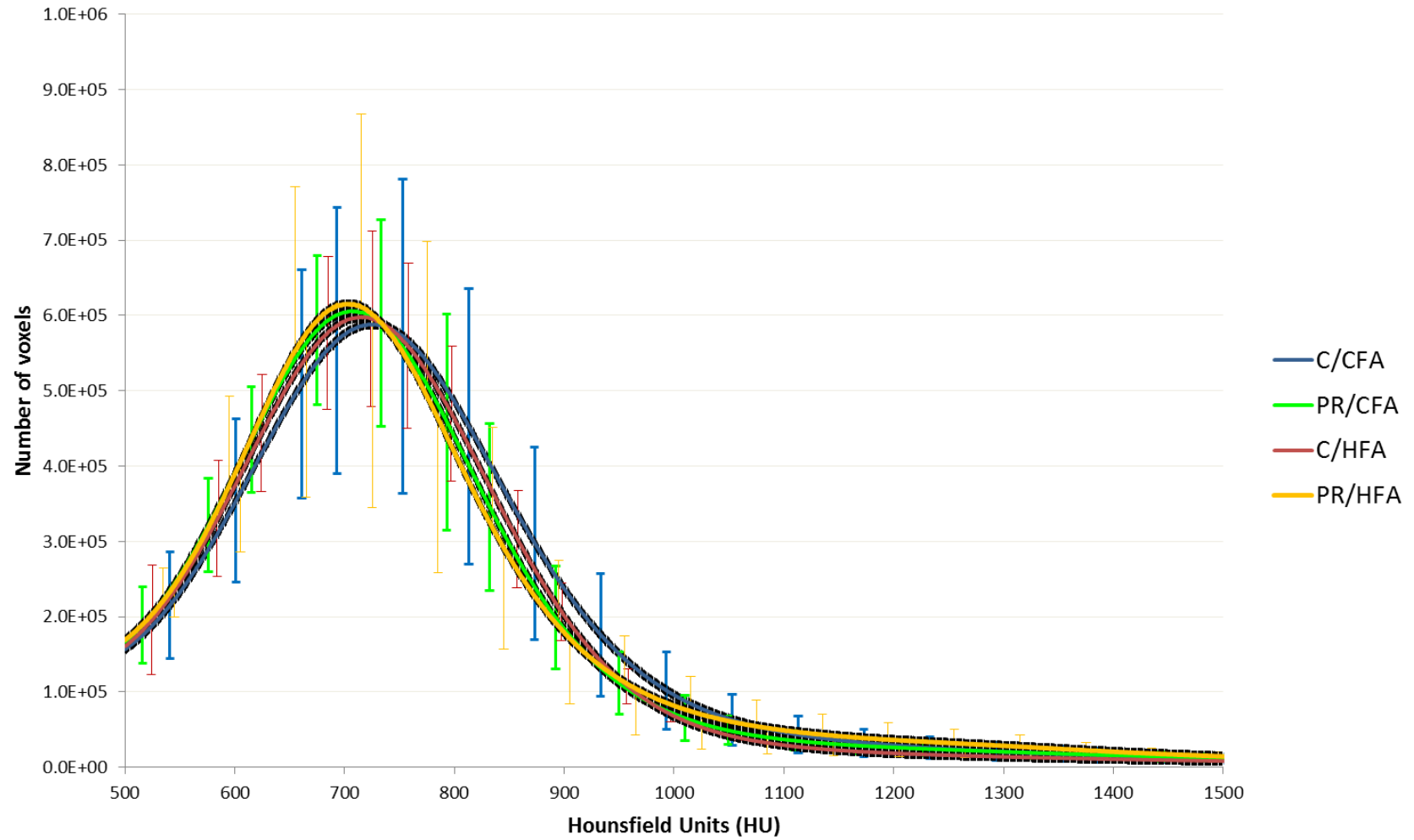


Figure 3-10 Whole femur bone mineral density data for female 12 week young adult offspring from C (control)/ PR (protein restricted) dams, with CFA (control folic acid)/ HFA (high folic acid) during the juvenile period. Data displayed as mean \pm SD.



Midshaft cortical femur

The midshaft cortical femur in female offspring (Table 3-10) showed a decreased wall mean thickness due to the high folic acid juvenile diet ($P < 0.001$) and combined maternal and juvenile diet PR/HFA ($P = 0.02$) compared to controls. A decrease in wall mean thickness would lead to a weaker cortical midshaft.

Whole femur BMD

Figure 3-9 represents the BMD values of young adult males from all diet groups. The largest difference is seen between the C/HFA and the PR/CFA groups with the C/HFA group having more dense bone in the femur. This has not been analysed for statistical significance at this point and is therefore just a qualitative observation.

Figure 3-10 represents the BMD values of young adult females from all diet groups, which appear very similar although again this is just a qualitative observation.

3.3.4 Three point bend testing

Midshaft femur three point bend testing data for 12 week young adult offspring from control/ protein restricted dams, with control/ high folic acid during the juvenile period is displayed below in Table 3-11.

Table 3-11 Midshaft femur three point bend testing data for 12 week young adult offspring from control/ protein restricted dams, with control/ high folic acid during the juvenile period. Data displayed as mean \pm SD with associated P-values. Diet groups- C/CFA(control/control folic acid) n=6, C/HFA (C/High folic acid) n=4 , PR/CFA (protein restricted/CFA) n=5 , PR/HFA n=4 and the diet comparisons were JP (juvenile pubertal diet) and M (maternal diet). – indicates no significance.

	C/CFA	C/HFA	PR/CFA	PR/HFA	P-value		
	Mean	Mean	Mean	Mean	JP diet	M diet	JP x M diet
Males							
Max load at ultimate failure (N)	166.4 \pm 15.8	138.2 \pm 19.1	156.6 \pm 25.1	151.81 \pm 10.6	–	–	–
Max displacement at ultimate failure (mm)	0.96 \pm 0.31	1.49 \pm 0.28	1.07 \pm 0.29	1.29 \pm 0.3	–	–	–
Max load at total displacement (N)	165.4 \pm 15.9	134.9 \pm 23.5	151 \pm 17.5	138.7 \pm 15.8	–	–	–
Max displacement at total displacement (N)	1.0 \pm 0.39	1.67 \pm 0.20	1.23 \pm 0.41	1.56 \pm 0.4	–	–	–
Work to failure (J)	85.8 \pm 6.6	128.5 \pm 21.3	1.7.7 \pm 71.9	135.0 \pm 47.9	–	–	–
Stiffness (N/mm)	300 \pm 43	201 \pm 69	246.8 \pm 70.8	232 \pm 80	–	–	–
Females							
Max load at ultimate failure (N)	118.1 \pm 5.7	104 \pm 5.97	114 \pm 12.1	108.7 \pm 6.2	0.05	–	–
Max displacement at ultimate failure (mm)	1.18 \pm 0.24	1.05 \pm 0.10	1.08 \pm 0.24	1.16 \pm 0.30	–	–	–
Max load at total displacement (N)	118.1 \pm 15.8	103 \pm 5.26	111.2 \pm 116.3	106.3 \pm 8.2	–	–	–
Max displacement at total displacement (N)	1.19 \pm 0.25	1.12 \pm 0.15	1.28 \pm 0.22	1.27 \pm 0.0.33	–	–	–
Work to failure (J)	78 \pm 4.7	79 \pm 13.7	91 \pm 19.4	98 \pm 29.9	–	–	–
Stiffness (N/mm)	181 \pm 16	157 \pm 7	169 \pm 21	171 \pm 37	–	–	–

Three point bend testing

Neither the juvenile, maternal nor combination diets induced statistically significant results in the male young adult rats (Table 3-11). The juvenile diet did however significantly reduce the maximum load at ultimate failure in female rat offspring at 12 weeks compared to controls ($P=0.05$). $N=3$ samples are shown here for the PR/HFA diet both male and female due to sample complications resulting in unsuitable results.

3.3.5 Body weight of animals

The weights of the young adult rats discussed in this chapter are not available, but the weights of young adult rat offspring from the same cohort are available from Burdge et al. (2009) as shown in Figure 3-11. As mentioned in the figure legend below, maternal diet did not affect body weight and so the data are not shown. However, for both male and female offspring from either maternal diet additional folic acid during the juvenile stage increased body weight compared to controls. This increase occurred earlier in females than males and was more pronounced in the maternal control groups compared to the maternal PR groups.

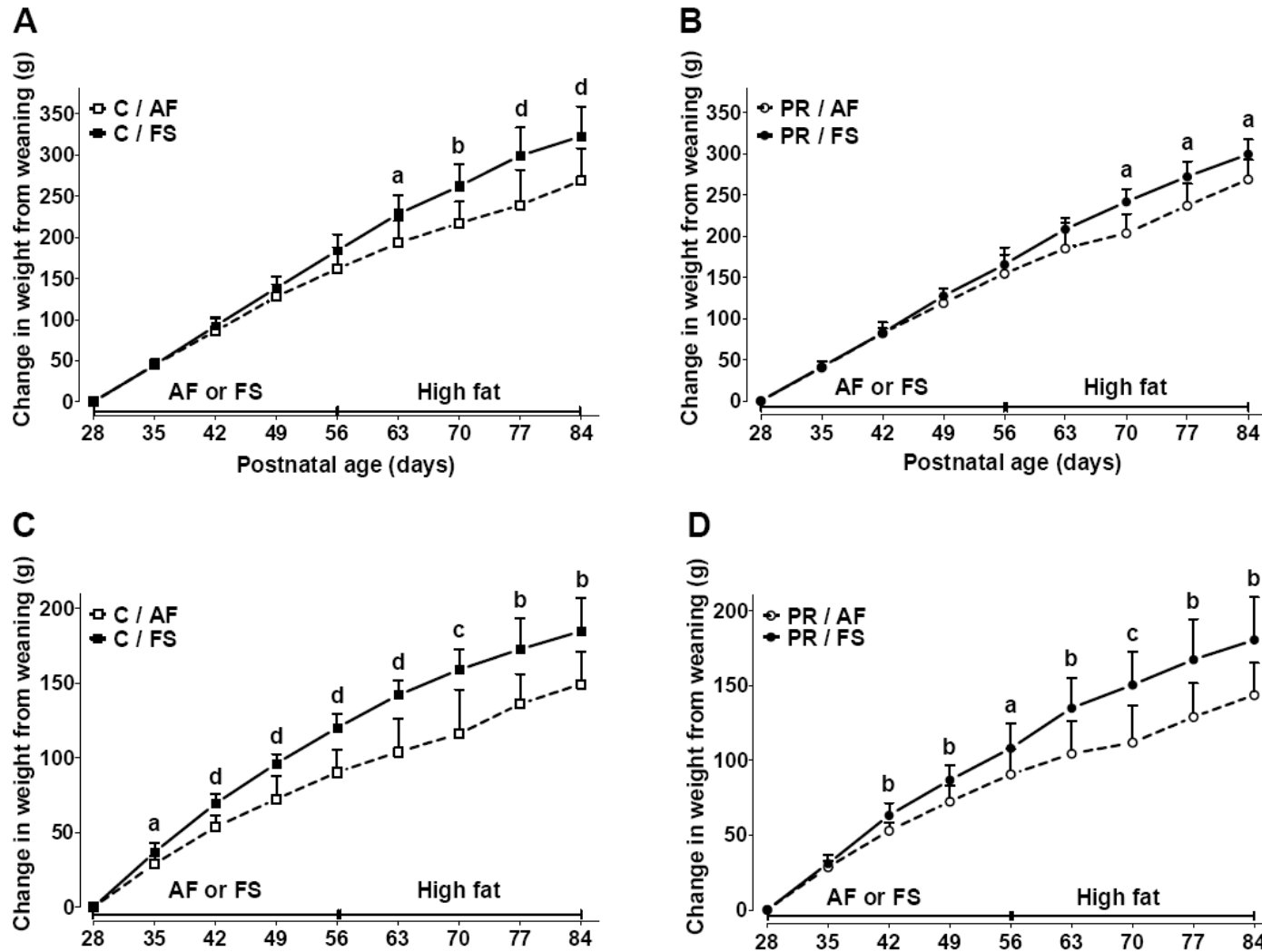


Figure 3-11 from Burdge et al. (2009) Whole body weight gain from weaning (mean \pm 1SD) in (A) male C, (B) male PR, (C) female C and (D) female PR offspring. The periods of feeding diets with different folic acid contents, and the high fat diet are indicated above the x-axis. Comparisons between groups at each time point are indicated by ^a $P < 0.05$, ^b $P < 0.01$, ^c $P < 0.001$ and ^d $P < 0.0001$. Since there were no significant effect of maternal diet, only comparisons between control/control folic acid C/CFA (C/AF) vs. control/ high folic acid C/HFA (C/FS) and protein restricted/ control folic acid PR/CFA (PR/AF) vs. protein restricted/ high folic acid PR/HFA (PR/FS) are shown.

3.3.6 Result summary

Juvenile folic acid supplementation produced site specific effects throughout the vertebra and femur of female young adult rats. Differences that would likely result in stronger bone structures compared to controls were observed at the cortical vertebral body (thicker and more concave) and trabecular neck of femur (increased connectivity). At the midshaft cortical femur the thickness and subsequent strength was reduced by additional juvenile folic acid. It appears that the cortical femur is being sacrificed in order to protect the vertebra in this case. Male young adult rats showed significant differences as a result of folic acid supplementation but only at the trabecular neck of femur. These included decreased bone volume, bone surface density and trabecular number, and increased structural model index, trabecular pattern factor and trabecular separation- resulting in a predicted less concave weaker trabecular structure.

The maternal protein restriction during pregnancy induced potentially advantageous changes at the cortical vertebra and trabecular distal femur in young adult female rat that included- increased bone volume and a more concave thicker cortical vertebra and a less dense but more connective trabecular structure at the distal femur. The young adult male rats were affected adversely by maternal protein restriction at the trabecular neck of femur with an increase in trabecular separation.

The combination of maternal protein restriction during pregnancy and juvenile folic acid addition resulted in complex outcomes for both male and female young adult rats. The combination diet resulted in increased bone volume in the trabecular and cortical vertebral body in female rats which is advantageous but a thinner midshaft cortical which would result in a weaker bone. Again, the vertebra is being prioritised over the midshaft cortical femur. Young adult male rats however adapted differently as result of the combination diet. Similarly to the female rats, male rats had increased bone volume at the cortical vertebral body, but the BMD at this site was reduced. Also, an advantageous adaptation in the trabecular structure is seen at the head of femur with increased anisotropy, but conversely at the neck trabecular neck of femur lower bone

volume is observed. Again, it is evident that adaptations due to the combination diet have been seen in male young adult rats with changes in the cortical vertebral body and the femoral head being prioritised slightly over the femoral neck.

3.4 Discussion

It has previously been shown that protein restriction during pregnancy affects the bone structure of rat offspring (Lanham et al. 2008). Folic acid supplementation during periods of growth, such as pregnancy, has been shown to reverse the negative effects of protein restriction in other tissues (Lillycrop et al. 2005; Torrens et al. 2010, 2006). Puberty is an important growth period for bone and in which additional folic acid may be able to alter the effects of maternal protein restriction. The data displayed in this results chapter show how the addition of folic acid during the juvenile period alters the effect of maternal protein restriction, inducing sex specific effects on the trabecular and cortical bone of male and female young adult rat offspring.

Maternal protein restriction resulted in structural differences in the female offspring and one difference in the male offspring at 12 weeks. Higher bone volume and an enhanced negative trabecular pattern factor at the cortical vertebral body predict a stronger, more concave bone, in the female young adult rats from protein restricted dams. The structure described for the female cortical vertebral body predicts a strong bone that would withstand bone loss due to aging without losing structural integrity. At the distal femur a better-connected but less dense trabecular network was also observed for the female PR/CFA offspring. The outcome for the structure at the distal femur for PR/CFA rats is harder to predict- the decrease in bone surface density will decrease strength while increased connections would likely lead to a more robust trabecular structure. A higher trabecular separation was seen at the neck of femur for the male offspring, which one would expect to result in a weaker structure in later life. In a previous study, Lanham et al. found that maternal protein restriction had a negative effect on the trabecular femoral head and trabecular vertebrae and a positive effect on the trabecular femoral necks in 75 week old female offspring (Lanham et al. 2008). The 12 week female samples studied here produced no significant differences at either the head or neck of femur or trabecular vertebral body, suggesting the differences observed in 75 week samples were not evident at this time point (Lanham et al. 2011). Contrary to the result seen in this study, Lanham et al. found males from protein restricted mothers had significantly longer femurs than those from the

control group at 12 weeks when corrected for mass, but the μ CT analysis showed no differences in the male offspring at 75 weeks (Lanham et al. 2011). No such differences in femur length were observed in this study; however, the high fat diet given to the samples discussed here from day 56 onwards probably accounts for this as an increase in weight would require an increase in bone volume in order to support the extra weight. Burdge et al. found no significant differences in weight between either male or female offspring from protein restricted dams, from birth to 12 weeks (Burdge et al. 2009). Maternal protein restriction produced sex specific differences on 12 week old offspring with a high fat diet from 56-84 days: differences that are likely to be advantageous were observed in the female offspring, and only one difference was observed in male offspring. Previous studies using rat models have shown negative effects from protein restriction during pregnancy: namely hypertension risk (Woods et al. 2001) and brain development issues in early life, and type II diabetes in later life (Fernandez-Twinn et al. 2005). Protein restriction of similar magnitude was found by Woods et al. to impair renal development and to programme adult hypertension in later life (Woods et al. 2001). Fernandez-Twinn et al. showed that the same protein restriction regime in pregnancy resulted in increased insulin resistance and risk of type II diabetes in later life (Fernandez-Twinn et al. 2005). Maternal protein restriction during pregnancy may also affect fetal development, in particular in the brain, by inducing alterations in maternal liver metabolism, as shown by Torrens et al. (2010).

The addition of folic acid to rats between 29-56 days induced strong site specific differences in both female and male young adult rats. In female offspring, folic acid supplementation produced a thicker more concave structure in the cortical vertebral body and increased trabecular connectivity at the neck of femur. These adaptations would likely result in a strong bone structure that could withstand age related bone loss. Conversely the mean wall thickness at the midshaft cortical and subsequent maximum load at ultimate failure was lower for the female C/HFA young adult rats. Male young adult rats with additional folic acid showed substantial differences at the neck of femur compared to controls. A less concave cortical structure with decreased bone volume and a decreased number of trabeculae would strongly suggest folic acid had a specific effect on male juvenile samples that is likely to produce a

weakened structure at this site. There are no previous studies assessing the addition of folic acid during the juvenile period on bone. As described in 3.3.5 Burdge et al. found using animals from the same cohort that the folic acid and high fat regime used in this study significantly increased body weight for both males (from 63 days) and females (from 35 days) (Burdge et al. 2009). The effects observed in the young adult female rats suggest that a predictive adaptive response is evident in which a strong vertebra has been sought at the expense of the midshaft femur strength. This alone may be as a result of the increased weight observed in C/HFA females compared to C/CFA females in this cohort by Burdge et al. One reason that the vertebra is prioritised could be that a strong spine is required to successfully produce offspring. The differences observed in young adult male due to folic acid supplementation are very site specific to the neck of femur. Why these potentially detrimental effects are seen at the neck of femur specifically is not known. It is likely however that the resources required for the C/HFA male rats to grow approximately 50 g heavier have been acquired at the cost of the neck of femur trabecular structure and potentially other organs not investigated here.

While there are no other studies to date concerning juvenile folic acid addition on bone, Huot et al. have investigated the effect of high folic acid (HFA) (20mg/kg feed) during pregnancy and early life (up to 20 weeks), in female rat offspring (Huot et al. 2013). HFA during pregnancy had a negative effect on the femur morphology, bone mineral content (BMC) and biomechanical strength of 20 week old female rats. HFA after weaning resulted in lower L4 anterior posterior width, BMC and bone mineral density (BMD). The folic acid diet used by Huot et al. was four times higher than in this study (5mg/kg feed) and the samples were eight weeks older than the samples discussed here. Furthermore, the L4 vertebra was found to hold significant differences by Huot et al. but the L1-L3 vertebra were not, a result which was not explained in their discussion. The lumbar vertebra investigated here was the L3. However, Huot et al. (2013) results show that folic acid had a negative effect on the vertebra are contradictory to the results reported here that folic acid produced a positive effect on the cortical vertebral body. The effects seen here in the male trabecular neck of femur are in keeping with the Hout et al. results, but Huot et al. only investigated the effects on females. However, different techniques were

used in the analysis; Huot et al. used DEXA scans for BMD and this study used μ CT. The evidence presented by Huot et al. suggests that folic acid supplementation during pregnancy can have potentially detrimental effects on female rat bone density and structure at 20 weeks, but this study has shown that the addition of folic acid during the juvenile stage produced beneficial differences in female 12 week old rats and the differences are sex dependent.

The combined effect of protein restriction and folic acid addition (PR/HFA) was investigated relative to controls without any additional folic acid (C/CFA). The combination of protein restriction during pregnancy and folic acid addition to the juvenile offspring produced site and sex specific changes on the young adult rat offspring. Bone volume was increased at the trabecular and cortical vertebral body in female offspring and a thinner midshaft femur was also observed. The protein restriction and folic acid addition (PR/HFA) had an effect on the female rats similar to that seen for the C/HFA offspring, with the vertebra being prioritised over the midshaft femur although arguably to a lesser extent as the resulting strength of the femur was not compromised but the cortical vertebral body was in this case also affected. The male young adult rats showed a decrease in bone volume at the neck of femur but an increase in anisotropy at the head of femur, and an increase in bone volume at cortical vertebral body but a subsequent decrease in BMD at this site. The effects on male rats at the femur are relatively minor as only one parameter is significant, although this does indicate a response. The changes in the male cortical vertebra are more interesting as the bone volume is increased but there are have been no structural changes, and the BMD has been decreased as well. There is obviously some adaption taking place at the cortical vertebral body but the subsequent predicted outcome of this on the strength of the bone is not clear. The results for the male neck of femur for PR/HFA samples are consistent with the previous results seen for the PR/CFA, C/HFA male rats, all diet combinations affect the trabecular neck of femur in a detrimental manner. Burdge et al. found that with this diet regime both male (after day 70) and female offspring (after day 42) had significantly higher body weight (Burdge et al. 2009). The increased bone volume at the trabecular and cortical vertebral body corresponds with the additional body weight noted by Burdge et al.- as the extra body weight would require a stronger spine. The increased body weight in the males along with the predicted reduced strength observed at the

neck of femur could result in a phenotype with a potential increased likelihood of fracture at the neck of femur in later life. The differences observed for the combination diet at the neck of femur in males may again be as a result of the large increase in weight. This adaptation is probably to increase chances of breeding at the expense of long term bone strength.

Other studies have highlighted the importance of folic acid addition at the correct time point in order to obtain the desired effect. Protein restriction during pregnancy altered the epigenetic regulation of hepatic gene expression as discussed in 3.1 (Lillycrop et al. 2005). Folic acid addition and protein restriction during pregnancy resulted in a reversal of the PR effect on hepatic gene expression. However, Burdge et al. went on to show that the same folic acid addition (during the juvenile period), did not reverse the effects, but resulted in changes to the hepatic gene expression previously unseen (Burdge et al. 2009). Thus, the time point at which folic acid is added to the diet has an effect on the outcome of the diet. The negative outcomes for the male offspring in this study may be due to the time point at which the additional folic acid was given. As other time points have not been investigated at this time this is unconfirmed.

Differences have been observed as a result of all diet combinations. The differences were predominantly observed in the female offspring as previously seen, however significant male data were also observed. Two points must be considered when evaluating this study. It is important to remember that the protein restriction is only a small reduction (from 18% to 9%) and all animals received an isocaloric diet at all times. In addition, the time point studied here was during the growth phase for the rat, in which dietary manipulations may alter the trajectory of the bone development. Previous data from Lanham et al. relates to 75 week old females. At 12 weeks rats would have reached skeletal maturity at 10 weeks of age, but not yet peak bone mass which is at 40 weeks of age (Jee and Yao 2001). Considering this, the differences in the data produced have shown that small changes to the maternal and juvenile diets can have a large impact on bone- whether these changes persist into old age remains to be seen. However, it is known the foundations for strong long lasting bones are established up until peak bone mass and that therefore this

is a very crucial time. Data presented on the effect of protein restriction with additional folic acid, compared to high folic acid controls, on female offspring raise an interesting question considering the folic acid fortification of cereals and bread in the UK- what unexpected effects are the general population encountering due to folic acid supplementation? Thus, however it remains to be determined what effects folic acid fortification is having on development in tissues, such as bone, at other time points.

4. Multigenerational study into the effect of protein restriction during pregnancy (F0) on the bone structure, mechanical properties, and gene expression of offspring up to F3 generation

4.1 Introduction

The effect of maternal protein restriction has been shown to influence hypertension (Harrison and Langley-Evans 2009) and glucose tolerance (Benyshek et al. 2006) in subsequent offspring. The effect of environmental influences on the F1 generation has been shown through epidemiological and animal studies to influence chronic disease states including coronary heart disease, diabetes, and osteoporosis as discussed in Chapter 1. Additional studies have been conducted to establish if the effects extend to the F2 and F3 generations and the mechanisms therein (Figure 4-1).

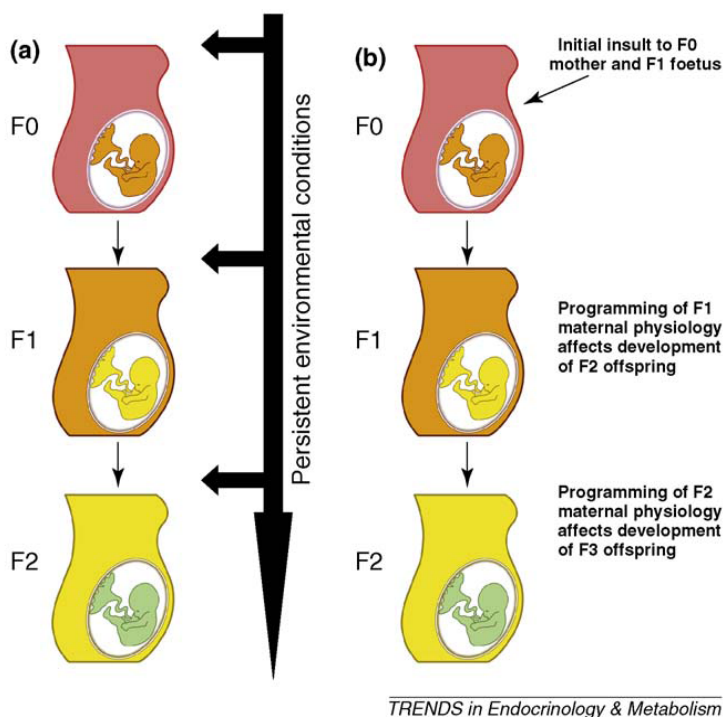


Figure 4-1 Mechanisms for the intergenerational transmission of programming effects. (a) Persistence of an adverse external environment can result in the reproduction of the phenotype in multiple generations. (b) The induction of programmed effects in the F1 offspring following in utero exposure (e.g. programmed changes in maternal physiology or size) results in programmed effects on the developing F2 fetus and so on. Taken from Drake and Liu (2010).

The theory proposed by Drake et al. was that the initial insult to the F0 generation during pregnancy affects the F1 offspring as previously shown, but these effects are seen in the F2 female offspring as the germ cells of the female F1 offspring (which will become the F2 offspring) were developing during the F0 pregnancy (Drake and Liu 2010). The germ cells that would go on to form the F3 offspring were not present during the F0 pregnancy and so should not be epigenetically marked due to the suffered insult.

In order to interrogate the mechanism(s) involved, a number of studies have been conducted. The studies discussed here all have maternal protein restriction during pregnancy as their environmental insult. Burdge et al. showed that maternal protein restriction in rats altered the metabolic phenotype observed, which was seen as discreet methylation changes on gene promoters, were present in F2 males from F0 dams that were protein restricted during pregnancy (Burdge et al. 2007). The effect on F2 females or F3 offspring, was not stated. Harrison et al. showed that F0 protein restriction during pregnancy produced F1 and F2 but not F3 offspring with increased blood pressure in both sexes (Harrison and Langley-Evans 2009). Benyshek et al. demonstrated that F0 rats that were protein restricted during pregnancy went on to produce reduced insulin secretion in the F1 generation and insulin resistance in the F2 generation. Altered glucose–insulin homeostasis was noted in the F3 generation but was less severe than in the F2 generation (Benyshek et al. 2006).

The effect of protein restriction during pregnancy on the offspring's bone structure has been established as discussed in Chapter 1. However the effect on subsequent generations with regards to bone has not been investigated.

Hypothesis

- **Protein restriction during F0 pregnancy reduces bone quality and mechanical properties in F1 and F2, but not F3 offspring**

4.2 Methods

4.2.1 Animal experimentation

Information for animal experimentation was taken from published material by Hoile et al. using these samples (Hoile et al. 2011). Female Wistar rats (about 220 g) obtained from a breeding colony were maintained on standard chow for 14 days and then mated (Figure 4-2). No male was mated with any of its progeny. F0 dams were fed either a control (C) or protein restricted (PR) diet (n= 6 per dietary group) during pregnancy which provided an increase in energy of approximately 25% compared to the diet fed to the breeding colony (Table 4-1). Dams were fed diet 93G from the American Institute for Nutrition (AIN-93G) during lactation and offspring were weaned onto AIN-93M on postnatal day 28. Litters were standardised to 8 offspring within 24 hours of birth, with bias towards females to ensure sufficient stock for mating. F1 and F2 females were mated on postnatal day 70 (n= 6 per F0 dietary group). F1 and F2 dams were fed the control diet during pregnancy and AIN-93G during lactation (Table 4-1). Offspring were weaned onto AIN-93M. All female offspring which were not mated were fasted for 12 hours (20:00 to 08:00) and then killed by carbon dioxide asphyxiation on postnatal day 70. Samples were stored at -80°C. All experimental design up to this point was carried out by Hoile et al. Once defrosted, femurs were taken for molecular analysis and lumbar spine and femurs were taken for anthropometric analysis, μ CT, microindentation and three point bend testing.

Table 4-1 Diet compositions. PR-protein restriction

	Pregnancy Diets		Lactation Diet	Maintenance diet
	Control (all generations)	PR (F0 generation)	AIN-93G	AIN-93M
Caesin (g/kg)	18.3	92	200	140
Cornstarch (g/kg)	420	482	397	466
Sucrose (g/kg)	213	243	100	100
Choline (g/kg)	2.8	2.8	2.5	2.5
Methionine (g/kg)	9.7	7.4	5.2	3.6
Crude fibre (g/kg)	50	50	50	50
Oil (g/kg)	100	100	70	40
Total metabolisable energy (MJ/kg)	17.2	17.4	16.4	15.78

All diets were supplied by PMI Nutrition International.

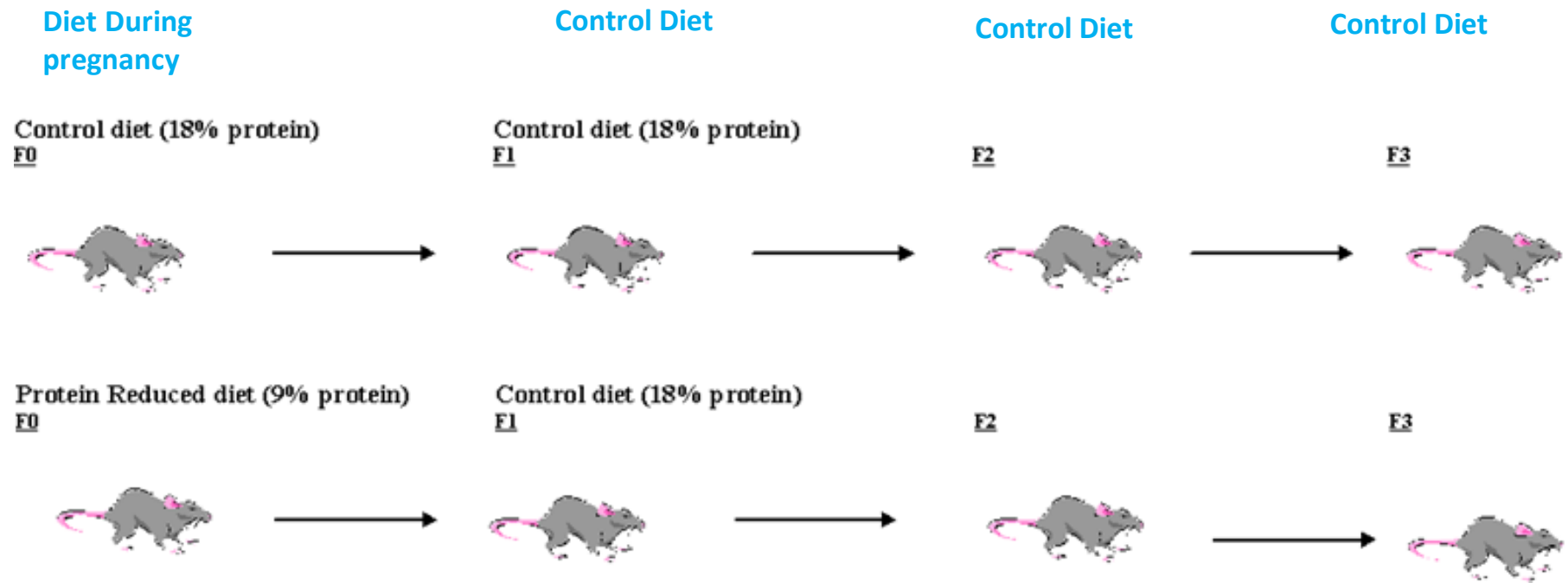


Figure 4-2 Simplified schematic of the study design and dietary manipulations

4.2.2 Anthropometric analysis of femurs

All experimentation and data analysis were carried out as in General methods sections 2.1.1 and 2.1.2.

4.2.3 Micro computed tomography

All experimentation and data analysis were carried out as in General methods sections 2.3.1, 2.3.5, 2.3.6 and 2.3.7.2.

4.2.4 Bone mineral density

All experimentation and data analysis were carried out as in General methods sections 2.4.2.

4.2.5 Three point bend testing

All experimentation and data analysis were carried out as in General methods sections 2.5.2.

4.2.6 Microindentation testing

All experimentation and data analysis were carried out as in General methods sections 2.6.

4.2.7 Molecular analysis

All experimentation and data analysis were carried out as in General methods sections 2.7.

4.2.8 Statistical analysis

The statistical analyses were conducted according to General Methods section 2.8.

4.3 Results

All femur lengths were measured using digital callipers and the data are shown in Figure 4-3. The protein restricted (PR) and control (C) young adult rats were compared within each generation for the F1, F2 and F3 generations.

4.3.1 Anthropometric analysis of femurs

Data from Figure 4-3 show that F1 PR 10 week old female femurs were statistically longer than those of the F1 C young adult rats ($P=0.05$). There were no other significant differences within the F2 or F3 generations.

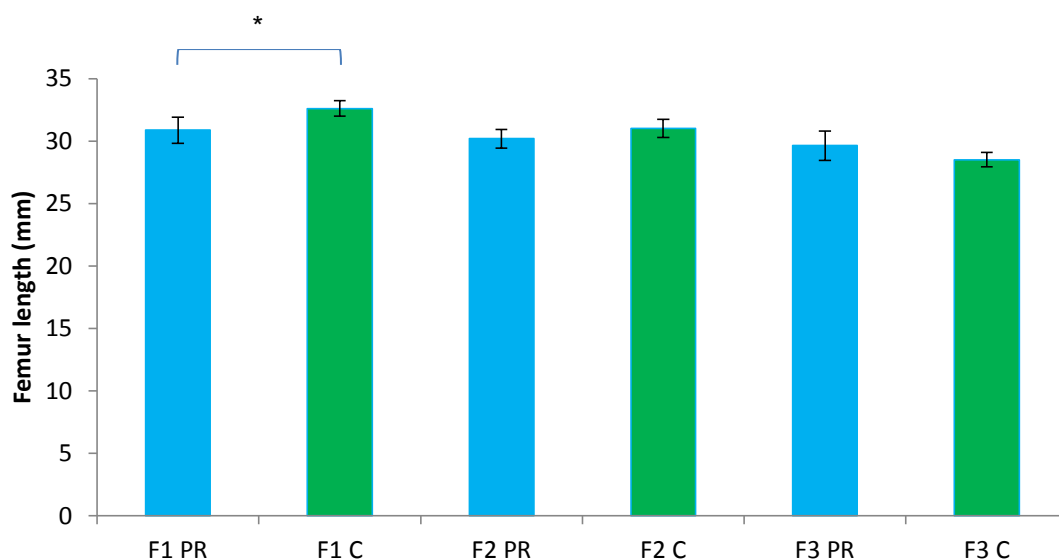


Figure 4-3 Anthropometric analysis of 10 week old female femur data for F1-F3 10 week old females from F0 PR (protein restricted) and C (control) dams. N = 5 samples per group, per generation. Data are mean \pm SD and significance is displayed as $P\leq 0.05$ (*).

4.3.2 Micro Computed Tomography Analysis of Bone Structure

Vertebral body trabecular bone analysis

As in Chapter 3, the L3 vertebral bodies were selected for micro computed tomography analysis. The trabecular and cortical bone within the vertebral bodies were analysed separately-the data are displayed in Figures 4-4 and 4-5.

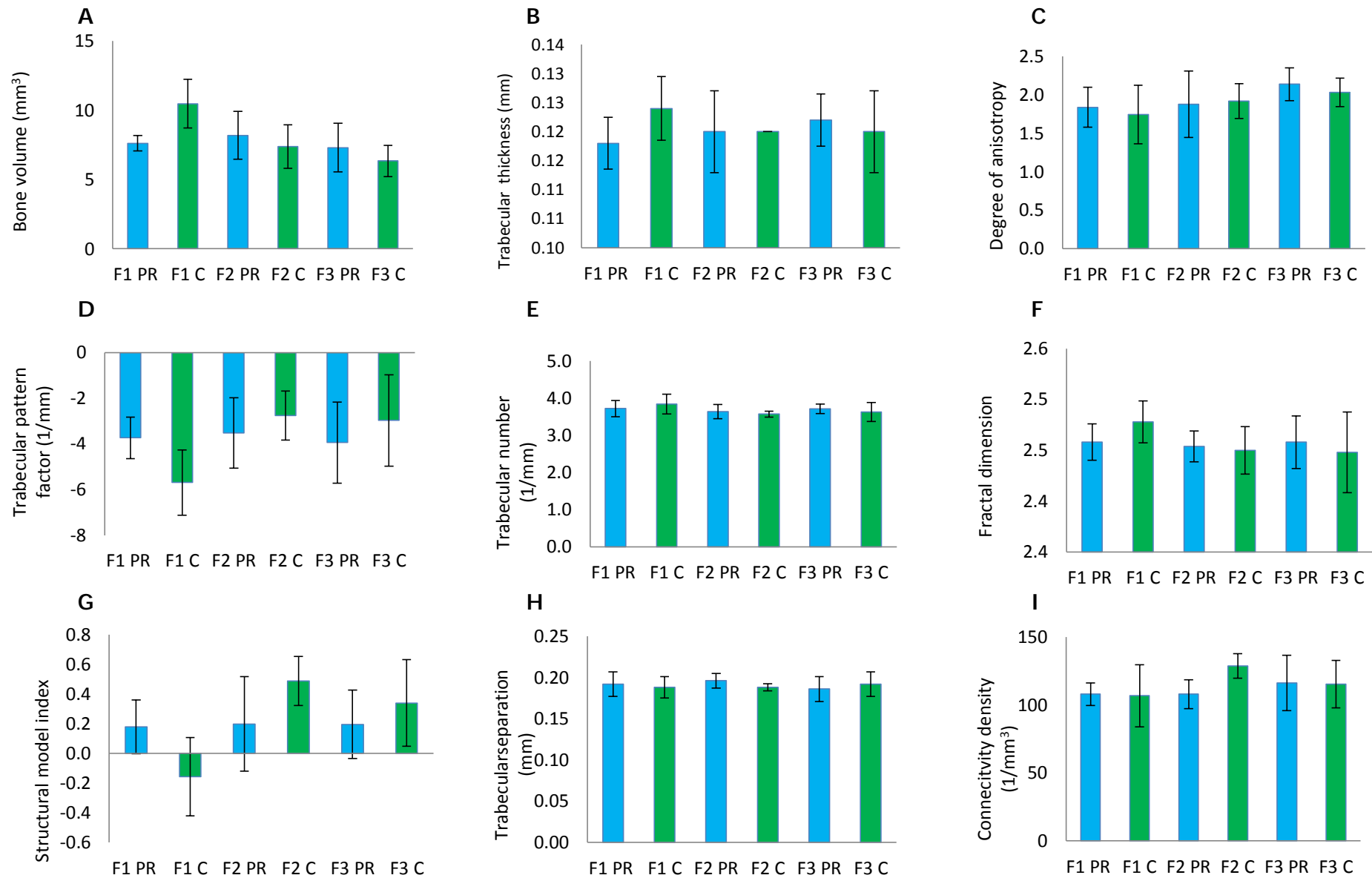


Figure 4-4 Vertebral body trabecular bone data for F1-F3 10 week old females from F0 PR (protein restricted) and C (control) dams. N = 5 samples per group, per generation. Data are mean \pm SD.

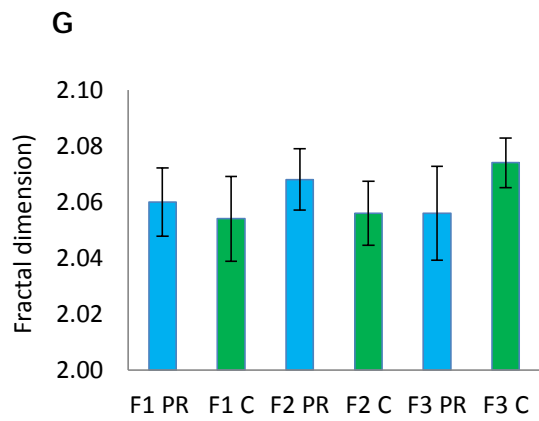
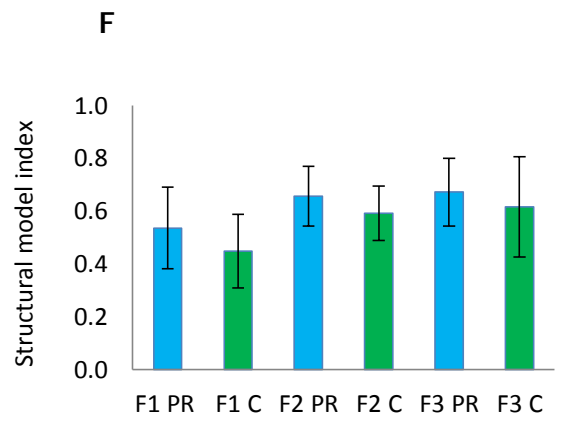
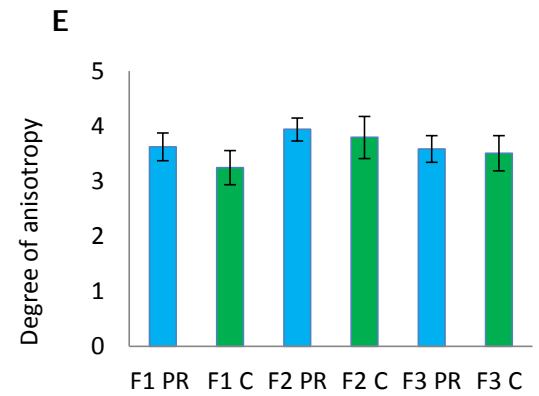
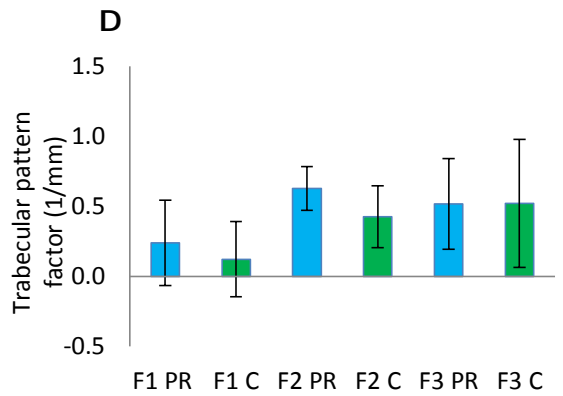
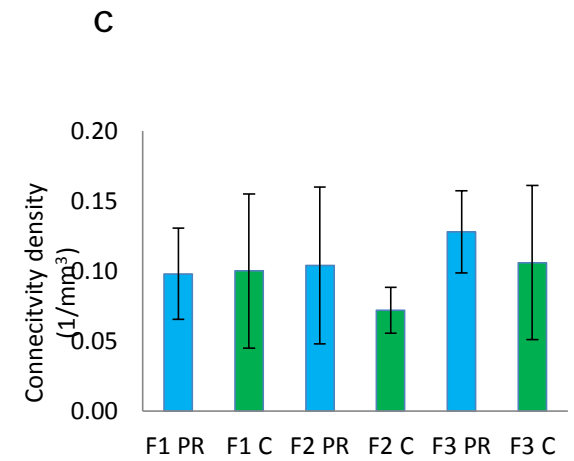
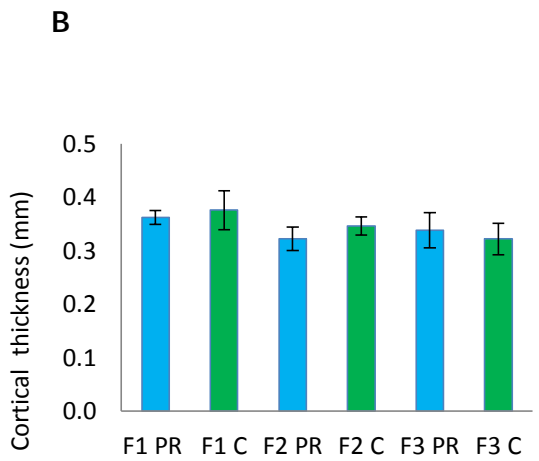
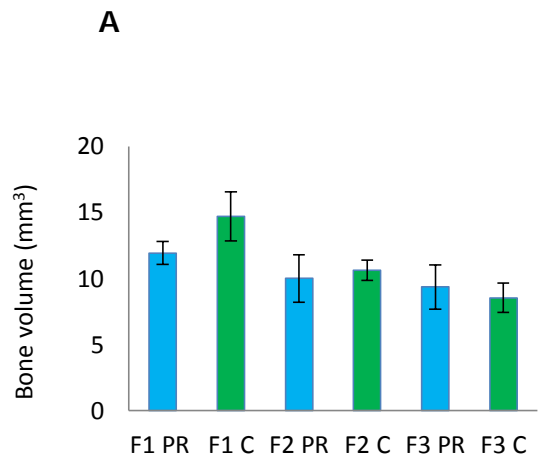


Figure 4-5 Vertebral body cortical bone data for F1-F3 10 week old females from F0 PR (protein restricted) and C (control) dams. N = 5 samples per group, per generation. Data are mean \pm SD.

Vertebral body results

There were no significant differences between the PR and C trabecular or cortical vertebral body analyses within the F1, F2 or F3 generations (Figure 4-4 and 4-5).

Head of femur trabecular bone analysis

The analysis on the head of femur is different than that in Chapter 3 due to additional input from the μ CT manufacturer Bruker. As the growth plate (primary spongiosa) at the proximal end of the femur, including the femoral head is traditionally excluded from histomorphometric analysis, Bruker suggest excluding this from the μ CT analysis also (Figure 4-6). For this reason a standard offset is applied to each sample in order to avoid all growth plate bone. The trabecular bone was separated from the cortical bone and then analysed independently (Figure 4-7).

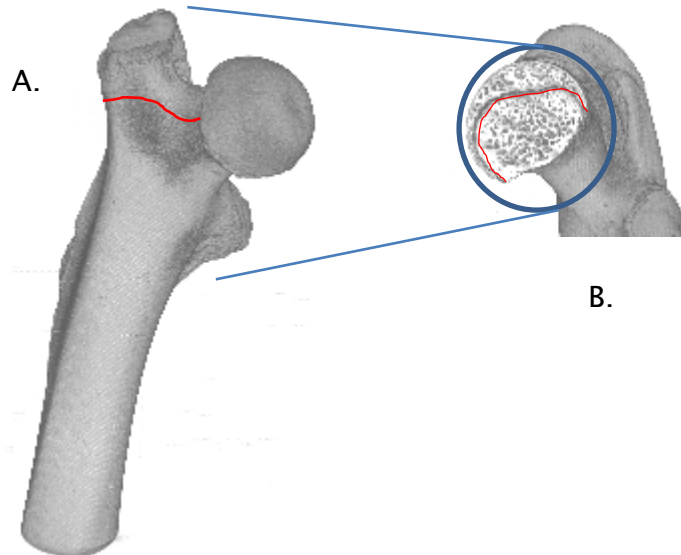


Figure 4-6 In order to avoid the growth plate at the proximal femur (red), including the femoral head, an offset was applied before analysis. A. proximal femur, B. Close up of femoral head with the growth plate and trabecular bone exposed.

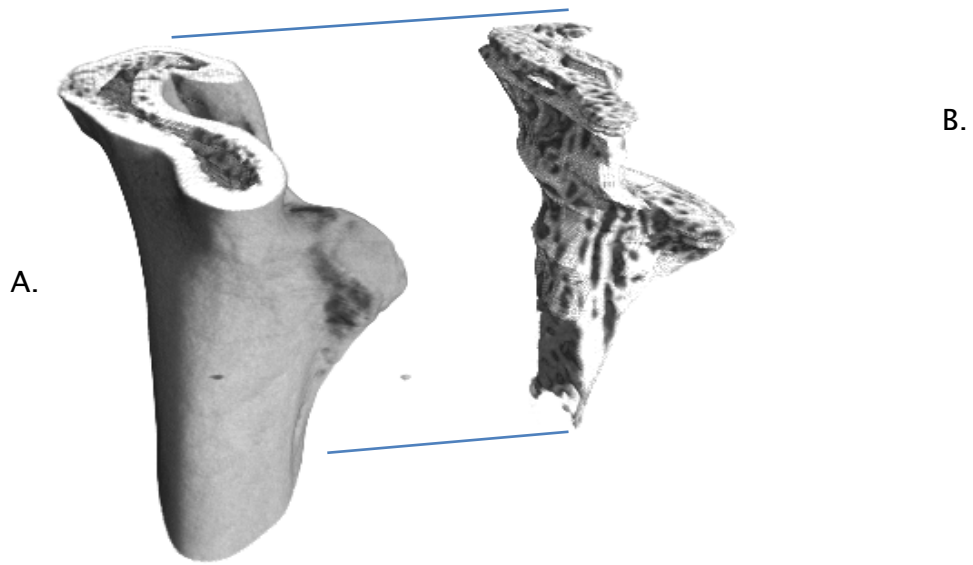


Figure 4-7 Representations of the cortical and trabecular bone analysed for the head of femur. A. cortical bone and B. trabecular bone.

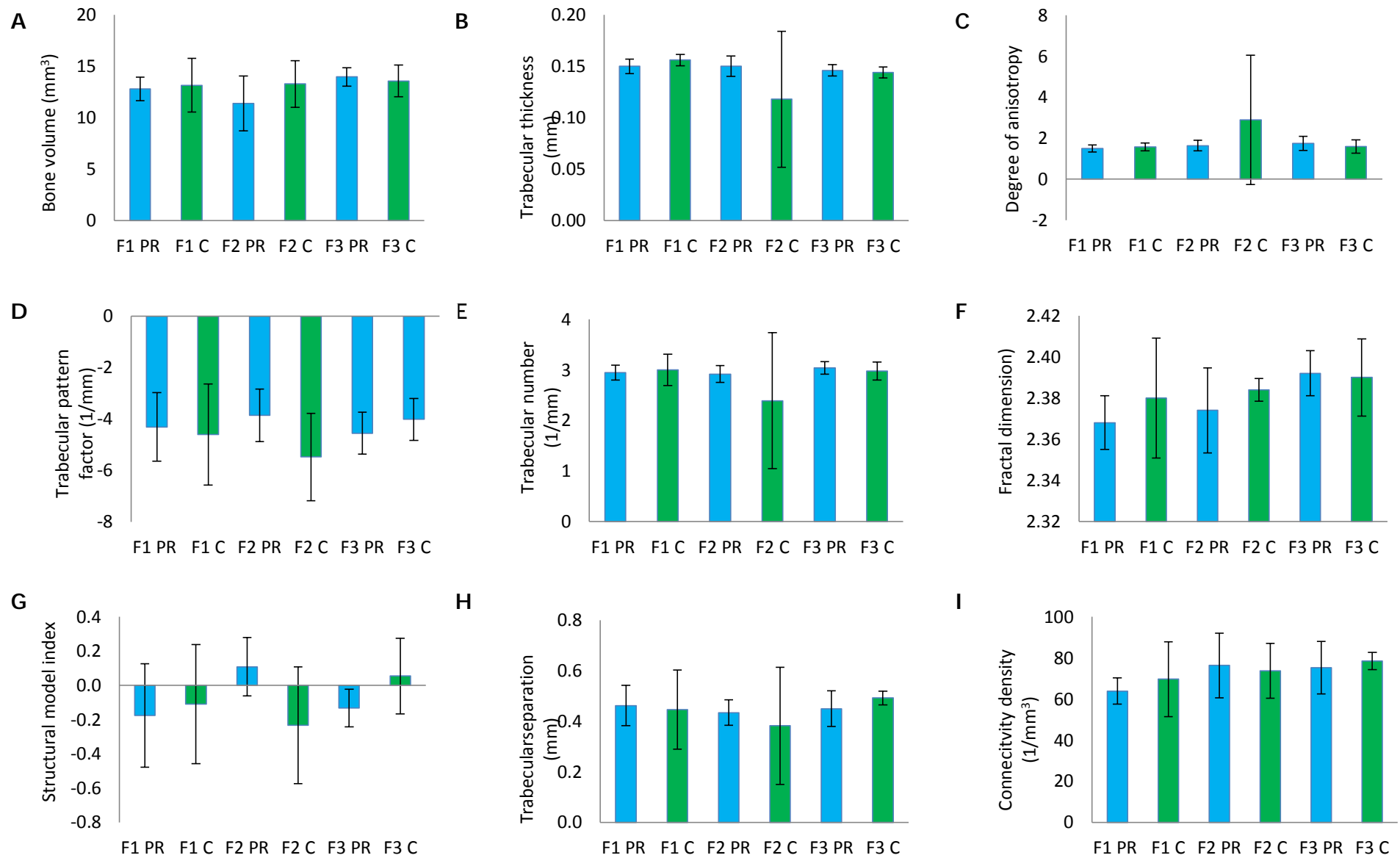


Figure 4-8 Head of femur trabecular bone data for F1-F3 10 week old females from F0 PR (protein restricted) and C (control) dams. N = 5 samples per group, per generation. Data are mean \pm SD.

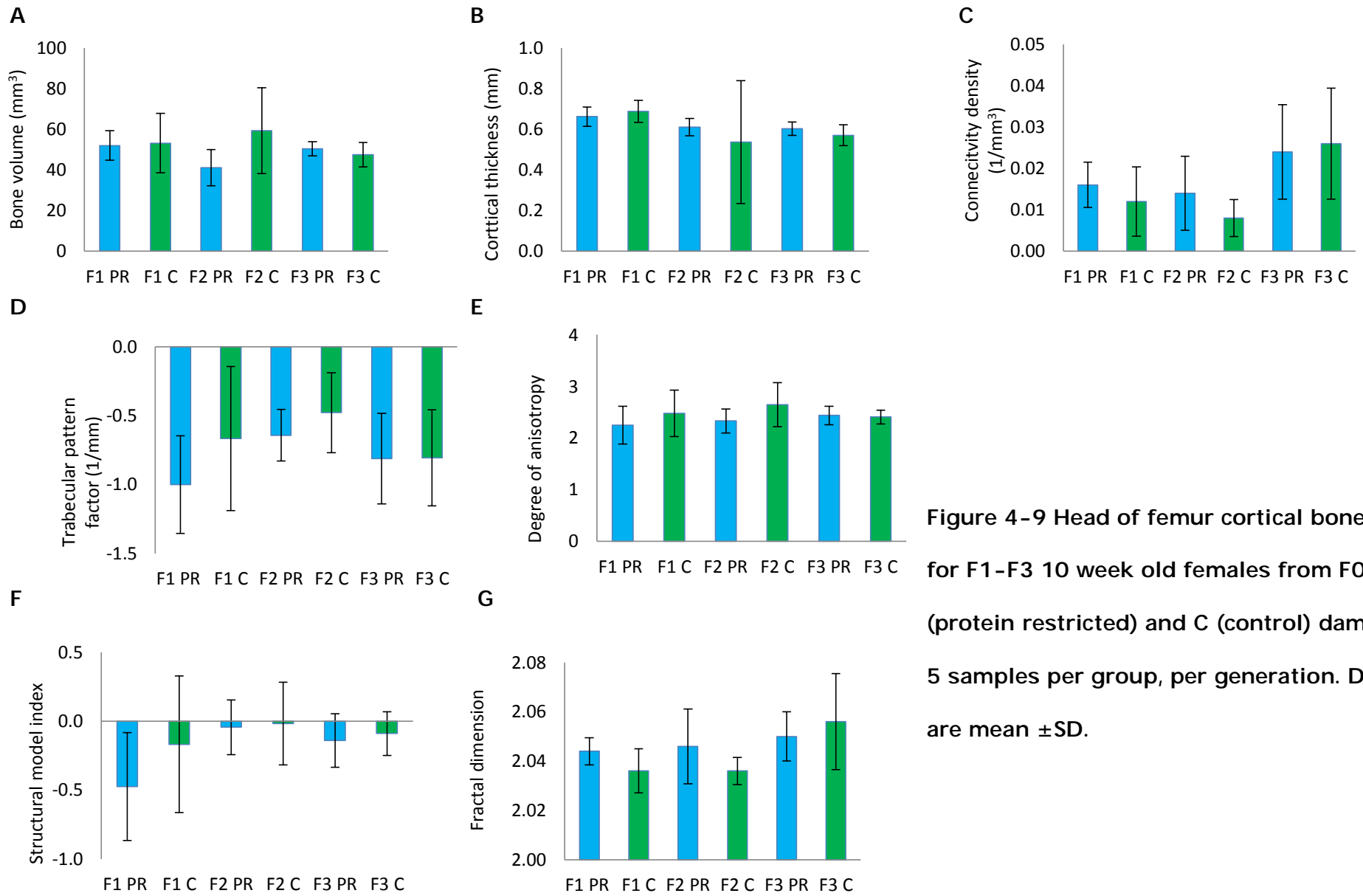


Figure 4-9 Head of femur cortical bone data for F1-F3 10 week old females from F0 PR (protein restricted) and C (control) dams. N = 5 samples per group, per generation. Data are mean \pm SD.

Head of femur results

No significant differences were observed for either the trabecular or cortical head of femur data when comparing PR and C young adult rats within the F1, F2 or F3 generations (Figures 4-8 and 4-9).

Distal femur trabecular bone analysis

The analysis on the distal femur is different to that in Chapter 3 due to additional input from the μ CT manufacturer Bruker. As the growth plate (primary spongiosa) at the distal femur is traditionally excluded from histomorphometric analysis, Bruker suggest excluding this bone from the μ CT analysis also (Figure 4-10). For this reason a standard offset is applied to each sample in order to avoid all growth plate bone. The trabecular bone was separated from the cortical bone and then analysed independently (Figure 4-11). The areas of trabecular and cortical bone analysed are larger for the distal femur than for the head of femur or vertebral body, resulting in large differences between values for parameters such as bone volume. These differences in size are a consequence of using physiological landmarks for the analysis and not set sized cuboids.

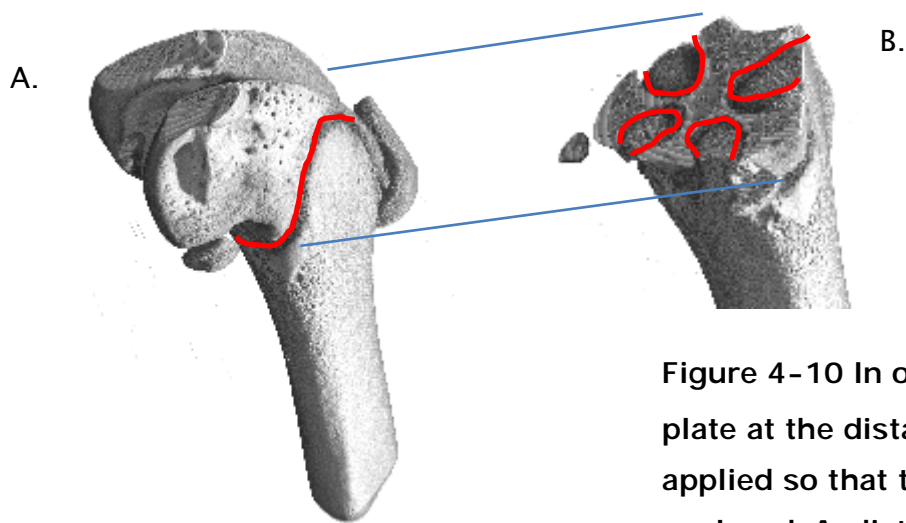


Figure 4-10 In order to avoid the growth plate at the distal femur (red) an offset was applied so that the growth plate was not analysed. A. distal femur, B. segment of the distal femur with the growth plate and trabecular bone exposed.

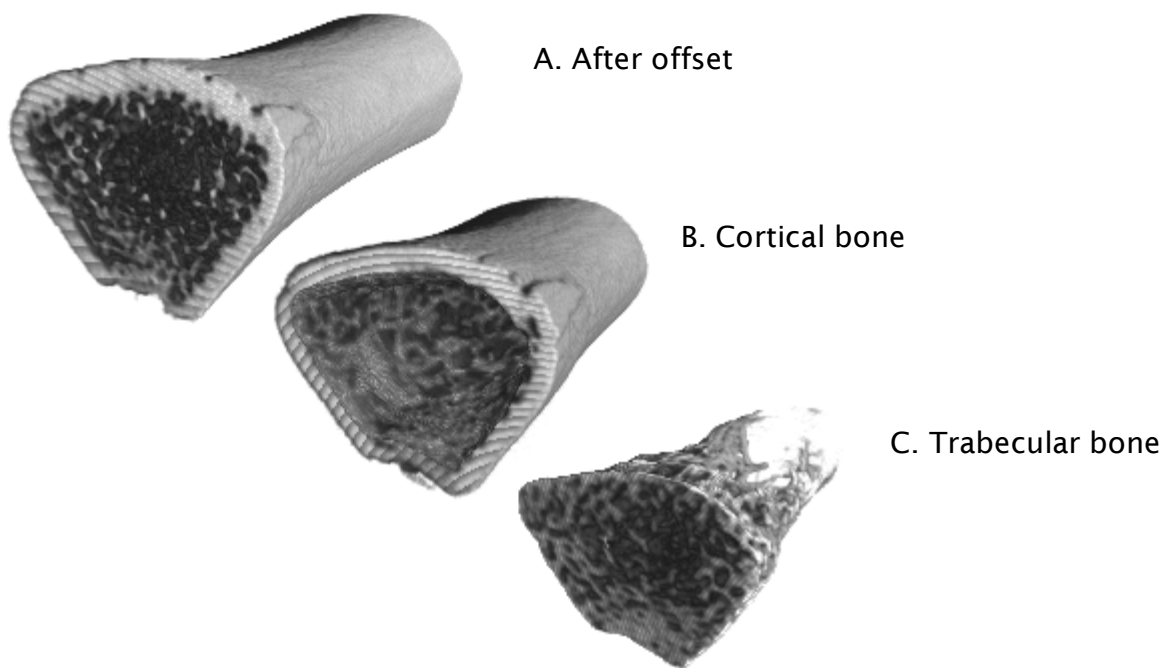


Figure 4-11 Illustration representing the cortical and trabecular bone analysed for the distal femur. A. distal femur after offset, B. cortical bone and C. trabecular bone.

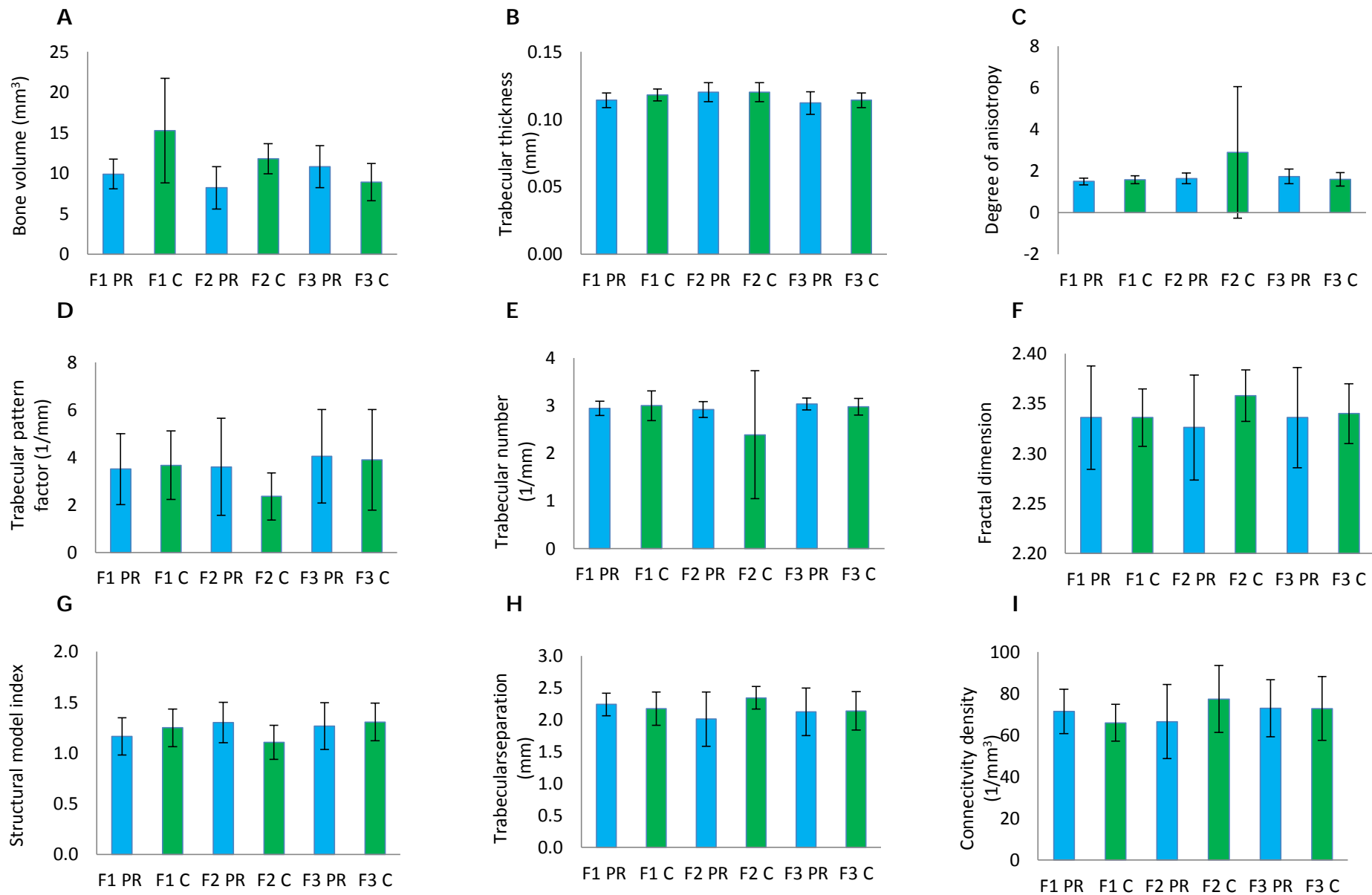


Figure 4-12 Distal femur trabecular bone data for F1-F3 10 week old females from F0 PR (protein restricted) and C (control) dams. N = 5 samples per group, per generation. Data are mean \pm SD.

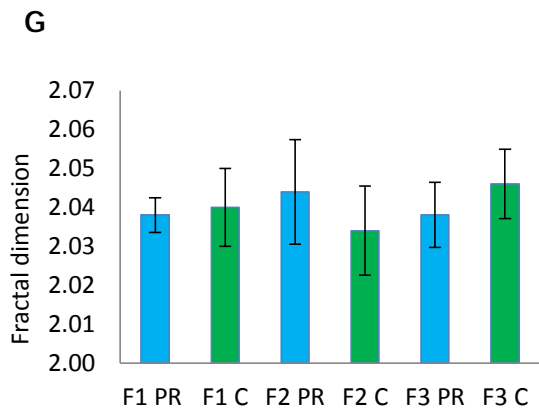
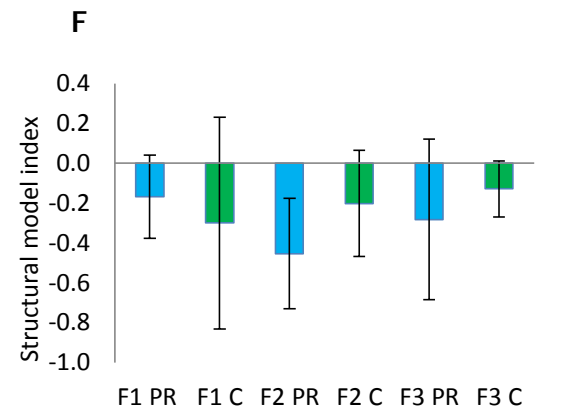
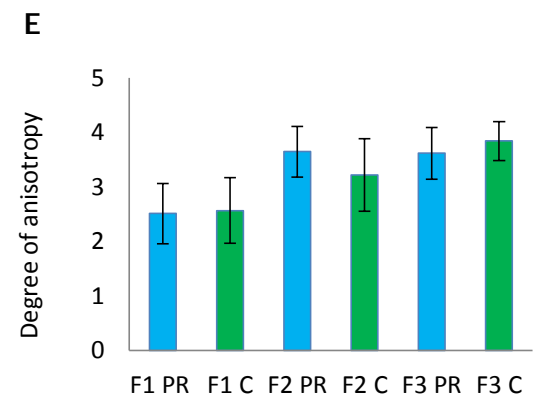
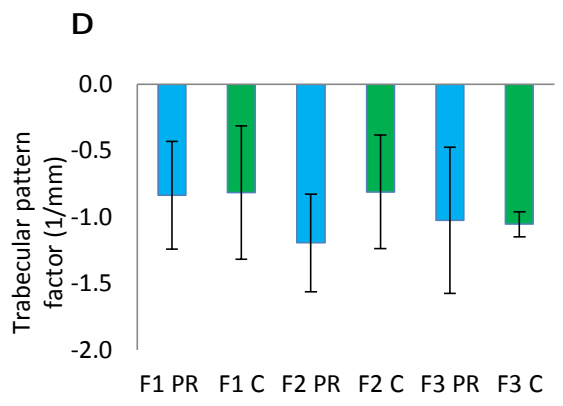
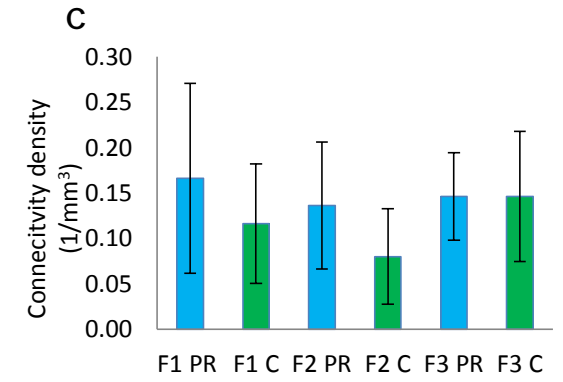
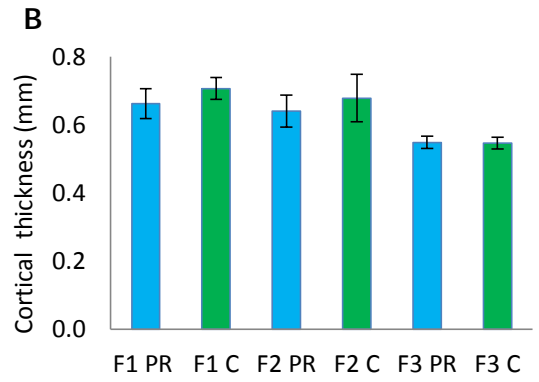
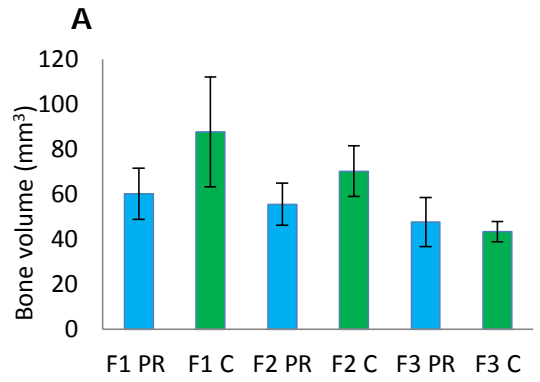


Figure 4-13 Distal femur cortical bone data for F1-F3 10 week old females from F0 PR (protein restricted) and C (control) dams. N = 5 samples per group, per generation. Data are mean \pm SD.

Distal femur results

The F1, F2 and F3 PR vs C analysis at the distal femur, both trabecular and cortical yielded no statistically significant results (Figures 4-12 and 4-13).

4.3.3 Bone Mineral Density (BMD)

Bone mineral density analysis data are presented in Figure 4-14 below.

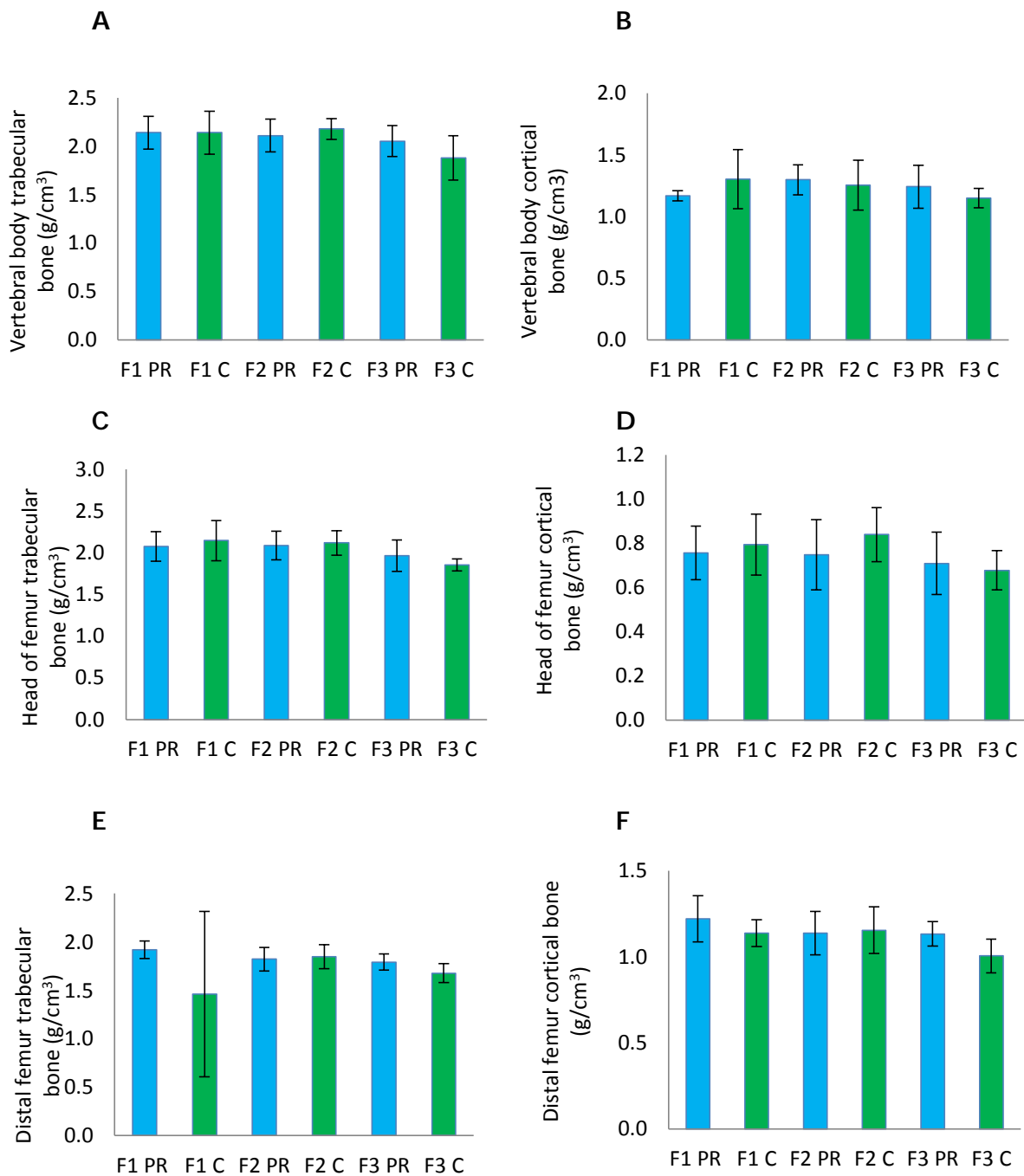


Figure 4-14 Bone mineral density data for F1-F3 10 week old females from F0 PR (protein restricted) and C (control) dams. N = 5 samples per group, per generation. Data are mean \pm SD.

There were no significant differences in the BMD for the trabecular or cortical bone at the vertebral body, head of femur or distal femur found between the PR vs C rats within any of the F1-F3 generational comparisons (Figure 4-14).

4.3.4 Three Point Bend Testing

All femurs were three point bend tested to destruction. The data are displayed in Figure 4-15 for all generations PR vs C.

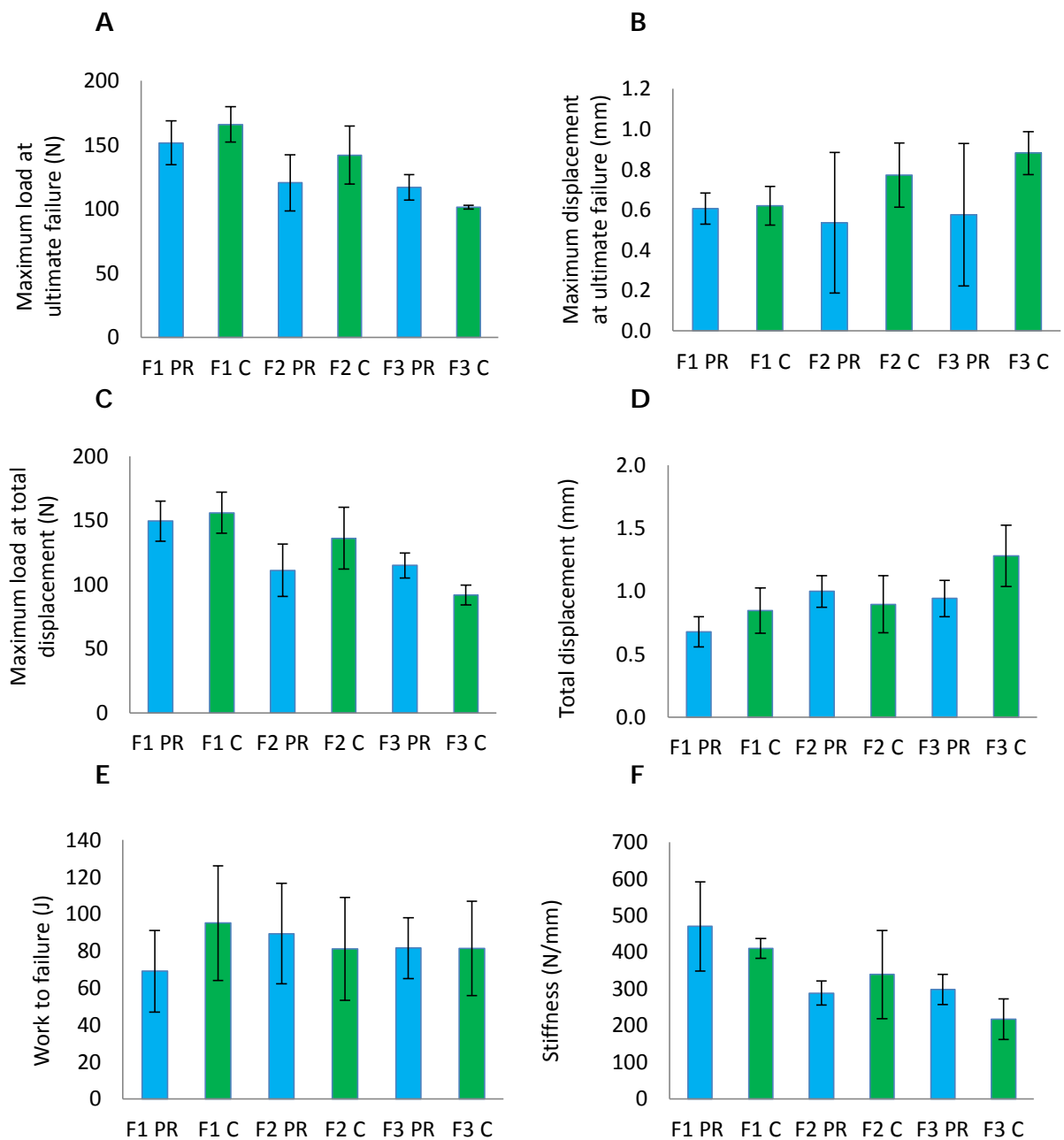


Figure 4-15 Three point bend testing data for F1-F3 10 week old females from F0 PR (protein restricted) and C (control) dams. N = 5 samples per group, per generation. Data are mean \pm SD.

When comparing the PR vs C offspring the three point bend data produced no significant differences for F1, F2 or F3 generations (Figure 4-15).

4.3.5 Microindentation Analysis

Selected sites on the femurs of 10 week old females from either PR or C F0 dams were microindentation tested. These sites are detailed in General methods 2.6- head of femur, neck of femur and four positions along the anterior side of the femoral midshaft (1-4), and an additional position between the epicondyles. The data for the head and neck of femur and the midshaft femur 1 are displayed in Figure 4-16.

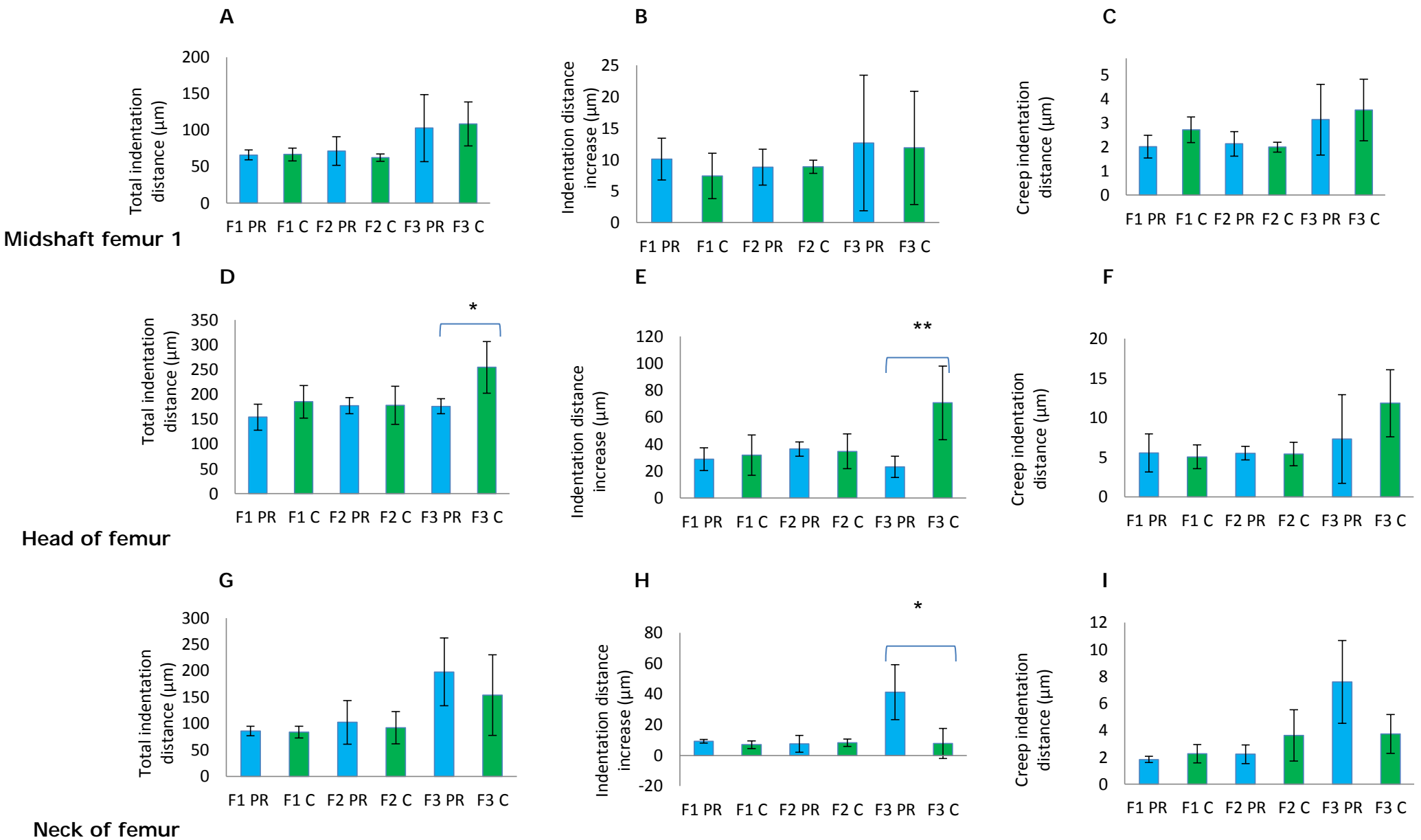


Figure 4-16 Microindentation data for the head and neck of femur and midshaft femur 1 for F1-F3 10 week old females from F0 PR (protein restricted) and C (control) dams. N = 5 samples per group, per generation. Data are mean \pm SD and $P \leq 0.05$ significances are $P < 0.05$ (*) and $P < 0.01$ (**).

Microindentation results

At the head of femur the F3 PR femurs showed a significantly lower total indentation distance and indentation distance increase, $P=0.02$ and $P<0.01$ respectively (Figure 4-14 D and E). The decrease in indentation displayed here indicates a cortical bone more resistant to fracture.

At the neck of femur the F3 PR femurs showed a significant increase in indentation distance increase compared to controls $P<0.01$ (Figure 4-14 H). This result is contrary to the data from the head of femur, suggesting a site specific effect in the F3 generation.

No significant differences in the microindentation data were found between the F1, F2 or F3 PR vs C rats at the midshaft femur site 1 (Figure 4-14 A-C). The data for the midshaft femur sites 2-4 and the epicondyle can be found in Appendix 5 and also showed no significant differences.

4.3.6 Quantitative PCR analysis

Expression data were collected for eight genes from the distal femur bone tissue of F1, F2 and F3 offspring from protein restricted and control dams (F0). The eight genes selected are all known to be expressed by osteoblasts and are important for bone formation at different stages. The genes investigated were runt-related transcription factor 2 (Runx 2), collagen 1 (Col 1), osteonectin (ON), osteopontin (OP), insulin-like growth factor I (IGF-I), insulin-like growth factor II (IGF-II), bone sialoprotein (BSP) and osteocalcin (OCN). The data have been presented as a relative expression level, with the highest $\Delta\Delta CT$ value for an F1 control sample set to 1, and the other F1 control samples and F1 protein restricted samples shown relative to that sample (Figure 4-11). The absolute means (ΔCT), standard deviations, and p-values can be found in Appendix 6. The error bars are the standard deviation of the five different rats used for each diet group in the analysis. Only one statistically significant difference was observed from the molecular data. In the F2 generation the PR osteocalcin expression was significantly lower than the C ($P=0.02$; Figure 4-17).

One outlier was removed from the F2 PR BSP data.

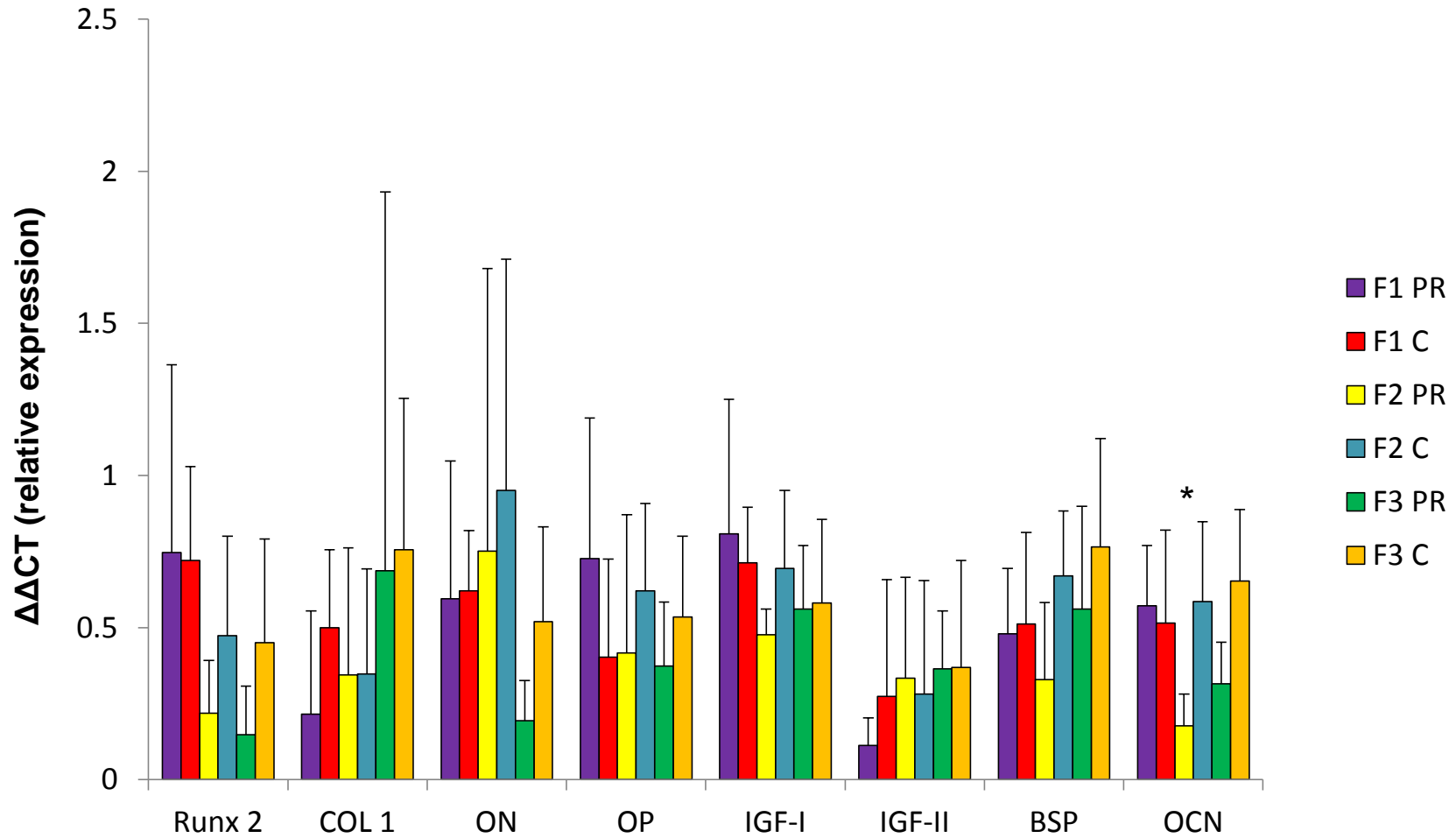


Figure 4-17 Relative gene expression data for F1-F3 10 week old females from F0 PR (protein restricted) and C (control) dams. N = 5 samples per group, per generation. Data are mean \pm SD and $P \leq 0.05$ significances is displayed as (*).

4.3.7 Results summary

Each generation, F1, F2 and F3 showed significant results, however the results were different in each generation. The F1 PR offspring had significantly shorter femur length than the F1 controls ($P=0.05$). The F2 PR offspring had a lower osteocalcin expression than the F2 controls ($P=0.02$). A decreased level of expression means that there are a smaller number of mature osteoblasts and is a sign of decreased bone formation. The F3 PR offspring had a femoral head more resistant to fracture (lower total indentation distance and indentation distance increase, $P=0.02$ and $P<0.01$ respectively) and a femoral neck less resistant to fracture (increase in indentation distance increase $P<0.01$) compared to the F3 controls. This suggests a site specific effect in the F3 generation with the femoral head prioritised over the femoral neck.

4.4 Discussion

Protein restriction during F0 pregnancy has been shown to cause hypertension in F2 offspring (Harrison et al. 2009) and alter methylation states in the liver (Burdge et al. 2007) in F1 and F2 offspring. Benyshek et al. describe a difference in glucose metabolism at the F3 generation as a result of protein restriction during pregnancy in the F0 generation (Benyshek et al. 2006). This study aimed to establish if differences in bone induced by maternal protein restriction during F0 pregnancy, were present in the F1, F2 and F3 generation offspring. No additional dietary conditions were imposed on the F1, F2 and F3 offspring and all were culled and studied at 10 weeks of age. Data presented here suggest limited site specific effects in the F1, F2 and F3 generations.

The F1 PR offspring were found to have significantly shorter femurs than F1 offspring from control dams. Lanham et al. 2008 produced data showing no difference in female femur length at either 8 or 12 weeks. Although the samples studied here are taken at 10 weeks, the result from this study is contrary to the findings from Lanham et al 2008. No differences were observed here in the expression levels of IGF-II between the F1 PR and control offspring. Previously, male offspring from protein restricted dams have been shown to have significantly higher IGF-II expression in the liver after delivery (Gong et al. 2010).

The F2 PR offspring had significantly lower osteocalcin gene expression compared to F2 controls, indicating a decrease in bone formation by osteoblasts. Although it did not reach statistical significance, most of the genes investigated were down regulated in the protein restricted F2 offspring compared to controls. The SDs for the qPCR data are large as they represent comparisons between multiple different rats and not just replicates of the same sample, which would therefore show large natural genetic variations. This down regulation is interesting as it suggests that the osteoblast function has been altered by maternal protein restriction at F0. No previous data have been published on any of the techniques used here with regards to offspring from protein restricted dams in the F2 or F3 generation. Harrison et al.

observed increased systolic blood pressure and nephron number and subsequent hypertension in the F2 generation (Harrison and Langley 2009). The significant result in the F2 generation seen by Harrison and Langley-Evans was not seen in the F3 generation, indicating the effects on blood pressure are only present for two subsequent generations.

When comparing the F3 PR offspring against F3 controls, the microindentation data showed the F3 PR offspring were more resistant to fracture at the head of femur and less resistant to fracture at the neck of femur. The trend of lower gene expression in the F2 protein restricted samples was evident in the F3 protein restricted samples as well, but is still not statistically significant. While other previous studies into tissues other than bone have shown no difference in the F3 generation from protein restricted dams, Benyshek et al. showed insulin resistance in F2 offspring and impaired glucose metabolism at the F3 offspring (Benyshek et al. 2006). Although the effect of F0 protein restriction during pregnancy was less pronounced in F3 offspring compared to F2 offspring suggesting a return to control glucose metabolism levels. Therefore, F3 differences have previously been seen in other systems, a finding that may support the differences observed here in bone for the F3 offspring from protein restricted dams.

As with the previous chapter it is important to note the dietary manipulation during the F0 pregnancy was mild (9% protein for the PR and 18% for the controls) and all diets are isocaloric. Also, the samples studied here are even younger (10 weeks) than the samples studied in the previous study (12 weeks).

The differences induced in the F1, F2 and F3 offspring by the F0 protein restriction differ with each generation, but all differences were observed at the femur. This may however be because the micro computed tomography analysis produced no significant results and other analysis techniques were conducted only on the femur. The number of significant changes observed in this study is very low considering the amount of data presented in this chapter. This may be as a result of the time point being investigated here. The F1 differences in trabecular bone observed by Lanham et al. were only present in 75 week old

offspring (Lanham et al. 2008). It may also be due to the sample size being too small to detect any effect that may be present at this time point. As the phenotype we are investigating using maternal protein restriction is one that resembles osteoporotic bone it not surprising that this is not present in 10 week old rat offspring. If the offspring had been kept until old age before analysis was conducted then we may have seen different results. However this was these rats were not kept until old age in this study. Another technique that would have provided insight here is epigenetic analysis of the DNA. This could have provided further evidence as to whether the F0 PR had influenced further generations but time did not allow for it. The data presented here show that F0 protein restriction influences F1, F2 and F3 femurs and that these changes differ depending on the generation being investigated.

5. General Discussion

Chronic diseases in later life, such as heart disease, hypertension, type II diabetes, and osteoporosis can be influenced in the intrauterine environment. Lanham et al. have previously shown that maternal protein restriction in rodents during pregnancy affects bone structure in the offspring (Lanham et al. 2008). Can the effects of maternal protein restriction on offspring's bone be reversed by folic acid supplementation, and are the effects of maternal protein restriction evident in subsequent generations?

The results in Chapter 3 showed that maternal protein restriction led to structural differences in the female offspring and a single difference in the male offspring at 12 weeks. The young adult female offspring displayed a cortical vertebral body structure predicted to be stronger than that of the control females. Therefore the structure resulting from maternal protein restriction would be likely to better withstand age related bone loss than the controls. Lanham et al. did not investigate the cortical vertebral body structure in the 75 week offspring so no direct comparison can be made here (Lanham et al. 2008). However, Lanham et al. did find that the vertebra of the protein restricted samples had a higher BMD and the images provided appear quantitatively as if more cortical bone is present than the controls. The strength testing data presented also concur that the enhanced cortical structure present as a result of protein restriction resulted in a stronger bone. This comparison would agree that the changes observed from Chapter 3 do in fact predict a stronger cortical vertebra. At the distal femur a better-connected but less dense trabecular network was also observed for the female PR/CFA offspring in Chapter 3. Lanham et al. did not investigate the distal femur but did find that the bone surface density at the femoral neck of 75 week offspring was reduced due to protein restriction. This therefore suggests that a site specific and possible time specific difference in bone surface density is seen in the femur as a result of protein restriction. Results from Chapter 4 using 10 week old females showed that protein restriction resulted in significantly shorter femurs compared to controls. This result was not seen at 12 weeks of age for Lanham et al but was seen at 75 weeks (Lanham et al. 2008). There is only a two week difference between the samples from Chapters 3 and 4 however profound changes are seen. The significances observed at the

vertebral body and distal femur may be as a result of the age difference: the younger animals would be just entering puberty and the subsequent period of plasticity. Alternatively it may be the high fat diet given between days 56-84 in Chapter 3. The increase in weight associated with the high fat diet may have precipitated the differences in phenotype. Maternal protein restriction and juvenile high fat produced advantageous differences in the female offspring at 12 weeks, which were not present for 10 week offspring who lacked the high fat diet.

As only female offspring were investigated in Chapter 4 comparisons with the slightly older offspring from Chapter 3 are not possible. In the male offspring in Chapter 3 a higher trabecular separation was seen at the neck of femur. One could speculate that increased trabecular separation would decrease potential strength, but this would be more likely if other parameters had been affected, such as a decrease in trabecular number. Lanham et al. did not find any structural differences in male offspring at 75 weeks (Lanham et al. 2011). The 12 week female samples studied in Chapter 3 produced no significant differences at either the head or neck of femur or trabecular vertebral body, suggesting the differences Lanham et al. observed in 75 week samples were not evident at this time point. Contrary to the result seen in this study, Lanham et al. found males from protein restricted mothers had significantly longer femurs than those from the control group at 12 weeks when corrected for mass, but the μ CT analysis showed no differences in the male offspring at 75 weeks (Lanham et al. 2011).

Using the same cohort of animals as presented in Chapter 3, Burdge et al. found no differences in weight for either sex between the protein restricted and control offspring at any time from birth to 12 weeks (Burdge et al. 2009). In the same study Burdge et al. also found that protein restriction increased fasting plasma triglyceride (TAG) and β -hydroxybutyrate concentrations as a result of altered lipid metabolism. This is probably enhanced due to the high fat diet as in the results presented here. Protein restriction during pregnancy has also been shown to affect other systems in the offspring. Maternal protein restriction was shown by Woods et al. to impair renal development and to programme adult hypertension in later life (Woods et al. 2001). Fernandez-

Twinn et al. showed that protein restriction during pregnancy resulted in increased insulin resistance and increased risk of type II diabetes in later life (Fernandez-Twinn et al. 2005). Torrens et al. revealed that gestational protein restriction impaired fetal brain development by inducing alterations in maternal liver metabolism as a result of lipid composition (Torrens et al. 2010). Bone has recently been identified as an endocrine organ due to the effects of osteocalcin on glucose metabolism and testosterone production (Guntur and Rosen 2012). Differences in brain development are also altered as a result of osteocalcin which is expressed by osteoblasts. Oury et al. showed that osteocalcin knock out mice suffered learning and memory deficiencies (Oury et al. 2013). Maternal osteocalcin can be transported through the placenta to the offspring. It would be interesting to investigate if osteocalcin expression differed in either the mother or fetus during pregnancy as a result of protein restriction. Osteocalcin expression levels at 10 weeks were shown to be the same as controls in Chapter 4.

Whether the effects of maternal protein restriction during pregnancy on bone can be altered by folic acid addition during periods of growth, such as gestation or puberty, has not yet been examined. Folic acid is a strong candidate to alter the effects of protein restrictions as it is an important methyl donor that contributes methyl groups through one-carbon metabolism to epigenetic control of gene expression (Giudicelli et al. 2013). Folic acid is recommended as a supplement for women during pregnancy due to its prevention of neural tube defects. Adequate folic acid intake is so crucial that bread and cereals in the UK are fortified with folic acid. Folic acid supplementation and fortification make it a very important candidate for investigation through animal models, especially for periods of intense growth. Lillycrop et al. have shown using a rat model that maternal protein restriction induced alterations in hepatic gene expression in the livers of the offspring at 34 days: PPAR gene methylation was 20.6% lower and expression 10.5-fold higher, and GR gene methylation was 22.8% lower and expression 200% higher in PR offspring compared with controls (Lillycrop et al. 2005). However these alterations were reversed by folic acid supplementation during pregnancy. Burdge et al. then went on to show that sex, and not maternal protein restriction or folic acid supplementation during pregnancy, regulates the fatty acid composition of hepatic phospholipids in 15 week old offspring (Burdge et

al. 2008). The proportions of liver phospholipids (18:0, 20:4n-6 and 22:6n-3) was higher in females than in males and hepatic TAG composition did not differ between sexes. $\Delta 5$ Desaturase expression was found to be higher in females than in males, although neither $\Delta 5$ or $\Delta 6$ desaturase expression was related to polyunsaturated fatty acid concentrations. Torrens et al. found that folic acid addition during pregnancy restored systolic blood pressure to control levels, which is a reversal of the increased systolic blood pressure induced by maternal protein restriction (Torrens et al. 2006). So there is some evidence that the alteration in phenotype caused by protein restriction can be reversed by folic acid supplementation at the same time. Is it just during gestation that folic acid has this effect? Are other periods of plasticity affected in a similar way by folic acid supplementation?

Folic acid supplementation during the juvenile period altered the effects of maternal protein restriction in young adult rats as described in Chapter 3. These differences were site and sex specific. In the female offspring bone volume increased for both the trabecular and cortical vertebral bodies resulting in a predicted strength increase. This is probably due to the associated increase in body weight that all folic acid supplemented offspring encountered, as discussed for the same cohort in (Burdge et al. 2009). Increases in weight of approximately 40g would require an associated increase in strength in the vertebra. The females suffered a reduction in femur wall mean thickness, but this did not reduce the strength as measured by three point bend testing. This may suggest that the femur has been sacrificed at 12 weeks in order to protect the vertebra in female offspring, although this is not to the detriment of the femur. The combination diet (PR/HFA) also affected the vertebral body bone structure of male young adult rats with an increase in cortical bone volume, but a decrease in BMD at the same site. The male offspring exhibited decreased bone volume at the neck of femur and increased anisotropy at the head of femur in male young adult offspring due to the combination diet. The differences observed in Chapter 3 provide strong evidence that juvenile folic acid supplementation produced sex specific differences in young adult rats from protein restricted dams. In 2009 Burdge et al. investigated the effect of juvenile folic acid supplementation on young adult rats from protein restricted mothers using the same cohort as the data from Chapter 3. In this case Burdge

et al. showed that the folic acid supplementation altered the effect of the maternal protein restriction, but did not reverse the effects as maternal folic acid supplementation had (Burdge et al. 2009). The results presented here concur that juvenile folic acid addition produces a distinct phenotype, including increased weight gain and structural changes in the vertebra that would support this, in young adult rats from protein restricted dams. This illustrates again how the juvenile pubertal period is one of plasticity and intense development. Intervention during this period results in sex specific differences partly due to the enormous changes happening as a result of the developmental stage being studied. The results presented here are not all favourable with particularly the folic acid supplemented male young adult rats exhibiting a trabecular structure at the head and neck of femur that one would expect to be structurally weaker at this stage. This is almost certainly due to the increased body weight that these samples display relative to controls, but this could have serious consequences that are not being considered. There is no evidence as to how rats under these diet conditions would continue to develop and age but this is an area that warrants further study.

Similarly the effect of protein restriction on future generations is a question that needs to be answered for bone. Previously, intergenerational effects of maternal protein restriction have not been investigated on bone microarchitecture and mechanical properties. Results presented here in Chapter 4 show that maternal protein restriction induced minor effects in the young adult female offspring's bone structure and mechanical properties up to F3 generation. The data presented for Chapter 4 F1 offspring have been discussed in comparison to other F1 protein restricted studies earlier in this chapter.

The F2 PR offspring had a significantly lower osteocalcin gene expression compared to F2 controls, indicating a decrease in bone formation by osteoblasts. Osteocalcin is a marker of mature osteoblasts (Hopayan et al. 1999). A decreased level of expression means that there are a smaller number of mature osteoblasts and is a sign of decreased bone formation. According to the Oury et al. (2013) and Guntur and Rosen (2012) papers discussed earlier this could also affect a wide range of functions such as glucose metabolism, testosterone production and fetal learning and memory. None of these have been investigated as a result of protein restriction during pregnancy on the F2

generation. Harrison et al. have also determined that protein restriction during F0 pregnancy increased systolic blood pressure in F2 offspring in 8 week old rats leading to an increase in hypertension risk (Harrison and Langley-Evans 2009). Similar findings of increased blood pressure and endothelial cell dysfunction were also seen by Torrens et al. in 11 and 25 week old rats (Torrens et al. 2008). There is therefore reasonable evidence that F2 offspring have altered blood pressure at a range of ages including around the time studied in Chapter 4. However, contrary to the findings for vascular tissue, marked phenotypical changes were not observed in the data presented here for bone. Similarly to the data presented here for bone, Hoile et al. showed that hepatic gene expression was altered relative to both F1 and F3 in the F2 generation, but that these changes were not transmitted between generations (Hoile et al. 2011). The data presented for bone also follow this pattern with differences observed in all generations that were not transmitted across generations. Hoile et al. also found that fasting plasma glucose was higher in the F2 generation compared to controls. This may tie into the reduced osteocalcin expression reported here as a decrease in osteocalcin expression would lead to a reduction in glucose metabolism and therefore an increase in plasma glucose as found by Hoile et al.

The effects seen in the F3 offspring for both Chapter 4 and Hoile et al. (2011) were different for those observed for the F2 generation. The microindentation analysis for the F3 PR offspring demonstrated more resistance to fracture at the head of femur and less resistance to fracture at the neck of femur compared to F3 controls. Hoile et al. (2011) did not find increased fasting plasma glucose in the F3 generation in 10 week old samples. Contrary to this however Benyshek et al. did show a reduction in glucose metabolism at the F3 generation from protein restricted dams at 10 weeks (Benyshek et al. 2006). However in the Benyshek et al. study the dams were also fed a protein restricted diet during lactation as well as during pregnancy, so the discrepancy could also be as a result of this. No statistically significant difference for osteocalcin was observed between the F3 PR vs F3 C samples in Chapter 4, although the result was near to significance ($P=0.056$).

The effects of F0 protein restriction increase from the F1 to the F3 generation, with the largest number of sites affected in the F3 generation. The adaptations seen in F3 PR females could indicate a predictive adaptive response by the offspring in response to cues encountered in the intrauterine environment, as described by Gluckman and Hanson (2004). However, as the changes are relatively small and inconsistent across all generations there is insufficient evidence that this is the case at this time point. If the rats from Chapter 4 had been studied at old age, then maybe an altered, potentially osteoporotic phenotype would have been seen in the PR offspring in order to conclude a predictive adaptive response.

A number of method developments were made during the studies discussed in this thesis. Due to the mild nature of the maternal insult studied in this thesis and following the analysis of the results in Chapter 3, modifications were made to the techniques and protocols in order to achieve higher sensitivity in the parameters examined. Histological analysis as used in Chapter 3 was deemed of low sensitivity when evaluating changes on such a small scale and hence, histological analysis was not used for the results in Chapter 4. The μ CT protocol was further developed with input from Bruker staff to better conform to traditional bone histomorphometric standards. This involved selecting regions of interest that were determined by physiological landmarks, such as the cartilage bridge at the epiphyseal growth plate in the distal femur, in order to select a region of bone that is mature trabecular bone and independent of bone size. The modified protocol also allowed for analysis of cortical bone at the head of femur and distal femur. Leppänen et al. have established that three point bend testing is a valid method of assessing bone strength at the midshaft of femurs (Leppänen et al. 2006). However, three point bend testing provides negligible information as to the structural integrity of the trabecular or cortical bone at the head, neck, or distal femur. For this reason in addition to three point bend testing, microindentation was used in Chapter 4 to assess cortical bone at different sites on the femur. The microindentation data produced in Chapter 4 show significant differences at the neck of femur for the F3 protein restricted samples that would not have been detected by three point bend testing alone. However, microindentation analysis also has limitations, as shown in the research presented here. Thus the error on head of femur and neck of femur investigations is sometimes as much as 40%. This is due to the

cartilage on the head of femur or neck of femur being displaced before the test probe makes contact with the cortical bone. Furthermore, microindentation does not assess the trabecular bone strength. Both the three point bend testing data and μ CT data presented in this study had an error of 10-20 % which is significantly lower than the error for the microindentation testing. The error associated with microindentation testing does not negate its usefulness, but it does mean that observations at the femoral head need to be carefully examined. Further investigation would have included strength testing of the vertebral bodies and epigenetic analysis of the bone tissue from Chapter 4 if time had allowed.

There are three well known diet regimes used to investigate bone that mimic maternal nutritional insults and allow one to study the subsequent outcomes. Two are undernutrition models: the maternal protein restricted model where isocaloric diets have altered protein levels, 9% casein PR and 18% casein control, and the maternal total nutrient restriction model one example of which is bilateral uterine vessel ligation surgery reduces the nutrients received by the fetus. The final model is an over nutritional model: the maternal high fat model (dams and potentially their offspring are fed a high fat diet).

The isocaloric maternal gestational protein restriction model was originally developed by Langley-Evans and was used here (although modified to include additional high fat in Chapter 3). This is an interesting and well used nutritional challenge model, which on application has produced significant changes in many different tissues, now including multiple time points for bone as detailed here. As it is only protein levels that are reduced in this model, it could be said that as a nutritional challenge the diet is mild compared to total caloric restriction models. This means that it better resembles sections of the Western diet, where calorie content is not reduced, but the composition is not optimal.

The other undernutrition model, total nutrition restriction, was used by Romano et al. who found that a restricted gestational environment reduced bone mineral content (BMC) and bone strength in all offspring regardless of postnatal environment (Romano et al. 2009). Romano et al. used bilateral uterine vessel ligation surgery to reduce the blood flow and subsequent

nutrient flow to the fetus either during pregnancy and/ or during weaning. Control dams were sham operated. Nutrient restriction during pregnancy reduced the BMC of 26 week old male and female rats regardless of the weaning environment. Differences in strength and structure were observed between male and female offspring suggesting sex differences as evident in the data presented in Chapter 3 and Lanham et al. (2008).

The only over nutritional model used to assess maternal nutrition and bone is high fat. In the high fat model, offspring from mouse dams that had been fed either standard chow (C) or a lifetime high-fat diet (HF) were maintained on a HF diet into adulthood. Lanham et al. (2009) used a mouse model to study the effects of a HF diet during gestation on subsequent offspring's bone structure (Lanham et al. 2009). A maternal HF diet during pregnancy was shown to increase bone marrow adiposity and alter bone structure in female offspring. However, female offspring from HF dams who were then fed a postnatal HF diet exhibited a reduced femur length, bone volume, bone density, trabecular thickness, and spacing to levels seen in the control samples. A predictive adaptive response has also been seen here: in the case of the high fat diet used by Lanham et al., female offspring responded to maternal high fat in that when the offspring were maintained on a high fat diet, bone structure similar to controls was observed. In the total nutrient restriction model, bilateral uterine vessel ligation was conducted at 18 days of gestation in the restricted group, in order to reduce blood flow to the fetus and induce restricted fetal growth. Control rats were sham operated. Pups were then cross-fostered onto different control (normal lactation) or restricted (impaired lactation) mothers 1 day after birth. A high fat diet in male mice given from either 7-31 weeks (extended high fat) or 28-31 weeks (short term high fat), has also been shown to be detrimental to trabecular bone structure, with a less extensive effect on cortical bone (Patsch et al. 2011). Bone volume was reduced for both the short term (12%) and extended high fat (19%) diet groups compared to controls. Although the nutritional insult was not given during pregnancy it is evident that even the short term high fat diet produced a distinctly altered phenotype- which is similar to that of osteoporosis. Furthermore, it has been shown that phenotypic changes in the body size of mice offspring induced by maternal high fat have been transmitted down the paternal line to the F3 generation females (Dunn and Bale 2011). No bone analysis was conducted by Dunn et al,

but changes in body size would suggest an increase in bone length and volume (Dunn et al. 2011). The combined protein restriction and high fat diet given in Chapter 3 did exacerbate the phenotype observed from just protein restriction alone.

However, the question of which of the nutritional models used to study maternal nutrition is the most relevant is still unanswered. There is evidence that all of the models discussed have their own merits and all have been shown to influence the phenotype evident in bone at a young age. The age of the offspring studied in any investigation is also going to influence the efficacy of the model. For example, the maternal protein restriction isocaloric model does not increase or decrease the amount of energy the offspring receives so any changes in phenotype may take longer to become evident. That is one reason why a high fat diet was given from 56-84 days in Chapter 3. Another reason is that high fat is becoming more prominent in Western society as obesity rates rise and as highlighted by Patsch et al. (2011) high fat diets even for short periods can have a significant influence on bone structure. Total nutrient restriction is a valid model for the many undernourished people in developing countries. So a case could be made for further investigation into any of the current models.

Further investigation into protein restriction during pregnancy is warranted due to the growing body of evidence that rat offspring's bone microarchitecture and strength are altered. The addition of folic acid to low protein diets during pregnancy poses an interesting research topic due to its methyl donor properties and recommended supplementation, especially as folic acid supplementation during pregnancy has not been investigated in bone. One could hypothesise that similar to the Lillycrop et al. (2005) study, the addition of folic acid during pregnancy may reverse the effects induced by maternal protein restriction. Investigations from Chapter 4 confirm that a much later time point than 10 weeks would be required in order to be able to assess this, so a 75 week time point as investigated by Lanham et al. (2008) would be essential in order to model osteoporosis. Further protein restriction investigations would include both male and female samples from protein restricted dams during pregnancy. Samples would be analysed during the

juvenile stage 12 weeks of age as here and also at peak bone mass at 40 weeks of age (Jee and Yao 2001) and in old age at 75 weeks (Lanham et al. 2008). Techniques would include anthropometric analysis, gene expression, μ CT analysis, microindentation testing, and three point bend testing as used in this thesis. Additional methylation studies would be conducted on bone tissue similar to those previously used by Burdge et al. (2009) to investigate liver epigenetic control of gene expression. Methylation studies would help in elucidating the potential epigenetic mechanisms by which maternal protein restriction induces alterations in offspring bone structure and the role that folic acid supplementation may play in this. Additional studies into the role of intergenerational high fat along both the maternal and paternal lines would prove interesting, again using the same time points and techniques as highlighted above. This area of research still demands thorough investigation and is of high importance in the field of osteoporosis research.

This thesis demonstrates that maternal protein restriction produces minor and non-transmitted effects on offspring bone for three subsequent generations, and that folic acid addition during the juvenile period alters the phenotype of young adult offspring from protein restricted dams. In Chapter 4 F1 protein restricted offspring showed reduced femur length, F2 offspring showed reduced osteocalcin expression and the microindentation analysis for the F3 protein restriction offspring demonstrated more resistance to fracture at the head of femur and less resistant to fracture at the neck of femur than controls. This shows that a response has been made as a result of the F0 PR. In Chapter 3 folic acid addition at the juvenile stage altered the phenotype of both male and female young adult rat offspring from protein restricted dams. Effects that predict a stronger bone were seen in the female offspring vertebral bodies, and effects that predict a weaker bone were seen in the midshaft femur of female offspring and in the trabecular structure at the neck of femur of male offspring. Comparison of the results for F1 offspring from protein restricted dams from both results chapters also showed that the addition of a high fat diet to young adult rats magnified structural and strength changes in bone not seen by protein restriction alone.

6. References

- Ammann, P., Laib, A., Bonjour, J.P., Meyer, J.M., Regsegger, P., and Rizzoli, R. 2002. Dietary essential amino acid supplements increase bone strength by influencing bone mass and bone microarchitecture in ovariectomized adult rats fed an isocaloric low-protein diet. *Journal of Bone and Mineral Research*, 17, (7) 1264-1272
- Aubin, J.E. 2001. Regulation of osteoblast formation and function. Reviews in *Endocrine and Metabolic Disorders*, 2, (1) 81-94
- Barker, D.J., Bull, A.R., Osmond, C., and Simmonds, S.J. 1990. Fetal and placental size and risk of hypertension in adult life. *British Medical Journal*, 301, (6746) 259-262
- Barker, D.J.P. 1990. The fetal and infant origins of adult disease. *British Medical Journal*, 301, (6761) 1111
- Barker, D.J.P. 1995. Fetal origins of coronary heart disease. *British Medical Journal*, 311, (6998) 171-174
- Barker, D.J.P. 2007. Introduction: the window of opportunity. *Journal of Nutrition*, 137, (4) 1058-1059
- Barker, D.J.P. and Osmond, C. 1986. Infant mortality, childhood nutrition, and ischemic heart disease in England and Wales. *The Lancet*, 327, (8489) 1077-1081
- Baron, R., Ferrari, S., and Russell, R.G. 2011. Denosumab and bisphosphonates: different mechanisms of action and effects. *Bone*, 48, (4) 677-692
- Benyshek, D., Johnston, C., and Martin, J. 2006. Glucose metabolism is altered in the adequately-nourished grand-offspring (F3 generation) of rats malnourished during gestation and perinatal life. *Diabetologia*, 49, (5) 1117-1119
- Bilezikian, J.P., Raisz, L.G., and Martin, T.J. 2009. *Principles of Bone Biology*, 3rd ed, San Diego: Academic Press; 2008

Black, D.M., Delmas, P.D., Eastell, R., Reid, I., Boonen, S., Cauley, J.A., Cosman, F., Lakatos, P., Leung, P.C., Man, Z., Mautalen, C., Mesenbrink, P., Hu, H., Caminis, J., Tong, K., Rosario-Jansen, T., Krasnow, J., Hue, T.F., Sellmeyer, D., Eriksen, E.F. and Cummings, S.R. 2007. Once-yearly Zoledronic acid for treatment of postmenopausal osteoporosis. *The New England Journal of Medicine*, 356, (18) 1809-1822

Blaus, B. Structure of a long bone,
http://en.wikipedia.org/wiki/File:Structure_of_a_Long_Bone.png. 20-8-2013.

Bonewald, L.F. 2007. Osteocytes as dynamic multifunctional cells. *Skeletal Biology and Medicine*, Pt A, 1116, 281-290

Boskey, A. 2006. Assessment of bone mineral and matrix using backscatter electron imaging and FTIR imaging. *Current Osteoporosis Reports*, 4, (2) 71-75

Boyde, A. Osteoclast. Breakfast, lunch and dinner for an osteoclast!
<http://www.brsoc.org.uk/gallery/index.htm> , 2010.

Brown, J.P., Prince, R.L., Deal, C., Recker, R.R., Kiel, D.P. and de Gregorio L.H. 2009. Comparison of the effect of denosumab and alendronate on BMD and biochemical markers of bone turnover in postmenopausal women with low bone mass: a randomized, blinded, phase 3 trial. *Journal of Bone and Mineral Research*, 24, (1) 153-161

Bruce, K.D., Cagampang, F.R., Argenton, M., Zhang, J., Ethirajan, P.L., Burdge, G.C., Bateman, A.C., Clough, G.F., Poston, L., Hanson, M.A., McConnell, J.M., and Byrne, C.D. 2009. Maternal high-fat feeding primes steatohepatitis in adult mice offspring, involving mitochondrial dysfunction and altered lipogenesis gene expression. *Hepatology*, 50, (6) 1796-1808

Burdge, G.C., Lillycrop, K.A., Phillips, E.S., Slater-Jefferies, J.L., Jackson, A.A., and Hanson, M.A. 2009. Folic acid supplementation during the juvenile-pubertal period in rats modifies the phenotype and epigenotype induced by prenatal nutrition. *Journal of Nutrition*, 109, 1054-1060

Burdge, G.C., Slater-Jefferies, J., Torrens, C., Phillips, E.S., Hanson, M.A., and Lillycrop, K.A. 2007. Dietary protein restriction of pregnant rats in the F-0

generation induces altered methylation of hepatic gene promoters in the adult male offspring in the F-1 and F-2 generations. *British Journal of Nutrition*, 97, (3) 435-439

Burdge, G.C., Slater-Jefferies, J.L., Grant, R.A., Chung, W.S., West, A.L., Lillycrop, K.A., Hanson, M.A., and Calder, P.C. 2008. Sex, but not maternal protein or folic acid intake, determines the fatty acid composition of hepatic phospholipids, but not of triacylglycerol, in adult rats. *Prostaglandins, Leukotrienes and Essential Fatty Acids*, 78, (1) 73-79

Butler, N.R., Goldstein, H., and Ross, E.M. 1972. Cigarette smoking in pregnancy: its influence on birth weight and perinatal mortality. *British Medical Journal*, 2, (5806) 127-130

Chappard, D., Legrand, E., Haettivh, B., Chales, G., Auvinet, B., Eschard, J.P., Hamelin, J.P., Basle, M.F., and Audran, M. 2001. Fractal dimension of trabecular bone: comparison of three histomorphometric computed techniques for measuring the architectural two-dimensional complexity. *The Journal of Pathology*, 195, (4) 515-521

Chia, P.H., Gualano, L., Seevanayagam, S., and Weinberg, L. 2013. Outcomes following fractured neck of femur in an Australian metropolitan teaching hospital. *Bone and Joint Research*, 2, (8) 162-168

Cole, Z.A., Gale, C.R., Javaid, M.K., Robinson, S.M., Law, C., Boucher, B.J., Crozier, S.R., Godfrey, K.M., Dennison, E.M., and Cooper, C. 2009. Maternal dietary patterns during pregnancy and childhood bone mass: a longitudinal study. *Journal of Bone and Mineral Research*, 24, (4) 663-668

Cooper, C. 1996. The problem- health impact of osteoporosis. *Scandinavian Journal of Rheumatology* (25) 3-5

Cooper, C. 2010. Osteoporosis: disease severity and consequent fracture management. *Osteoporosis International*, 21, (0) 425-429

Cooper, C. and Aihie, A. 1995. Osteoporosis. *Baillieres Clinical Rheumatology*, 9, (3) 555-564

- Cooper, C., Eriksson, J.G., Forsen, T., Osmond, C., Tuomilehto, J., and Barker, D.J.P. 2001. Maternal height, childhood growth and risk of hip fracture in later life: a longitudinal study. *Osteoporosis International*, 12, (8) 623-629
- Cooper, C., Fall, C., Egger, P., Hobbs, R., Eastell, R., and Barker, D. 1997. Growth in infancy and bone mass in later life. *Annals of the Rheumatic Diseases*, 56, (1) 17-21
- Cooper, C., Javaid, M.K., Taylor, P., Walker-Bone, K., Dennison, E., and Arden, N. 2002. The fetal origins of osteoporotic fracture. *Calcified Tissue International*, 70, (5) 391-394
- Cooper, C., Walker-Bone, K., Arden, N., and Dennison, E. 2000. Novel insights into the pathogenesis of osteoporosis: the role of intrauterine programming. *Rheumatology*, 39, (12) 1312-1315
- Coxon, J.P., Oades, G.M., Colston, K.W., and Kirby, R.S. 2004. Advances in the use of bisphosphonates in the prostate cancer setting. *Prostate Cancer and Prostatic Diseases*, 7, (2) 99-104
- Cramer, J., Gold, D., Silverman, S., and Lewiecki, E. 2007. A systematic review of persistence and compliance with bisphosphonates for osteoporosis. *Osteoporosis International*, 18, (8) 1023-1031
- Dequeker, J. and Johnell, O. 1993. Osteoarthritis protects against femoral neck fracture: the MEDOS study experience. *Bone*, 14 Suppl 1, S51-S56
- Diez-Perez, A., Guerri, R., Nogues, X., Caceres, E., Pena, M.J., Mellibovsky, L., Randall, C., Bridges, D., Weaver, J.C., Proctor, A., Brimer, D., Koester, K.J., Ritchie, R.O., and Hansma, P.K. 2010. Microindentation for in vivo measurement of bone tissue mechanical properties in humans. *Journal of Bone and Mineral Research*, 25, (8) 1877-1885
- Doblhammer, G. and Vaupel, J.W. 2001. Lifespan depends on month of birth. *Proceedings of the National Academy of Sciences of the United States of America*, 98, (5) 2934-2939

- Dolinoy, D.C., Das, R., Weidman, J.R., and Jirtle, R.L. 2007. Metastable epialleles, imprinting, and the fetal origins of adult diseases. *Pediatric Research*, 61, (5 Part 2) 30R-37R
- Drake, A.J. and Liu, L. 2010. Intergenerational transmission of programmed effects: public health consequences. *Trends in Endocrinology and Metabolism*, 21, (4) 206-213
- Dunn, G.A. and Bale, T.L. 2011. Maternal high-fat diet effects on third-generation female body size via the paternal lineage. *Endocrinology*, 152, (6) 2228-2236
- Earl, S., Cole, Z.A., Holroyd, C., Cooper, C., and Harvey, N.C. 2010. Session 2: other diseases: dietary management of osteoporosis throughout the life course. *Proceedings of the Nutrition Society*, 69, (1) 25-33
- Fernandez-Twinn, D.S., Wayman, A., Ekizoglou, S., Martin, M.S., Hales, C.N., and Ozanne, S.E. 2005. Maternal protein restriction leads to hyperinsulinemia and reduced insulin-signaling protein expression in 21-mo-old female rat offspring. *American Journal of Physiology - Regulatory Integrative and Comparative Physiology*, 288, (2) R368-R373
- Ganss, B., Kim, R.H., and Sodek, J. 1999. Bone sialoprotein. *Critical Reviews in Oral Biology and Medicine*, 10, (1) 79-98
- Gilbert, S.F. 2000. *Developmental Biology*, 6th Edition ed. Sinauer Associates Inc., U.S.
- Giudicelli, F., Brabant, A.L., Grit, I., Parnet, P., and Amarger, V.r. 2013. Excess of methyl donor in the perinatal period reduces postnatal leptin secretion in rat and interacts with the effect of protein content in diet. *Public Library of Science One*, 8, (7) e68268
- Gluckman, P.D. and Hanson, M.A. 2004. Living with the past: evolution, development, and patterns of disease. *Science*, 305, (5691) 1733-1736
- Gluckman, P.D., Hanson, M.A., Buklijas, T., Low, F.M., and Beedle, A.S. 2009. Epigenetic mechanisms that underpin metabolic and cardiovascular diseases. *Nature Reviews Endocrinology*, 5, (7) 401-408

Gluckman, P.D., Hanson, M.A., Cooper, C., and Thornburg, K.L. 2008. Effect of in utero and early-life conditions on adult health and disease. *New England Journal of Medicine*, 359, (1) 61-73

Gluckman, P.D. and Hanson, M.A., 2006. *Developmental Origins of Health and Disease*. Cambridge University Press. 1st ed.

Godfrey, K., Walker-Bone, K., Robinson, S., Taylor, P., Shore, S., Wheeler, T., and Cooper, C. 2001. Neonatal bone mass: influence of parental birth weight, maternal smoking, body composition, and activity during pregnancy. *Journal of Bone and Mineral Research*, 16, (9) 1694-1703

Gong, L., Pan, Y.X., and Chen, H. 2010. Gestational low protein diet in the rat mediates Igf2 gene expression in male offspring via altered hepatic DNA methylation. *Epigenetics*, 5, (7) 619-626

Guntur, A. and Rosen, C. 2012. Bone as an endocrine organ. *Endocrine Practice*, 18, (5) 758-762

Hahn, M., Vogel, M., Pompesius-Kempa, M., and Delling, G. 2007. Trabecular bone pattern factor-a new parameter for simple quantification of bone microarchitecture. *Bone*, 13, (4) 327-330

Hales, C.N. and Barker, D.J.P. 2001. The thrifty phenotype hypothesis: type 2 diabetes. *British Medical Bulletin*, 60, (1) 5-20

Hanson, M.A. and Gluckman, P.D. 2008. Developmental origins of health and disease: New Insights. *Basic and Clinical Pharmacology and Toxicology*, 102, (2) 90-93

Harrison, M. and Langley-Evans, S.C. 2009. Intergenerational programming of impaired nephrogenesis and hypertension in rats following maternal protein restriction during pregnancy. *British Journal of Nutrition*, 101, (7) 1020-1030

Harvey, N.C., Javaid, M.K., Arden, N.K., Poole, J.R., Crozier, S.R., Robinson, S.M., Inskip, H.M., Godfrey, K.M., Dennison, E.M., and Cooper, C. 2010. Maternal predictors of neonatal bone size and geometry: the Southampton women's survey. *Journal of Developmental Origins of Health and Disease*, 1, (1) 35-41

- Hauschka, P.V., Frenkel, J., DeMuth, R., and Gundberg, C.M. 1983. Presence of osteocalcin and related higher molecular weight 4-carboxyglutamic acid-containing proteins in developing bone. *Journal of Biological Chemistry*, 258, (1) 176-182
- Heaney, R.P., Abrams, S., Dawson-Hughes, B., Looker, A., Looker, A., Marcus, R., Matkovic, V., and Weaver, C. 2000. Peak bone mass. *Osteoporosis International*, 11, (12) 985-1009
- Hildebrand, T. and Regsegger, P. 1997. Quantification of bone microarchitecture with the structure model index. *Computer Methods in Biomechanics and Biomedical Engineering*, 1, (1) 15-23
- Hill, P.A. 1998. Bone remodelling. *Journal of Orthodontics*, 25, (2) 101-107
- Hochberg, Z., Feil, R., Constancia, M., Fraga, M., Junien, C., Carel, J.C., Boileau, P., Le Bouc, Y., Deal, C.L., Lillycrop, K., Scharfmann, R., Sheppard, A., Skinner, M., Szyf, M., Waterland, R.A., Waxman, D.J., Whitelaw, E., Ong, K., and Albertsson-Wikland, K. 2011. Child health, developmental plasticity, and epigenetic programming. *Endocrine Reviews*, 32, (2) 159-224
- Hoile, S.P., Lillycrop, K.A., Thomas, N.A., Hanson, M.A., and Burdge, G.C. 2011. Dietary protein restriction during F-0 pregnancy in rats induces transgenerational changes in the hepatic transcriptome in female offspring. *Public Library of Science One*, 6, (7)
- Hopyan, S., Gokgoz, N., Bell, R.S., Andrulis, I.L., Alman, B.A., and Wunder, J.S. 1999. Expression of osteocalcin and its transcriptional regulators core-binding factor alpha 1 and MSX2 in osteoid-forming tumours. *Journal of Orthopaedic Research*, 17, (5) 633-638
- Huot, P.S., Dodington, D.W., Mollard, R.C., Reza-Lopez, S.A., Sanchez-Hernandez, D., Cho, C.E., Kuk, J., Ward, W.E., and Anderson, G.H. 2013. High folic acid intake during pregnancy lowers body weight and reduces femoral area and strength in female rat offspring. *Journal of Osteoporosis*, 2013, 154109
- Jee, W.S. and Yao, W. 2001. Overview: animal models of osteopenia and osteoporosis. *Journal of Musculoskeletal and Neuronal Interactions*, 1, (3) 193-207

- Jones, G., Riley, M., and Dwyer, T. 1999. Maternal smoking during pregnancy, growth, and bone mass in prepubertal children. *Journal of Bone and Mineral Research*, 14, (1) 146-151
- Jundt, G., Berghñuser, K.H., Termine, J.D., and Schulz, A. 1987. Osteonectin - a differentiation marker of bone cells. *Cell and Tissue Research*, 248, (2) 409-415
- Kanis, J., Burlet, N., Cooper, C., Delmas, P., Reginster, J.Y., Borgstrom, F., Rizzoli, R., and 2008. European guidance for the diagnosis and management of osteoporosis in postmenopausal women. *Osteoporosis International*, 19, (4) 399-428
- Kanis, J.A. 2002. Diagnosis of osteoporosis and assessment of fracture risk. *The Lancet*, 359, (9321) 1929-1936
- Kanis, J.A. 2010. Osteoporosis. *Journal of Medical Sciences*, 3, (3) 124-130
- Kanis, J.A. and Kanis, J.A. 1994. Assessment of fracture risk and its application to screening for postmenopausal osteoporosis: synopsis of a WHO report. *Osteoporosis International*, 4, (6) 368-381
- Kanis, J.A., Delmas, P., Burckhardt, P., Cooper, C., and Torgerson, D. 1997. Guidelines for diagnosis and management of osteoporosis. *Osteoporosis International*, 7, (4) 390-406
- Kirkham GR and Cartmell SH. 2007. Genes and proteins involved in the regulation of osteogenesis. *Topics in Tissue Engineering* 3.
- Kloosterboer, H.J. and Ederveen, A.G.H. 2002. Pros and cons of existing treatment modalities in osteoporosis: a comparison between Tibolone, SERMs and Estrogen (Progestogen) treatments. *The Journal of Steroid Biochemistry and Molecular Biology*, 83, (1-5) 157-165
- Knight, S. 2003. *Muscles, Bones and Skin*, Second Edition ed. Elsevier Science.
- Koo, W.K., Walters, J., Esterlitz, J.O.Y., Levine, R.J., Bush, A.J., and Sibia, B.A.H.A. 1999. Maternal calcium supplementation and fetal bone mineralization. *Obstetrics and Gynecology*, 94, (4) 577-582

- Langley-Evans, S.C. and McMullen, S. 2010. Developmental origins of adult disease. *Medical Principles and Practice*, 19, (2) 87-98
- Lanham, S.A., Roberts, C., Hollingworth, T., Sreekumar, R., Elahi, M.M., Cagampang, F.R., Hanson, M.A., and Oreffo, R.O. 2009. Maternal high-fat diet: effects on offspring bone structure. *Osteoporosis International*, 21(10) 1703-14
- Lanham, S.A., Roberts, C., Perry, M.J., Cooper, C., and Oreffo, R.O.C. 2008. Intrauterine programming of bone. part 2: alteration of skeletal structure. *Osteoporosis International*, 19, (2) 157-167
- Lanham, S.A., Bertram, C., Cooper, C., and Oreffo, R.O. 2011. Animal Models of Maternal Nutrition and Altered Offspring Bone Structure-Bone Development Across the Lifecourse. *European cells and materials*, 22, 321-332
- Lelovas, P.P., Xanthos, T.T., Thoma, S.E., Lyritis, G.P., and Dontas, I.A. 2008. The laboratory rat as an animal model for osteoporosis research. *Comparative Medicine*, 58, (5) 424-430
- Leppänen, O., Sievönen, H., Jokihaara, J., Pajamäki, I., and Järvinen, T.L. 2006. Three-point bending of rat femur in the mediolateral direction: introduction and validation of a novel biomechanical testing protocol. *Journal of Bone and Mineral Research*, 21, (8) 1231-1237
- Leslie, W.D. 2012. Ethnic differences in bone mass - clinical implications. *Journal of Clinical Endocrinology and Metabolism*, 97, (12) 4329-4340
- Lillycrop, K.A., Phillips, E.S., Jackson, A.A., Hanson, M.A., and Burdge, G.C. 2005. Dietary protein restriction of pregnant rats induces and folic acid supplementation prevents epigenetic modification of hepatic gene expression in the offspring. *Journal of Nutrition*, 135, (6) 1382-1386
- Livak, K.J. and Schmittgen, T.D. 2001. Analysis of relative gene expression data Using real-time quantitative PCR and the 2 delta CT method. *Methods*, 25, (4) 402-408
- Lucas, A. 1991. Programming by early nutrition in man. *Ciba Foundation Symposia*, 156, 38-55

- Major, P.P., Lipton, A., Berenson, J., and Hortobagyi, G. 2000. Oral bisphosphonates. *Cancer*, 88, (1) 6-14
- Marieb, E.N. 2006. *Essentials of Human Anatomy and Physiology*, Ingram, 8ed.
- Marquis, M.E., Lord, E., Bergeron, E., Drevelle, O., Park, H., Cabana, F., Senta, H. and Faucheux, N. 2009. Bone cells-biomaterials interactions. *Frontiers in Bioscience*, 14, (3) 1023-1067
- Martini, F.E.A. 2007. *Anatomy and Physiology*. Pearson Education Inc.
- Mazzali, M., Kipari, T., Ophascharoensuk, V., Wesson, J.A., Johnson, R., and Hughes, J. 2002. Osteopontin - a molecule for all seasons. *QJM: An International Journal of Medicine*, 95, (1) 3-13
- McCance, D.R., Pettitt, D.J., Hanson, R.L., Jacobsson, L.T.H., Knowler, W.C., and Bennett, P.H. 1994. Birth weight and non-insulin dependent diabetes: thrifty genotype, thrifty phenotype, or surviving small baby genotype? *British Medical Journal*, 308, (6934) 942-945
- McHorney, C.A., Schousboe, J.T., Cline, R.R., and Weiss, T.W. 2007. The impact of osteoporosis medication beliefs and side-effect experiences on non-adherence to oral bisphosphonates. *Current Medical Research and Opinion*, 23, (12) 3137-3152
- Meunier, P.J. 1998. *Osteoporosis: diagnosis and management*, illustrated ed. Taylor and Francis.
- Mullender, M.G. and Huiskes, R. 1997. Osteocytes and bone lining cells: which are the best candidates for mechano-sensors in cancellous bone? *Bone*, 20, (6) 527-532
- National Institute for Health and Clinical Excellence 2010, NICE technology appraisal guidance 204 Denosumab for the prevention of osteoporotic fractures in postmenopausal women.
- National Osteoporosis Society 2010. Clinician's guide to prevention and treatment of osteoporosis. Washington, DC: *National Osteoporosis Foundation*.

Odgaard, A. 1997. Three-dimensional methods for quantification of cancellous bone architecture. *Bone*, 20, (4) 315-328

Office of the Surgeon General. 2004 U.S. Department of Health and Human Services. The 2004 surgeon general's report on bone health and osteoporosis: what it means to you. *U.S. Department of Health and Human Services*.

Oury, F., Khrimian, L., Denny, C., Gardin, A., Chamouni, A., Goeden, N., Huang, Y.y., Lee, H., Srinivas, P., Gao, X.B., Suyama, S., Langer, T., Mann, J., Horvath, T., Bonnin, A., and Karsenty, G. 2013. Maternal and offspring pools of osteocalcin influence brain development and functions. *Cell*, 155, (1) 228-241

Patsch, J.M., Kiefer, F.W., Varga, P., Pail, P., Rauner, M., Stupphann, D., Resch, H., Moser, D., Zysset, P.K., Stulnig, T.M., and Pietschmann, P. 2011. Increased bone resorption and impaired bone microarchitecture in short-term and extended high-fat diet induced obesity. *Metabolism*, 60, (2) 243-249

Pitkin, R.M. 2007. Folate and neural tube defects. *The American Journal of Clinical Nutrition*, 85, (1) 285S-288S

Ralston, S.H. 2002. Genetic control of susceptibility to osteoporosis. *Journal of Clinical Endocrinology and Metabolism*, 87, (6) 2460-2466

Ralston, S.H. and Uitterlinden, A.G. 2010. Genetics of osteoporosis. *Endocrine Reviews*, 31(5) 629-62

Ralston, S. 2012. Osteoporosis: Recommended Diagnosis and Management. *Prescriber*, 23, (22) 27-34

Recker, R.R. Ish-Shalom, S. Marín, F.Hawkins, F. and Stepan, J. 2009. Comparative effects of Teriparatide and Strontium Ranelate on bone biopsies and biochemical markers of bone turnover in postmenopausal women with osteoporosis. *Journal of Bone and Mineral Research*, 24, (8) 1359-1368

Remy, E. and Thiel, E. 2002. Medial axis for chamfer distances: computing look-Up tables and neighbourhoods in 2D or 3D. *Pattern Recognition Letters*, 23, (6) 649-661

Rey, C., Combes, C., Drouet, C., and Gilmcher, M.J. 2009. Bone mineral: update on chemical composition and structure. *Osteoporosis International*, 20, 1013-1021

Riggs, B.L., Kholsa, S., and Melton, L.J. 1998. A unitary model for involuntional osteoporosis: oestrogen deficiency causes both type I and type II osteoporosis in postmenopausal women and contributes to bone loss in aging men. *Journal of Bone and Mineral Research*, 13, (5) 763-773

Romano, T., Wark, J.D., Owens, J.A., and Wlodek, M.E. 2009. Prenatal growth restriction and pstnatal growth restriction followed by accelerated growth independently program reduced bone growth and strength. *Bone*, 45, (1) 132-141

Royal College of Physicians. Osteoporosis; clinical guide-lines for prevention and treatment. *London: Royal College of Physicians of London*. 1999.

Ralston, S.H. and Uitterlinden, A.G. 2010. Genetics of osteoporosis. *Endocrine Reviews*, 31, (5)

Schulz, L.C. 2010. The Dutch hunger winter and the developmental origins of health and disease. *Proceedings of the National Academy of Sciences*, 107, (39) 16757-16758

SEER - U.S. National Cancer Institute's Surveillance, Epidemiology and End Results (SEER) Program. *Compact Bone and Spongy Bone*. (<http://training.seer.cancer.gov/anatomy/skeletal/tissue.html>) 2014

Thiebaud, D., Burckhardt, P., Kriegbaum, H., Huss, H., Mulder, H., Juttman, J.R., and Schóter, K.H. 1997. Three monthly intravenous injections of Ibandronate in the treatment of postmenopausal osteoporosis. *The American Journal of Medicine*, 103, (4) 298-307

Tobias, J.H., Steer, C.D., Emmett, P.M., Tonkin, R.J., Cooper, C., and Ness, A.R. 2005. Bone mass in childhood is related to maternal diet in pregnancy. *Osteoporosis International*, 16, (12) 1731-1741

Tobias, J.H. and Cooper, C. 2004. PTH/PTHrP Activity and the Programming of Skeletal Development in Utero. *Journal of Bone and Mineral Research*, 19, (2) 177-182

Torrens, C., Bautista, C.J., Tovar, A.R., Ordíz, G., Rodriguez-Cruz, M., Ortiz, V., Granados, O., Nathanielsz, P.W., Larrea, F., and Zambrano, E. 2010. Protein

restriction during pregnancy affects maternal liver lipid metabolism and fetal brain; lipid composition in the rat. *American Journal of Physiology - Endocrinology and Metabolism*, 298, (2) E270-E277

Torrens, C., Brawley, L., Anthony, F.W., Dance, C.S., Dunn, R., Jackson, A.A., Poston, L., and Hanson, M.A. 2006. Folate supplementation during pregnancy improves offspring cardiovascular dysfunction induced by protein restriction. *Hypertension*, 47, (5) 982-987

Torrens, C., Ethirajan, P., Bruce, K.D., Cagampang, F.R., Siow, R.C., Hanson, M.A., Byrne, C.D., Mann, G.E., and Clough, G.F. 2012. Interaction between maternal and offspring diet to impair vascular function and oxidative balance in high fat fed male mice. *Public Library of Science One*, 7, (12) e50671

Torrens, C., Poston, L., Hanson, M.A., Torrens, C., Poston, L., and Hanson, M.A. 2008. Transmission of raised blood pressure and endothelial dysfunction to the F-2 generation induced by maternal protein restriction in the F-0, in the absence of dietary challenge in the F-1 generation. *British Journal of Nutrition*, 100, (4) 760-766

Van Rietbergen, B., Huiskes, R., Eckstein, F., and Regsegger, P. 2003. Trabecular bone tissue strains in the healthy and osteoporotic human femur. *Journal of Bone and Mineral Research*, 18, (10) 1781-1788

Wald, N. 1991. Prevention of neural-tube defects - results of the medical-research-council vitamin study. *The Lancet*, 338, (8760) 131-137

Wald, N.J., Law, M.R., Morris, J.K., and Wald, D.S. 2001. Quantifying the effect of folic acid. *The Lancet*, 358, (9298) 2069-2073

Watkins, A.J., Lucas, E.S., Wilkins, A., Cagampang, F.R., and Fleming, T.P. 2011. Maternal periconceptual and gestational low protein diet affects mouse offspring growth, cardiovascular and adipose phenotype at 1 year of age. *Public Library of Science One*, 6, (12) e28745

Waugh, A. and Grant, A. 2001. *Ross and Wilson anatomy and physiology in health and illness*, 9 ed. Churchill Livingstone.

Weber, P. 2001. Vitamin K and bone health. *Nutrition*, 17, (10) 880-887

- Widdowson, E.M. and McCance, R.A. 1963. The effect of finite periods of undernutrition at different ages on the composition and subsequent development of the rat. *Proceedings of the Royal Society of London. Series B, Biological Sciences*, 158, (972) 329-342
- Wood, A.J.J., Riggs, B.L., and Hartmann, L.C. 2003. Selective estrogen-receptor modulators mechanisms of action and application to clinical practice. *New England Journal of Medicine*, 348, (7) 618-629
- Woods, L.L., Ingelfinger, J.R., Nyengaard, J.R., and Rasch, R. 2001. Maternal protein restriction suppresses the newborn renin-angiotensin system and programs adult hypertension in rats. *Pediatric Research*, 49, (4) 460-467
- World Health Organisation 1994, Assesment of fracture risk and its application to screening for postmenopausal osteoporosis. *Technical Report Series 84 Geneva*.
- Zhang, M., Xuan, S., Bouxsein, M.L., von Stechow, D., Akeno, N., Faugere, M.C., Malluche, H., Zhao, G., Rosen, C.J., Efstratiadis, A., and Clemens, T.L. 2002. Osteoblast-specific knockout of the insulin-like growth factor (IGF) receptor genereveals an essential role of IGF signaling in bone matrix mineralization. *Journal of Biological Chemistry*, 277, (46) 44005-4401

7. Appendices

Appendix 1 – Micro computed tomography CTAn task lists

Trabecular task list

- Thresholding-> *Adaptive (mean of min and max values)-> 2D space->Pre-thresholding-> Background : Dark-> Radius : 7-> Contrast : 0*
- Despeckle-> *Type : Remove white speckles-> 3D space-> Volume : less than 20 voxels-> Apply to : Image*
- 3D analysis-> *Basic values-> Additional values : all-> Save results as : both*
- Save bitmaps-> *Apply to : Image inside ROI-> file format : BMP->Convert to monochrome (1 bit)-> Copy shadow projection->Copy dataset log file*

Cortical task list

- Thresholding-> *Global*
- Bitwise Operations-> *Image=Image AND Region of Interest*
- Morphological operations-> *Type: Opening-> 3D space-> Kernel : Round-> Radius : 2-> Apply to : Image*
- Despeckle-> *Type : Sweep-> 3D space-> Remove : all except the largest object-> Apply to image*
- 3D analysis-> *Basic values-> Additional values : all except Trabecular separation-> Save results as : both*
- 2D analysis-> *Summary results*
- Save bitmaps-> *Apply to : Image inside ROI-> file format : BMP->Convert to monochrome (1 bit)-> Copy shadow projection->Copy dataset log file*

Appendix 2–Molecular protocols

Protocol for First-Strand cDNA Synthesis using SuperScript® VILO™ from Invitrogen.

The following protocol has been optimized for generating first-strand cDNA for use in two-step qRT-PCR. The reaction volume may be scaled as needed up to 100 μ l.

1. For a single reaction, combine the following components in a tube on ice. For multiple reactions, prepare a master mix without RNA.

5X VILO™ Reaction Mix 4 μ l

10X SuperScript® Enzyme Mix 2 μ l

RNA (up to 2.5 μ g) \times μ l

DEPC-treated water to 20 μ l

2. Gently mix tube contents and incubate at 25°C for 10 minutes.

3. Incubate tube at 42°C for 60 minutes.

4. Terminate the reaction at 85°C at 5 minutes.

5. Use diluted or undiluted cDNA in qPCR (see below), or store at -20°C until use.

RNA Isolation Procedure simplified from the TRIzol® Reagent protocol from Invitrogen

Always use the appropriate precautions to avoid RNase contamination when preparing and handling RNA.

RNA precipitation

1. When precipitating RNA from small sample quantities (<10⁶ cells or <10 mg tissue), add 5–10 μ g of RNase-free glycogen as a carrier to the aqueous phase.

Note: Glycogen is co-precipitated with the RNA, but does not inhibit first-strand synthesis at concentrations $\leq 4\text{mg/mL}$, and does not inhibit PCR.

2. Add 0.5 mL of 100% isopropanol to the aqueous phase, per 1 mL of TRIzol® Reagent used or homogenization.

3. Incubate at room temperature for 10 minutes.

4. Centrifuge at $12,000\times g$ for 10 minutes at 4°C . Note: The RNA is often invisible prior to centrifugation, and forms a gel-like pellet on the side and bottom of the tube.

RNA wash

1. Remove the supernatant from the tube, leaving only the RNA pellet.

2. Wash the pellet, with 1 mL of 75% ethanol per 1 mL of TRIzol® Reagent used in the initial homogenization. Note: The RNA can be stored in 75% ethanol at least 1 year 20°C , or at least 1 week at 4°C .

3. Vortex the sample briefly, then centrifuge the tube at $7500\times g$ for 5 minutes at 4°C . Discard the wash.

4. Vacuum or air dry the RNA pellet for 5–10 minutes. Do not dry the pellet by vacuum centrifuge. Note: Do not allow the RNA to dry completely, because the pellet can lose solubility. Partially dissolved RNA samples have an A_{260}/A_{280} ratio < 1.6 .

RNA resuspension

1. Resuspend the RNA pellet in RNase-free water or 0.5% SDS solution (20–50 μL) by passing the solution up and down several times through a pipette tip. Note: Do not dissolve the RNA in 0.5% SDS if it is to be used in subsequent enzymatic reactions.

2. Incubate in a water bath or heat block set at $55\text{--}60^{\circ}\text{C}$ for 10–15 minutes.

3. Proceed to downstream application, or store at -70°C .

Appendix 3- Housekeeping gene stability data

Two housekeeping genes β -Actin and R18S were selected for stability testing in order for qPCR analysis. Both housekeeping genes were run in duplicate with 18 of the rats studied in Chapter 4. The housekeeping gene whose CT values had the smallest standard deviation between all 36 measurements (total SD) was deemed the most stable and therefore used in all subsequent experiments. As shown in Table 7-1 the total SD for β -Actin was 1.20 and for R18s was 1.01. R18s was hence selected as the housekeeping gene of choice.

Table 7-1 Housekeeping gene CT data used to determine stability

Beta Actin					R18s				
	Cr	Cr Mean	Cr SD	Total SD		Cr	Cr Mean	Cr SD	Total SD
1	27.66419	27.79744	0.188448	1.20	1	11.78453	11.69176	0.131201	1.01
	27.93069	27.79744	0.188448			11.59898	11.69176	0.131201	
2	29.19563	29.30552	0.155419		2	11.20804	11.25127	0.061126	
	29.41542	29.30552	0.155419			11.29449	11.25127	0.061126	
3	27.71135	28.34676	0.898617		3	12.49349	12.21735	0.39052	
	28.98218	28.34676	0.898617			11.94121	12.21735	0.39052	
4	28.14451	28.55732	0.583793		4	10.09328	11.10881	1.43618	
	28.97012	28.55732	0.583793			12.12434	11.10881	1.43618	
5	28.52352	28.57073	0.066763		5	12.94224	13.21139	0.380629	
	28.61794	28.57073	0.066763			13.48053	13.21139	0.380629	
6	26.66804	27.43085	1.078771		6	12.70418	13.05626	0.497909	
	28.19365	27.43085	1.078771			13.40833	13.05626	0.497909	
7	28.78931	28.6364	0.216253		7	11.21105	11.09076	0.170111	
	28.48349	28.6364	0.216253			10.97047	11.09076	0.170111	
8	26.93706	27.73018	1.121643		8	12.3179	12.16074	0.222265	
	28.5233	27.73018	1.121643			12.00357	12.16074	0.222265	
9	29.75652	29.35534	0.567353		9	14.19027	13.35925	1.175233	
	28.95416	29.35534	0.567353			12.52824	13.35925	1.175233	
10	31.37453	31.76895	0.55779		10	14.19916	14.59305	0.557045	
	32.16336	31.76895	0.55779			14.98694	14.59305	0.557045	
11	27.60841	27.8086	0.283111		11	11.35837	11.76732	0.578338	
	28.00879	27.8086	0.283111			12.17626	11.76732	0.578338	
12	29.94256	29.7029	0.338931		12	11.95517	11.93629	0.026697	
	29.46324	29.7029	0.338931			11.91741	11.93629	0.026697	
13	27.60459	27.32383	0.397064		13	9.702315	11.19254	2.107497	
	27.04306	27.32383	0.397064			12.68277	11.19254	2.107497	
14	27.57227	27.41997	0.215385		14	12.35488	12.84032	0.686513	
	27.26767	27.41997	0.215385			13.32576	12.84032	0.686513	
15	27.01311	27.63495	0.879417		15	12.35832	12.35707	0.001764	
	28.2568	27.63495	0.879417			12.35582	12.35707	0.001764	
16	27.10532	27.07393	0.044391		16	11.35917	11.23669	0.173209	
	27.04254	27.07393	0.044391			11.11422	11.23669	0.173209	
17	27.38235	27.48133	0.139991		17	11.63025	11.60428	0.036726	
	27.58032	27.48133	0.139991			11.57831	11.60428	0.036726	
18	28.36142	28.65841	0.420019		18	11.90075	12.52925	0.888828	
	28.95541	28.65841	0.420019			13.15775	12.52925	0.888828	

Appendix 4- Primer sequences for qPCR

Table 7-2 Primer sequences for qPCR

Primer name	F/R	Primer sequence
Rat R18s	F	GCC GCG GTA ATT CCA GCT CCA
	R	CCC GCC CGC TCC CAA GAT C
Rat Col1A1	F	TGGCAAGAACGGAGATGA
	R	AGCTGTTCCAGGCAATCC
Rat Osteocalcin	F	CAG ACA CCA TGA GGA CCC TC
	R	GTC CAT TGT TGA GGT AGC GC
Rat Osteopontin	F	CTG CCA GCA CAC AAG CAG AC
	R	TCT GTG GCA TCG GGA TAC TG
Rat Osteonectin	F	GGA AGC TGC AGA AGA GAT GG
	R	TGC ACA CCT TTT CAA ACT CG
Rat BSP	F	CCG GCC ACG CTA CTT TCT TT
	R	TGG ACT GGA AAC CGT TTC AGA
Rat Runx 2	F	GCC GGA ATG ATG AGA ACT A
	R	TTG GGG AGG ATT TGT GAA GA
Rat IGF-II	F	CCA GGT GAC AGG ACT GGC AT
	R	CCT GAA AAC ACC CAT CCC AC

Rat IGF-I	F	GCT GCT GAA GCC GTT CAT TTA
	R	AAG AAA GGG CAG GGC TAA TGG
Rat β Actin	F	AGC CAT GTA CGT AGC CAT CCA
	R	TCT CCG GAG TCC ATC ACA ATG

Appendix 5- Microindentation data for midshaft points 2-4 and epicondyle site

Table 7-3 Mean values for the microindentation data for the midshaft femur 2 cortical bone of female F1 offspring (n=5) from protein restricted mothers (F0) compared to controls (n=5). P-values are derived from the One-Way ANOVA analysis.

Microindentation midshaft femur 2					
	F0 Control/ F1 Control (n=5)		F0 Protein restriction/ F1 Control (n=5)		P-value
	Mean	SD	Mean	SD	
Total indentation distance (µm)	63.2	4.0	75.0	22.4	1.00
Indentation distance increase (µm)	8.7	2.4	12.2	12.5	1.00
Creep indentation distance (µm)	1.99	0.40	4.56	4.39	1.00

Table 7-4 Mean values for the microindentation data for the midshaft femur 3 cortical bone of female F1 offspring (n=5) from protein restricted mothers (F0) compared to controls (n=5). P-values are derived from the One-Way ANOVA analysis.

Microindentation midshaft femur 3					
	F0 Control/ F1 Control (n=5)		F0 Protein restriction/ F1 Control (n=5)		P-value
	Mean	SD	Mean	SD	
Total indentation distance (µm)	72.6	17.3	103.9	42.9	0.59
Indentation distance increase (µm)	8.3	1.1	6.2	3.2	1.00
Creep indentation distance (µm)	3.03	2.07	3.74	2.46	1.00

Table 7-5 Mean values for the microindentation data for the midshaft femur 4 cortical bone of female F1 offspring (n=5) from protein restricted mothers (F0) compared to controls (n=5). P-values are derived from the One-Way ANOVA analysis.

Microindentation midshaft femur 4					
	F0 Control/ F1 Control (n=5)		F0 Protein restriction/ F1 Control (n=5)		P-value
	Mean	SD	Mean	SD	
Total indentation distance (µm)	221.7	82.4	220.4	86.3	1.00
Indentation distance increase (µm)	29.6	11.9	35.7	26.8	1.00
Creep indentation distance (µm)	7.15	4.27	7.15	4.94	1.00

Table 7-6 Mean values for the microindentation data midshaft femur 2 cortical bone of female F2 offspring (n=5) from protein restricted mothers (F0) compared to controls (n=5). P-values are derived from the One-Way ANOVA analysis.

Microindentation midshaft femur 2					
	F0 Control/ F2 Control (n=5)		F0 Protein restriction/ F2 Control (n=5)		P-value
	Mean	SD	Mean	SD	
Total indentation distance (µm)	73.1	10.9	83.4	16.7	1.00
Indentation distance increase (µm)	10.5	1.9	10.4	4.6	1.00
Creep indentation distance (µm)	5.27	5.18	2.64	1.07	1.00

Table 7-7 Mean values for the microindentation data midshaft femur 3 cortical bone of female F2 offspring (n=5) from protein restricted mothers (F0) compared to controls (n=5). P-values are derived from the One-Way ANOVA analysis.

Microindentation midshaft femur 3					
	F0 Control/ F2 Control (n=5)		F0 Protein restriction/ F2 Control (n=5)		P-value
	Mean	SD	Mean	SD	
Total indentation distance (µm)	67.5	7.7	81.8	16.5	1.00
Indentation distance increase (µm)	8.5	5.2	6.7	2.3	1.00
Creep indentation distance (µm)	2.12	0.50	2.31	1.14	1.00

Table 7-8 Mean values for the microindentation data midshaft femur 4 cortical bone of female F2 offspring (n=5) from protein restricted mothers (F0) compared to controls (n=5). P-values are derived from the One-Way ANOVA analysis.

Microindentation midshaft femur 4					
	F0 Control/ F2 Control (n=5)		F0 Protein restriction/ F2 Control (n=5)		P-value
	Mean	SD	Mean	SD	
Total indentation distance (µm)	220.2	73.6	179.3	64.4	1.00
Indentation distance increase (µm)	32.4	15.2	30.1	17.6	1.00
Creep indentation distance (µm)	7.00	3.41	5.32	2.79	1.00

Table 7-9 Mean values for the microindentation data for the midshaft femur 2 cortical bone of female F3 offspring (n=5) from protein restricted mothers (F0) compared to controls (n=4). P-values are derived from the One-Way ANOVA analysis.

Microindentation midshaft femur 2					
	F0 Control/ F3 Control (n=4)		F0 Protein restriction/ F3 Control (n=5)		P-value
	Mean	SD	Mean	SD	
Total indentation distance (µm)	78.0	17.8	74.0	6.5	1.00
Indentation distance increase (µm)	6.9	5.6	8.1	3.0	1.00
Creep indentation distance (µm)	2.31	0.65	2.39	0.44	1.00

Table 7-10 Mean values for the microindentation data for the midshaft femur 3 cortical bone of female F3 offspring (n=5) from protein restricted mothers (F0) compared to controls (n=4). P-values are derived from the One-Way ANOVA analysis.

Microindentation midshaft femur 3					
	F0 Control/ F3 Control (n=4)		F0 Protein restriction/ F3 Control (n=5)		P-value
	Mean	SD	Mean	SD	
Total indentation distance (µm)	73.4	18.9	66.7	8.1	1.00
Indentation distance increase (µm)	6.6	4.6	9.3	1.5	1.00
Creep indentation distance (µm)	2.59	1.49	2.14	0.42	1.00

Table 7-11 Mean values for the microindentation data for the midshaft femur 4 cortical bone of female F3 offspring (n=5) from protein restricted mothers (F0) compared to controls (n=4). P-values are derived from the One-Way ANOVA analysis.

Microindentation midshaft femur 4					
	F0 Control/ F3 Control (n=4)		F0 Protein restriction/ F3 Control (n=5)		P-value
	Mean	SD	Mean	SD	
Total indentation distance (µm)	132.3	78.7	110.2	73.5	1.00
Indentation distance increase (µm)	11.9	6.5	17.6	19.9	1.00
Creep indentation distance (µm)	2.90	0.94	3.89	2.47	1.00

Table 7-12 Mean values for the microindentation data for the epicondyle cortical bone of female F1 offspring (n=5) from protein restricted mothers (F0) compared to controls (n=4). P-values are derived from the One-Way ANOVA analysis.

Microindentation midshaft femur 4					
	F0 Control/ F1 Control (n=5)		F0 Protein restriction/ F1 Control (n=5)		P-value
	Mean	SD	Mean	SD	
Total indentation distance (µm)	139.4	25.3	132.5	6.2	1.00
Indentation distance increase (µm)	15.7	6.3	19.1	3.3	1.00
Creep indentation distance (µm)	5.00	2.77	4.05	1.52	1.00

Table 7-13 Mean values for the microindentation data for the epicondyle cortical bone of female F2 offspring (n=5) from protein restricted mothers (F0) compared to controls (n=4). P-values are derived from the One-Way ANOVA analysis.

Microindentation midshaft femur 4					
	F0 Control/ F2 Control (n=5)		F0 Protein restriction/ F2 Control (n=5)		P-value
	Mean	SD	Mean	SD	
Total indentation distance (µm)	162.1	17.2	210.1	133.4	1.00
Indentation distance increase (µm)	25.4	8.9	26.3	18.5	1.00
Creep indentation distance (µm)	5.87	3.17	6.43	1.51	1.00

Table 7-14 Mean values for the microindentation data for the epicondyle cortical bone of female F3 offspring (n=5) from protein restricted mothers (F0) compared to controls (n=4). P-values are derived from the One-Way ANOVA analysis.

Microindentation midshaft femur 4					
	F0 Control/ F3 Control (n=5)		F0 Protein restriction/ F3 Control (n=5)		P-value
	Mean	SD	Mean	SD	
Total indentation distance (µm)	215.5	138.7	215.7	91.0	1.00
Indentation distance increase (µm)	33.9	18.8	32.2	14.8	1.00
Creep indentation distance (µm)	6.38	3.47	7.48	4.26	1.00

Appendix 6- qPCR data

Table 7-15 Bone sialoprotein gene expression $\Delta\Delta CT$ (ddCT) for F1 Control and protein restricted samples

	mean dCT	ddCT	ddCT ²	mean	SD
F1 C	18.65	1.32	0.40	0.51	0.30
	17.36	2.62	0.16		
	19.97	0.00	1.00		
	19.45	0.52	0.70		
	18.24	1.73	0.30		
F1 PR	18.65	1.32	0.40	0.48	0.21
	16.97	3.01	0.12		
	18.94	1.03	0.49		
	19.31	0.66	0.63		
	19.56	0.41	0.75		

Table 7-16 Bone sialoprotein gene expression $\Delta\Delta CT$ (ddCT) for F2 Control and protein restricted samples

	mean dCT	ddCT	ddCT ²	mean	SD
F2 C	19.63	0.00	1.00	0.67	0.21
	18.82	0.81	0.57		
	19.20	0.43	0.74		
	18.10	1.53	0.35		
	19.09	0.54	0.69		
F2 PR	16.02	3.60	0.08	1.34	2.04
	22.06	-2.43	5.40		
	19.15	0.48	0.72		
	16.67	2.95	0.13		
	18.25	1.37	0.39		

Table 7-17 Bone sialoprotein gene expression $\Delta\Delta\text{CT}$ (ddCT) for F2 Control and protein restricted samples

	mean	ddCT	ddCT ²	mean	SD
F3 C	15.53	3.02	0.12	0.77	0.36
	18.04	0.51	0.70		
	18.77	-0.22	1.17		
	18.29	0.26	0.84		
	18.55	0.00	1.00		
F3 PR	17.75	0.80	0.57	0.56	0.34
	18.30	0.25	0.84		
	16.39	2.16	0.22		
	18.58	-0.03	1.02		
	15.82	2.73	0.15		

Table 7-18 Collagen 1 gene expression $\Delta\Delta\text{CT}$ (ddCT) for F1 Control and protein restricted samples

	mean	ddCT	ddCT ²	mean	SD
F1 C	18.19	1.19	0.44	0.50	0.26
	17.51	1.88	0.27		
	19.39	0.00	1.00		
	18.18	1.21	0.43		
	17.88	1.51	0.35		
F1 PR	16.08	3.30	0.10	0.22	0.34
	14.09	5.29	0.03		
	14.76	4.63	0.04		
	13.64	5.75	0.02		
	19.22	0.17	0.89		

Table 7-19 Collagen 1 gene expression $\Delta\Delta\text{CT}$ (ddCT) for F2 Control and protein restricted samples

	mean	ddCT	ddCT ²	mean	SD
F2 C	16.00	1.97	0.26	0.35	0.35
	16.50	1.47	0.36		
	17.97	0.00	1.00		
	13.83	4.14	0.06		
	14.13	3.84	0.07		
F2 PR	11.94	6.04	0.02	0.34	0.42
	18.04	-0.06	1.04		
	17.26	0.71	0.61		
	11.88	6.09	0.01		
	13.28	4.70	0.04		

Table 7-20 Collagen 1 gene expression $\Delta\Delta\text{CT}$ (ddCT) for F3 Control and protein restricted samples

	mean	ddCT	ddCT ²	mean	SD
F3 C	12.23	3.27	0.10	0.76	0.50
	14.14	1.36	0.39		
	15.50	0.00	1.00		
	16.12	-0.63	1.54		
	15.06	0.43	0.74		
F3 PR	11.32	4.18	0.06	0.69	1.25
	11.89	3.61	0.08		
	11.49	4.01	0.06		
	17.16	-1.67	3.18		
	11.29	4.20	0.05		

Table 7-21 IGF II gene expression $\Delta\Delta CT$ (ddCT) for F1 Control and protein restricted samples

	mean	ddCT	ddCT ²	mean	SD
F1 C	22.23	1.60	0.33	0.27	0.38
	17.85	5.99	0.02		
	23.84	0.00	1.00		
	17.44	6.40	0.01		
	17.75	6.09	0.01		
F1 PR	19.04	4.79	0.04	0.11	0.09
	21.94	1.90	0.27		
	17.77	6.07	0.01		
	20.97	2.87	0.14		
	20.66	3.17	0.11		

Table 7-22 IGF II gene expression $\Delta\Delta CT$ (ddCT) for F2 Control and protein restricted samples

	mean	ddCT	ddCT ²	mean	SD
F2 C	22.92	1.81	0.29	0.28	0.37
	17.95	6.78	0.01		
	21.48	3.25	0.11		
	17.44	7.28	0.01		
	24.73	0.00	1.00		
F2 PR	18.00	6.72	0.01	0.33	0.33
	23.60	1.12	0.46		
	19.97	4.76	0.04		
	24.59	0.14	0.91		
	22.74	1.99	0.25		

Table 7-23 IGF II gene expression $\Delta\Delta CT$ (ddCT) for F3 Control and protein restricted samples

	mean	ddCT	ddCT ²	mean	SD
F3 C	18.06	4.99	0.03	0.37	0.35
	22.00	1.05	0.48		
	21.00	2.05	0.24		
	19.62	3.43	0.09		
	23.05	0.00	1.00		
F3 PR	21.84	1.22	0.43	0.36	0.19
	21.20	1.86	0.28		
	21.71	1.34	0.39		
	19.25	3.80	0.07		
	22.43	0.62	0.65		

Table 7-24 IGF I gene expression $\Delta\Delta CT$ (ddCT) for F1 Control and protein restricted samples

	mean dCT	ddCT	ddCT ²	mean	SD
F1 C	15.79	0.53	0.69	0.71	0.18
	15.89	0.42	0.75		
	15.81	0.51	0.70		
	16.32	0.00	1.00		
	15.08	1.24	0.42		
F1 PR	16.22	0.10	0.93	0.81	0.44
	14.48	1.83	0.28		
	15.68	0.63	0.64		
	15.56	0.75	0.59		
	16.99	-0.67	1.59		

Table 7-25 IGF I gene expression $\Delta\Delta\text{CT}$ (ddCT) for F2 Control and protein restricted samples

	mean dCT	ddCT	ddCT ²	mean	SD
F2 C	16.68	0.00	1.00	0.69	0.26
	15.79	0.89	0.54		
	16.44	0.24	0.85		
	14.82	1.86	0.28		
	16.38	0.30	0.81		
F2 PR	15.22	1.46	0.36	0.48	0.08
	15.88	0.80	0.57		
	15.79	0.89	0.54		
	15.32	1.36	0.39		
	15.74	0.94	0.52		

Table 7-26 IGF I gene expression $\Delta\Delta\text{CT}$ (ddCT) for F3 Control and protein restricted samples

	mean dCT	ddCT	ddCT ²	mean	SD
F3 C	14.89	1.57	0.34	0.58	0.27
	14.89	1.57	0.34		
	16.46	0.00	1.00		
	16.16	0.30	0.82		
	15.20	1.26	0.42		
F3 PR	15.32	1.14	0.45	0.56	0.21
	15.13	1.33	0.40		
	16.40	0.06	0.96		
	15.66	0.80	0.57		
	15.20	1.25	0.42		

Table 7-27 Osteocalcin gene expression $\Delta\Delta\text{CT}$ (ddCT) for F1 Control and protein restricted samples

	mean dCT	ddCT	ddCT ²	mean	SD
F1 C	14.43	1.50	0.35	0.52	0.31
	13.53	2.40	0.19		
	14.16	1.76	0.29		
	15.93	0.00	1.00		
	15.49	0.44	0.74		
F1 PR	15.12	0.81	0.57	0.57	0.20
	13.78	2.14	0.23		
	15.16	0.77	0.59		
	15.25	0.68	0.62		
	15.69	0.24	0.85		

Table 7-28 Osteocalcin gene expression $\Delta\Delta\text{CT}$ (ddCT) for F2 Control and protein restricted samples

	mean dCT	ddCT	ddCT ²	mean	SD
F2 C	15.41	1.20	0.44	0.59	0.26
	16.20	0.40	0.76		
	16.61	0.00	1.00		
	15.56	1.04	0.49		
	14.63	1.98	0.25		
F2 PR	14.06	2.54	0.17	0.18	0.10
	15.20	1.41	0.38		
	13.63	2.98	0.13		
	12.97	3.63	0.08		
	13.65	2.95	0.13		

Table 7-29 Osteocalcin gene expression $\Delta\Delta\text{CT}$ (ddCT) for F3 Control and protein restricted samples

	mean dCT	ddCT	ddCT ²	mean	SD
F3 C	14.19	1.07	0.48	0.65	0.24
	15.06	0.21	0.86		
	15.27	0.00	1.00		
	14.35	0.92	0.53		
	13.93	1.34	0.40		
F3 PR	13.29	1.98	0.25	0.31	0.14
	13.51	1.76	0.30		
	12.60	2.66	0.16		
	14.45	0.81	0.57		
	13.51	1.76	0.30		

Table 7-30 Osteonectin gene expression $\Delta\Delta\text{CT}$ (ddCT) for F1 Control and protein restricted samples

	mean dCT	ddCT	ddCT ²	mean	SD
F1 C	14.36	0.67	0.63	0.62	0.20
	14.12	0.91	0.53		
	13.88	1.16	0.45		
	14.02	1.02	0.49		
	15.03	0.00	1.00		
F1 PR	13.18	1.86	0.28	0.59	0.45
	11.49	3.54	0.09		
	14.92	0.12	0.92		
	13.62	1.41	0.38		
	15.42	-0.39	1.31		

Table 7-31 Osteonectin gene expression $\Delta\Delta\text{CT}$ (ddCT) for F2 Control and protein restricted samples

	mean dCT	ddCT	ddCT ²	mean	SD
F2 C	13.80	0.51	0.70	0.95	0.76
	12.04	2.26	0.21		
	15.55	-1.25	2.38		
	14.30	0.00	1.00		
	13.19	1.11	0.46		
F2 PR	11.98	2.33	0.20	0.75	0.93
	13.33	0.97	0.51		
	15.68	-1.37	2.59		
	11.59	2.72	0.15		
	12.60	1.71	0.31		

Table 7-32 Osteonectin gene expression $\Delta\Delta\text{CT}$ (ddCT) for F3 Control and protein restricted samples

	mean dCT	ddCT	ddCT ²	mean	SD
F3 C	13.63	1.10	0.47	0.52	0.31
	12.59	2.14	0.23		
	14.73	0.00	1.00		
	14.28	0.45	0.73		
	12.21	2.52	0.17		
F3 PR	12.47	2.26	0.21	0.19	0.13
	11.98	2.75	0.15		
	11.02	3.71	0.08		
	13.55	1.18	0.44		
	11.34	3.39	0.10		

Table 7-33 Osteopontin gene expression $\Delta\Delta CT$ (ddCT) for F1 Control and protein restricted samples

	mean dCT	ddCT	ddCT ²	mean	SD
F1 C	20.14	1.39	0.38	0.40	0.32
	17.37	4.17	0.06		
	21.53	0.00	1.00		
	20.12	1.41	0.38		
	19.22	2.32	0.20		
F1 PR	20.05	1.49	0.36	0.73	0.46
	19.30	2.23	0.21		
	21.87	-0.34	1.26		
	20.55	0.98	0.51		
	21.91	-0.38	1.30		

Table 7-34 Osteopontin gene expression $\Delta\Delta CT$ (ddCT) for F2 Control and protein restricted samples

	mean dCT	ddCT	ddCT ²	mean	SD
F2 C	21.14	0.09	0.94	0.62	0.29
	19.79	1.45	0.37		
	20.06	1.18	0.44		
	19.76	1.48	0.36		
	21.24	0.00	1.00		
F2 PR	16.38	4.85	0.03	0.42	0.45
	21.61	-0.38	1.30		
	19.77	1.47	0.36		
	18.23	3.00	0.12		
	19.33	1.90	0.27		

Table 7-35 Osteopontin gene expression $\Delta\Delta CT$ (ddCT) for F3 Control and protein restricted samples

	mean dCT	ddCT	ddCT ²	mean	SD
F3 C	18.81	2.05	0.24	0.54	0.27
	19.26	1.61	0.33		
	19.88	0.99	0.50		
	20.14	0.73	0.60		
	20.87	0.00	1.00		
F3 PR	18.77	2.10	0.23	0.37	0.21
	19.66	1.21	0.43		
	20.01	0.85	0.55		
	20.15	0.72	0.61		
	16.18	4.69	0.04		

Table 7-36 Runx-2 gene expression $\Delta\Delta CT$ (ddCT) for F1 Control and protein restricted samples

	mean dCT	ddCT	ddCT ²	mean	SD
F1 C	15.35	1.83	0.28	0.72	0.31
	17.19	0.00	1.00		
	15.90	1.28	0.41		
	17.17	0.01	0.99		
	17.07	0.12	0.92		
F1 PR	16.57	0.62	0.65	0.75	0.62
	13.71	3.48	0.09		
	17.34	-0.16	1.11		
	14.41	2.78	0.15		
	17.98	-0.79	1.73		

Table 7-37 Runx-2 gene expression $\Delta\Delta CT$ (ddCT) for F2 Control and protein restricted samples

	mean dCT	ddCT	ddCT ²	mean	SD
F2 C	15.30	2.97	0.13	0.47	0.33
	16.95	1.33	0.40		
	18.27	0.00	1.00		
	17.70	0.57	0.67		
	15.67	2.60	0.16		
F2 PR	15.33	2.95	0.13	0.22	0.17
	16.04	2.24	0.21		
	17.41	0.86	0.55		
	13.99	4.29	0.05		
	15.51	2.76	0.15		

Table 7-38 Runx-2 gene expression $\Delta\Delta CT$ (ddCT) for F3 Control and protein restricted samples.

	mean dCT	ddCT	ddCT ²	mean	SD
F3 C	15.66	2.25	0.21	0.45	0.34
	15.52	2.39	0.19		
	17.40	0.51	0.70		
	17.91	0.00	1.00		
	15.13	2.78	0.15		
F3 PR	14.87	3.04	0.12	0.15	0.16
	14.18	3.73	0.08		
	13.31	4.60	0.04		
	16.79	1.11	0.46		
	13.16	4.75	0.04		

Table 7-39 Results of the Mann-Whitney U test for F1 C vs F1 PR samples.

	Null Hypothesis	Test	Sig.	Decision
1	The distribution of BSP is the same across categories of Diet_group.	Independent-Samples Mann-Whitney U Test	1.000 ¹	Retain the null hypothesis.
2	The distribution of COL1 is the same across categories of Diet_group.	Independent-Samples Mann-Whitney U Test	.095 ¹	Retain the null hypothesis.
3	The distribution of IGF2 is the same across categories of Diet_group.	Independent-Samples Mann-Whitney U Test	.690 ¹	Retain the null hypothesis.
4	The distribution of IGF1 is the same across categories of Diet_group.	Independent-Samples Mann-Whitney U Test	.310 ¹	Retain the null hypothesis.
5	The distribution of OCN is the same across categories of Diet_group.	Independent-Samples Mann-Whitney U Test	.841 ¹	Retain the null hypothesis.
6	The distribution of ON is the same across categories of Diet_group.	Independent-Samples Mann-Whitney U Test	.548 ¹	Retain the null hypothesis.
7	The distribution of OP is the same across categories of Diet_group.	Independent-Samples Mann-Whitney U Test	.310 ¹	Retain the null hypothesis.
8	The distribution of Runx2 is the same across categories of Diet_group.	Independent-Samples Mann-Whitney U Test	1.000 ¹	Retain the null hypothesis.

Table 7-40 Results of the Mann-Whitney U test for F2 C vs F1 PR samples.

	Null Hypothesis	Test	Sig.	Decision
1	The distribution of BSP is the same across categories of Diet_group.	Independent-Samples Mann-Whitney U Test	.548 ¹	Retain the null hypothesis.
2	The distribution of COL1 is the same across categories of Diet_group.	Independent-Samples Mann-Whitney U Test	.548 ¹	Retain the null hypothesis.
3	The distribution of IGF2 is the same across categories of Diet_group.	Independent-Samples Mann-Whitney U Test	.690 ¹	Retain the null hypothesis.
4	The distribution of IGF1 is the same across categories of Diet_group.	Independent-Samples Mann-Whitney U Test	.310 ¹	Retain the null hypothesis.
5	The distribution of OCN is the same across categories of Diet_group.	Independent-Samples Mann-Whitney U Test	.016 ¹	Reject the null hypothesis.
6	The distribution of ON is the same across categories of Diet_group.	Independent-Samples Mann-Whitney U Test	.421 ¹	Retain the null hypothesis.
7	The distribution of OP is the same across categories of Diet_group.	Independent-Samples Mann-Whitney U Test	.222 ¹	Retain the null hypothesis.
8	The distribution of Runx2 is the same across categories of Diet_group.	Independent-Samples Mann-Whitney U Test	.310 ¹	Retain the null hypothesis.

Table 7-41 Results of the Mann-Whitney U test for F3 C vs F3 PR samples.

	Null Hypothesis	Test	Sig.	Decision
1	The distribution of BSP is the same across categories of Diet_group.	Independent-Samples Mann-Whitney U Test	.690 ¹	Retain the null hypothesis.
2	The distribution of COL1 is the same across categories of Diet_group.	Independent-Samples Mann-Whitney U Test	.151 ¹	Retain the null hypothesis.
3	The distribution of IGF2 is the same across categories of Diet_group.	Independent-Samples Mann-Whitney U Test	.841 ¹	Retain the null hypothesis.
4	The distribution of IGF1 is the same across categories of Diet_group.	Independent-Samples Mann-Whitney U Test	.690 ¹	Retain the null hypothesis.
5	The distribution of OCN is the same across categories of Diet_group.	Independent-Samples Mann-Whitney U Test	.056 ¹	Retain the null hypothesis.
6	The distribution of ON is the same across categories of Diet_group.	Independent-Samples Mann-Whitney U Test	.056 ¹	Retain the null hypothesis.
7	The distribution of OP is the same across categories of Diet_group.	Independent-Samples Mann-Whitney U Test	.548 ¹	Retain the null hypothesis.
8	The distribution of Runx2 is the same across categories of Diet_group.	Independent-Samples Mann-Whitney U Test	.056 ¹	Retain the null hypothesis.